HYDROGEN SULFIDE MODULATES GLUCONEOGENESIS AND MITOCHONDRIAL BIOGENESIS IN MOUSE PRIMARY HEPATOCYTES

A Thesis

Presented to the Faculty of

Graduate Studies of Lakehead University

In Partial Fulfillment of the Requirements

For the Degree of Doctor of Philosophy

In Medical Biotechnology

By

ASHLEY UNTEREINER

PERMISSION TO USE

In presenting this thesis in partial fulfillment of the requirements for the Ph.D. degree from Lakehead University, I agree that the libraries of this University may make it freely available for inspection. I further agree that permission for copying of this thesis in any manner, in whole or in part, for scholarly purposes may be granted by the professor or professors who supervised my thesis work or, in their absence, by the head of the Department or the Dean of Graduate Studies in which my thesis work was done. It is understood that any copying or publication or use of thesis or parts thereof for financial gain shall not by allowed without my written permission. It is also understood that due recognition shall be given to me and to Lakehead University in any scholarly use which may be made of any material in my thesis.

Requests for permission to copy or to make other use of material in this thesis in whole or part should be addressed to:

Graduate Studies

Lakehead University

955 Oliver Road

Thunder Bay, ON, Canada

P7B 5E1

ABSTRACT

Among many endogenous substances that regulate hepatic energy production is the gasotransmitter hydrogen sulfide (H_2S). In the liver, H_2S production is largely catalyzed by cystathionine γ-lyase (CSE) and, to a lesser degree, by cystathionine β-synthase. We previously showed that H_2S stimulates glucose production in an immortalized carcinoma liver cell line ($HepG_2$ cells) as well as induce ATP generation in isolated vascular smooth muscle cells (VSMCs). Furthermore, we found that H_2S upregulates peroxisome proliferator-activated receptor-γ coactivator (PGC)-1α expression in rat VSMCs. PGC-1α is a crucial regulator of hepatic gluconeogenesis and mitochondrial biogenesis. Both of these PGC-1α-mediated energy processes are pivotal to maintain whole-body energy homeostasis, whereby their sustained disturbance may lead to the development of type 2 diabetes and metabolic syndrome. Therefore, we investigated the regulation of gluconeogenesis and mitochondrial biogenesis by CSE-generated H_2S under physiological conditions in isolated mouse hepatocytes.

We found that CSE-knockout (KO) mice had a reduced rate of gluconeogenesis, which was reversed by administration of NaHS (an H_2S donor) (i.p.). Interestingly, isolated CSE-KO hepatocytes exhibited a reduced glycemic response to chemical-induced activation of the cAMP/PKA and glucocorticoid pathways compared to wild-type (WT) hepatocytes. Treatment with the inhibitors for PKA (KT5720) or glucocorticoid receptor (RU-486) significantly reduced H_2S-stimulated glucose production from both WT and CSE-KO mouse hepatocytes. NaHS treatment upregulated the protein levels of key gluconeogenic transcription factors, such as PGC-1α and CCAAT-enhancer-binding proteins-β (C/EBP-β). Moreover, exogenous H_2S augmented the *S*-sulfhydration of the rate-limiting gluconeogenic enzymes and PGC-1α and increased their activities, which were lower in untreated CSE-KO hepatocytes. Finally, knockdown of PGC-1α,

but not C/EBP-β, significantly decreased NaHS-induced glucose production from the primary hepatocytes.

After determining that H_2S stimulates hepatic glucose production through the PGC-1α signaling pathway, we focused on whether or not H_2S induces hepatic mitochondrial biogenesis. We found that CSE-KO hepatocytes produced less mtDNA compared to WT hepatocytes. Mitochondrial content was decreased in CSE-KO hepatocytes compared to normal hepatocytes, which was restored with NaHS treatment. CSE-KO hepatocytes exhibited lower levels of mitochondrial transcription factors and the mitochondrial transcription coactivator, peroxisome proliferator-activated receptor-γ coactivator-related protein (PPRC) compared to WT hepatocytes. Interestingly, NaHS administration upregulated PPRC, yet downregulated PGC-1β protein level in mouse hepatocytes. Moreover, exogenous H_2S induced the *S*-sulfhydration of PPRC, which was lower in untreated CSE-KO hepatocytes, but not that of PGC-β. Finally, knockdown of either PGC-1α or PPRC significantly decreased NaHS-stimulated mitochondrial biogenesis in hepatocytes, where knockdown of both genes were required to completely abolish NaHS-induced mitochondrial biogenesis.

Overall this thesis demonstrates the stimulatory effect of endogenous H_2S on liver glucose production and reveals four underlying mechanisms. 1) H_2S upregulates the expression levels of PGC-1α and PEPCK *via* glucocorticoid receptor pathway. 2) H_2S upregulates the expression level of PGC-1α through the activation of the cAMP/PKA pathway, as well as PGC-1α activity *via S*-sulfhydration. 3) H_2S upregulates the expression and the activities (by *S*-sulfhydration) of G6Pase and FBPase. 4) H_2S augments the protein expression level and activity (*via S*-sulfhydration) of PPRC. By stimulating the combined activities of PPRC and PGC-1α,

H_2S induces mitochondrial biogenesis, thereby supplying energy to support its induction of hepatic glucose production.

This study may offer clues to the regulation of hepatic energy homeostasis under physiological conditions and its dysregulation in insulin-resistance diseases.

ACKNOWLEDGEMENTS

First and foremost, I would like to offer my sincere gratitude to my supervisors Dr. Lingyun Wu and Dr. Rui Wang. Their combined trust, guidance, and support helped me to become an independent thinker and a confident researcher. I have benefited tremendously from their keen scientific vision and the freedom to pursue my own research interests; making my research an exciting experience. I will always be grateful for their inspiration and support during my journey as a graduate student.

I thank my supervisory committee: Dr. Rui Wang, Dr. Lingyun Wu, Dr. Neelam Khaper, and Dr. Ingeborg Zehbe for their insightful and constructive comments during the course of my training and the preparation of this thesis. I would also like to thank my external examiner, Dr. Qingping Feng, for his advice and expertise on the final construction of my thesis.

I am grateful for my friends and colleagues: Ming Fu, Zaid Altaany, YoungJun Ju, Zoe Sun, Shuangshuang Li, Sarathi Mani, Kexin Zhao, and Katia Modis. They were always willing to offer a helping hand, their expertise, experience, and most importantly, a laugh.

I would like to show my gratitude to Rosanne (Roxanne) Licskai for her endless support and her wonderful comic relief. Roxanne's daily enthusiasm and sense of humour always brightened my day. I will never forget you!

I want to also acknowledge the financial support that I have received during my Ph.D. training. My gratitude goes to the Ontario Ministry of Education for awarding me the OGS, to CIHR for granting me the prestigious Doctoral Research Award, and to TBRRI and Lakehead University for their travel awards.

Finally, from the bottom of my heart I give a loving thanks to my parents Francis and Teresa Untereiner for their love, caring, and never ending support in helping me to achieve my dreams. They have allowed me to become the person I am today and for that I will always be grateful.

To my family,

for their unconditional

love and support

TABLE OF CONTENTS

LIST OF FIGURES

LIST OF TABLES

LIST OF ABBREVIATIONS

AGEs – advanced glycation end-products

AMPK – AMP-activated protein kinase

ApoE – apolipoprotein E

ATP1a5 – Na^+/K^+, ATPase-a5

BP – blood pressure

CAT – cysteine aminotransferase

CBS – cystathionine β-synthase

C/EBP-β – CCAAT-enhancer-binding proteins-β

CHOP – C/EBP homologous protein

CNS – central nervous system

CRE – cAMP response element

CREB – cAMP response element binding protein

CSE – cystathionine γ-lyase

CT – control

Dex – dexamethasone

DHAP – dihydroxyacetone phosphate

DHDY– tetrapeptide motif

DMEM – dulbecco's modified eagle medium

DMPD – *N*,*N*-dimethyl-p-phenylenediamine

ECL – enhanced chemiluminescence

EDRF – endothelium-derived relaxing factor

eNOS – endothelium nitric oxide synthase

ETC – electron transport chain

F-1,6-P – fructose-1,6-bisphosphate

F-6-P – fructose-6-phosphate

FACS – fluorescence-activated cell sorting

FBPase – fructose-1,6-bisphosphatase

FOXO1 – forkhead box protein O1

G-6-P – glucose-6-phosphate

G6Pase – glucose-6-phosphatase

GA3P – glyceraldehyde 3-phosphate

GI – gastrointestinal

GLUT – glucose transporter

GR – glucocorticoid receptor

GSH – reduced glutathione

GSSG – oxidized glutathione

HCF – host cell factor

Hcy – homocysteine

HDL – high-density lipoprotein

IL – interleukin

K_{ATP} – K^+-dependent-ATP

Kir – inwardly rectifying K^+ channel

KO – knockout

$_L$-cyt – $_L$-cysteine

LDL – low-density lipoproteins

LIRKO – liver-specific insulin receptor knockdown

LPS – lipopolysaccharide

MST – β-mercaptopyruvate sulfurtransferase

mtDNA – mitochondrial DNA

NOSM – Northern Ontario School of Medicine

NRF – nuclear respiratory factor

NSAID - Nonsteroidal anti-inflammatory drug

PAG - $_{DL}$-propargylglycine

PC – pyruvate carboxylase

PDE – phosphodiesterase

PEPCK – phosphoenolpyruvate carboxykinase

PGC-1α/β – peroxisome proliferator-activated receptor-γ coactivator-1α/β

PI3K – insulin receptor substrate-phosphatidylinositol 3-OH kinase

PKA – protein kinase A

PLP – pyridoxal 5'-phosphate

PPG – $_{DL}$-propargylglycine

PPRC – peroxisome proliferator-activated receptor-γ coactivator-related protein

PTT – pyruvate tolerance test

ROS – reactive oxygen species

SD – Sprague-Dawley

SHRs – spontaneously hypertensive rats

siRNA – short interfering RNA

SIRT – sirtuin

SOD – superoxide dismutase

SQR – sulfide:quinone oxidoreductase

SSH – *S*-sulfhydration

STZ – streptozotocin

SUR – sulfonylurea receptors

T1DM – type 1 diabetes mellitus

T2DM – type 2 diabetes mellitus

TCA – tricarboxylic acid cycle

Tfam – transcription factor A, mitochondrial

TNF-α – tumor necrosis factor-α

VSMCs – vascular smooth muscle cells

WT – wild type

ZDF – Zucker diabetic fatty

ZF – Zucker fatty

ZL – Zucker lean

LIST OF CHEMICAL FORMULAS

Ca_2^+ – calcium

CO – carbon monoxide

H_2O_2 – hydrogen peroxide

H_2S – hydrogen sulfide

HS^- – hydrosulfide anion

Na_2S – sodium sulfide

NaHS – sodium hydrosulfide

NO – nitric oxide

O_2 – oxygen

O_2^- – superoxide anion

$ONOO^-$ – peroxynitrite

S^{2-} – sulfide anion

CHAPTER 1

INTRODUCTION AND LITERATURE REVIEW

1.0 Glucose homeostasis

Our body strives to maintain our blood sugar level in the physiological range of 3.8-5.5 mM (1), which will rise and fall depending on diet and daily activities. Glucose in the bloodstream either comes from dietary sources or from glycogen breakdown (glycogenolysis) and/or *de novo* synthesis of glucose (gluconeogenesis) where both glycogenolysis and gluconeogenesis occur in the liver. Glucose is the most efficient and abundant energy substrate for mammalian cells, fueling numerous physiological functions, including cell proliferation and growth, protein and nucleic acid synthesis, fatty acid, and cholesterol synthesis, etc. This monosaccharide is used to produce ATP, the energy currency of the cell, *via* oxidative phosphorylation (in the mitochondria) and, to a lesser degree, anaerobic glycolysis (in the cytosol). Needless to say, glucose homeostasis is critical to maintaining the physiological function of our body, whereby its sustained disturbance may lead to the development of metabolic syndrome.

1.1 The impact of nutritional status on hepatic glucose metabolism

1.1.1. Immediately after consuming a meal (fed state)

The liver plays a fundamental role in whole-body glucose homeostasis. After a meal, the ingested nutrients absorbed from the gastrointestinal (GI) tract pass through the portal vein and enters the liver before entering the systemic circulation (2). In fact, the liver is a crucial player in regulating oral glucose tolerance. With the help of insulin, the liver removes the ingested glucose from the bloodstream to stabilize the rise in blood glucose level after a meal (2). Furthermore, when nutrients are not being absorbed from the GI tract, an increase of hepatic glucose production is required to meet the body's need for glucose to avoid hypoglycemia (low blood sugar level). Therefore, depending upon the concentration of the blood sugar level, the

liver alternates from a net consumer to a net producer of glucose to maintain whole-body glucose homeostasis.

1.1.1.1 Insulin-facilitated glucose utilization

Circulating glucose is recognized by and transported (*via* glucose transport machinery) into the liver, pancreas, skeletal muscle, and adipose tissues (Figure 1-1). These organs and tissues have their own characteristic patterns of metabolism and use glucose-derived metabolites or hormones as a means to communicate with each other. This complex, interconnected network is critical to maintain tissue-specific metabolic needs and to balance our blood sugar level.

For instance, after ingestion of a meal, plasma glucose level will spike which stimulates pancreatic β-cells to secrete insulin into the bloodstream (3). Insulin stimulates the uptake and utilization of glucose in the skeletal muscle, which burns glucose to meet its metabolic need, as well as in adipose tissue, which stores glucose to synthesize fat. The liver also responds to insulin signaling by absorbing glucose from the circulation and converting it into energy storage molecules (glycogen and fat). In fact, the liver is the major organ responsible for glucose production and its release into the circulation, *via* glycogenolysis and gluconeogenesis (discussed in section 1.1.2.1). To prevent the additional release of hepatic glucose into the bloodstream, insulin inhibits glycogenolysis and gluconeogenesis. Insulin secretion will continue until the GI tract completely absorbs the dietary nutrients and plasma glucose level is once again within the 3.8-5.5 mM range.

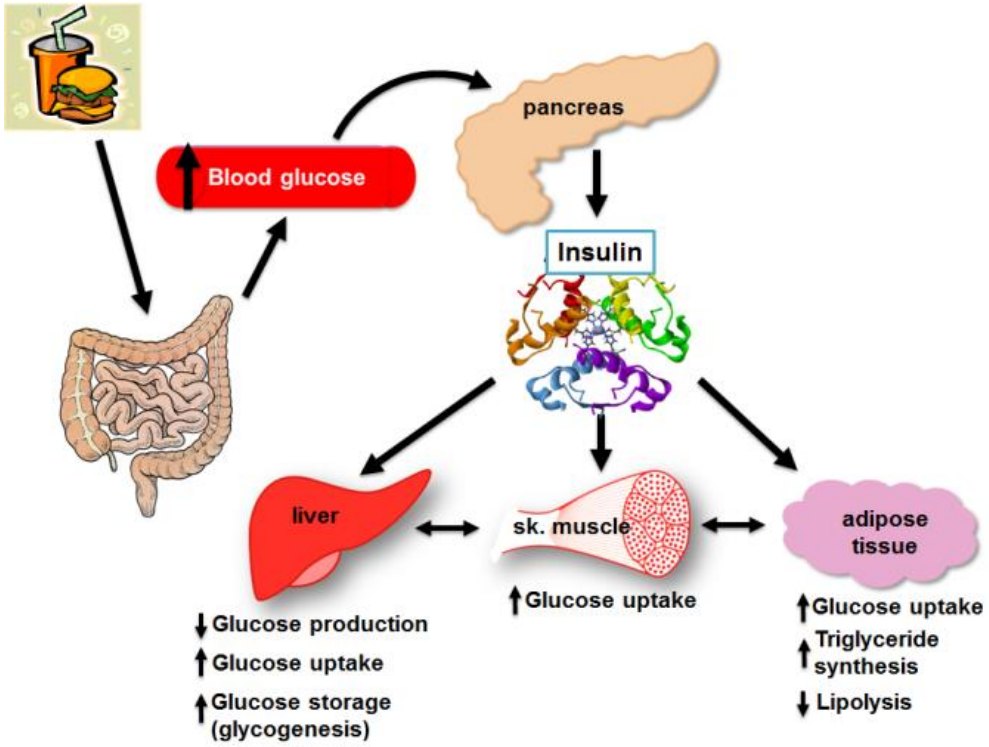

Figure 1-1: The interconnected network of insulin-sensitive tissues working synergistically to maintain glucose homeostasis after a meal. Adopted and modified from Kleinridders *et al.* (2009) (3).

1.1.1.2 Mechanism of insulin secretion

Insulin is a critical hormone used to lower blood glucose level. Therefore, the pancreas must respond appropriately to glucose fluctuations in the bloodstream to maintain glucose homeostasis. The first step in insulin secretion is the transportation of glucose into the pancreatic β-cell *via* glucose transporter (GLUT) 2 (4). Once inside, the glucose molecule is phosphorylated, yielding glucose-6-phosphate, which effectively traps glucose inside the β-cell. As glucose metabolism proceeds and more glucose enters the pancreatic β-cell, more ATP is produced in the mitochondria. As a result, this increases the ATP:ADP ratio that consequently closes the ATP-gated potassium channels in the β-cell membrane; thus preventing positively

charged potassium ions from leaving the cell. The rise in the positive charge inside the β-cell results in membrane depolarization, which then causes the voltage-gated calcium channels to open, allowing calcium ions to flow into the cell. Whereby, finally, the increase in intracellular calcium concentration triggers the release of insulin (*via* exocytosis) from the pancreatic β-cell (Figure 1-2).

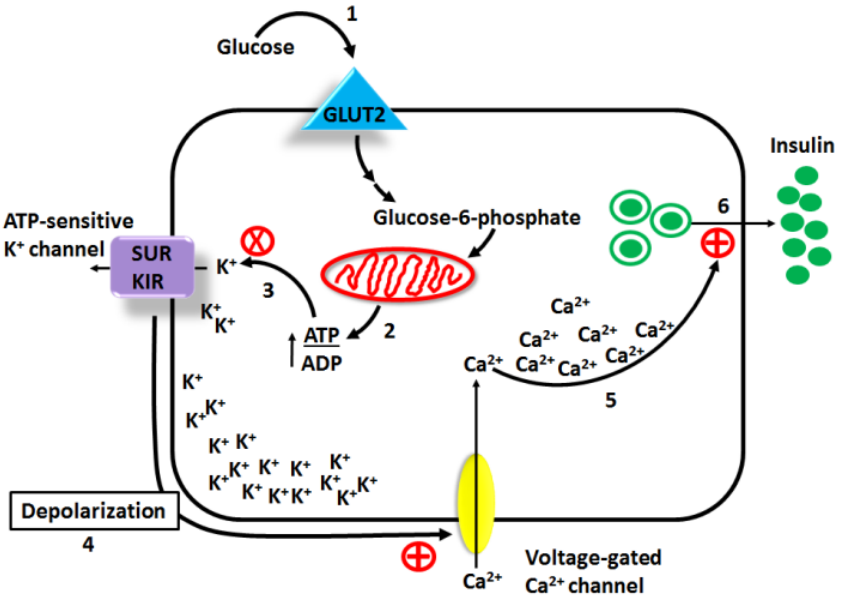

Figure 1-2: Glucose-stimulated insulin secretion from pancreatic β-cell. 1) Glucose enters pancreatic β-cell *via* glucose transporter (GLUT) 2. 2) Glucose metabolism increases the ATP:ADP ratio that (3) closes the ATP-gated potassium channels in the β-cell membrane, preventing positively charged potassium ions (K^+) from leaving the cell. 4) The increased positive charge inside the β-cell results in depolarization along its membrane, thus (5) opening the voltage-gated calcium channels, allowing calcium ions (Ca^{2+}) to enter the cell. 6) Increased intracellular Ca^{2+} concentration stimulates insulin exocytosis from the pancreatic β-cell. Kir: inwardly rectifying K^+ channel; SUR: sulfonylurea receptor. Adopted and modified from Fu *et al.* (2013) (4).

1.1.1.3 Actions of insulin on hepatocytes

The liver is the first organ to encounter the inflow of blood from the pancreas, *via* the portal vein (2). Consequently, the liver is exposed to considerably higher levels of pancreatic hormones (i.e.

insulin and glucagon) compared to other organs in the systemic circulation (2). The positioning of the liver to encounter more endocrine hormones released from pancreatic islets is strategic since glucagon primarily acts on hepatocytes to increase glucose production (*via* glycogenolysis and gluconeogenesis), whereas insulin counteracts the actions of glucagon on hepatocytes *via* inhibiting these glucose production mechanisms (as discussed below). Incredibly, ~60% of secreted insulin binds to hepatocyte insulin receptors, meaning that the liver is exposed to plasma insulin concentrations ~3-fold higher compared to other insulin-sensitive tissues in the body (2).

Upon binding to its receptor on hepatocytes, insulin activates the insulin receptor substrate (IRS)-phosphatidylinositol 3-OH kinase (PI3K) pathway. The PI3K pathway mediates insulin suppression on both glycogenolysis and gluconeogenesis processes. Accordingly, PI3K activates phosphoinositide-dependent kinase-1, which then phosphorylates the serine/threonine kinase AKT. Now, the pivotal point of insulin-mediated suppression of hepatic glucose production comes when AKT directly phosphorylates the transcription factor forkhead box O1 (FOXO1). This phosphorylation event causes FOXO1 to exit the nucleus, which consequently terminates the peroxisome proliferator-activated receptor-γ coactivator (PGC)-1α-mediated induction of the major gluconeogenic enzymes, such as phosphoenolpyruvate carboxykinase (PEPCK), fructose-1,6-bisphosphate (FBPase), and glucose-6-phosphatase (G6Pase). Furthermore, Akt also phosphorylates PGC-1α itself which increases PGC-1α protein degradation (5). Since the hepatic PGC-1α transduction pathway is abnormally stimulated in type 2 diabetes mellitus (T2DM) (discussed in Section 4.1.2), the AKT-FOXO1-PGC-1α mechanism is intensively studied and manipulated in insulin-resistant models, in the hopes of restoring and normalizing hepatic glucose production.

With the inhibition of hepatic glucose production, insulin then stimulates hepatic glucose uptake from the circulation, a mechanism that contributes to whole-body glucose homeostasis. Hepatic glucose uptake from the bloodstream subsequently stimulates glycogen and fatty acid synthesis. In fact, the liver is responsible for removing the equivalent of ~60-65% of glucose from the circulation (6). Therefore, it is pivotal that this function remains in intact, whereby impairments in glucose uptake into hepatocytes are associated with insulin-resistant diseases, such as metabolic syndrome and T2DM (discussed in section 1.2.1).

1.1.2 Roughly four hours after a meal (postprandial state)

When food is no longer being absorbed from the GI tract, plasma glucose level begins to decline which simultaneously stimulates the release of glucagon and inhibits the secretion of insulin into the circulation from pancreatic α- and β-cells, respectively. Fasting also stimulates the release of glucocorticoid into the bloodstream from the adrenal cortex that initiates only the gluconeogenic process in hepatocytes. Both the glucagon and glucocorticoid signaling pathways work synergistically to enhance glucose production and maintain glucose homeostasis.

1.1.2.1 Hepatic glucose production

1.1.2.1.1 Glycogenolysis

Glycogenolysis is the first glucose-delivery mechanism to be activated in the liver after ~4-5 hour fast (7). During this time, blood sugar level begins to fall which stimulates glucagon secretion from pancreatic α-cells. The increase in blood glucagon level is accompanied by a concomitant decrease in insulin secretion; a necessary measure since insulin opposes the actions of glucagon. Once released into the bloodstream, glucagon acts on the liver to stimulate glycogenolysis. With glycogenolysis, the liver can provide immediate energy supply by rapidly

converting glycogen into glucose which is then released into the bloodstream. In fact, the release rate of glucose is greater with glycogenolysis (5.0 μmol/kg/min) than with gluconeogenesis (3.0 μmol/kg/min) (7). The liver is the only organ in the body that undergoes glycogenolysis. However, the proportion of glucose release *via* glycogenolysis decreases with the duration of fasting, due to the depletion of hepatic glycogen stores (7). For example, in humans, after 24 hours from the last meal, glycogenolysis accounts for about 30% of all glucose released, and by 48 hours, it accounts for <10% of all glucose released into the circulation (8). Therefore, at this stage, the liver must switch to gluconeogenesis as the primary mechanism to release glucose into the bloodstream and to maintain glucose homeostasis.

1.1.2.1.2 Gluconeogenesis

Gluconeogenesis is the *de novo* synthesis of glucose from non-carbohydrate carbon compounds, such as lactate, pyruvate, alanine, and glycerol (Figure 1-3). This metabolic pathway is stimulated during periods of prolong fasting, low-carbohydrate diets, or intense physical activity. The vast majority of glucose is produced from hepatic gluconeogenesis (roughly 80%), and to a lesser extent, renal gluconeogenesis (approximately 20%; and it occurs in kidney cortex) (9; 10).

The rate of gluconeogenesis is determined by the unidirectional enzymes, pyruvate carboxylase (PC), PEPCK, FBPase, and G6Pase (11). These rate-limiting gluconeogenic enzymes are controlled *via* 3 mechanisms: 1) by transcriptional regulation (i.e. PC, PEPCK, and G6Pase) *via* insulin, glucagon, and/or glucocorticoid signaling; 2) through allosteric inhibition (i.e. FBPase) *via* fructose-2,6-bisphosphate; and 3) through inhibition/stimulation if the enzymes' substrate is absence/present (11). For example, G6Pase and PC are activated if glucose-6-phosphate or pyruvate, respectively, is present and is catalytically deactivated in its

absence. In fact, the activity rates of the gluconeogenic enzymes are regulated by the ATP:ADP ratio. ATP is a critical energy source for the *de novo* production of glucose, directly fueling the catalytic activity of PC and PEPCK, thereby indirectly determining the rate of FBPase and G6Pase due to their respective substrate levels (Figure 1-3).

One of the main transcriptional coactivators of hepatic gluconeogenesis is PGC-1α. The mechanism by which PGC-1α stimulates hepatic gluconeogenesis is described in detail in section 4.1.1.

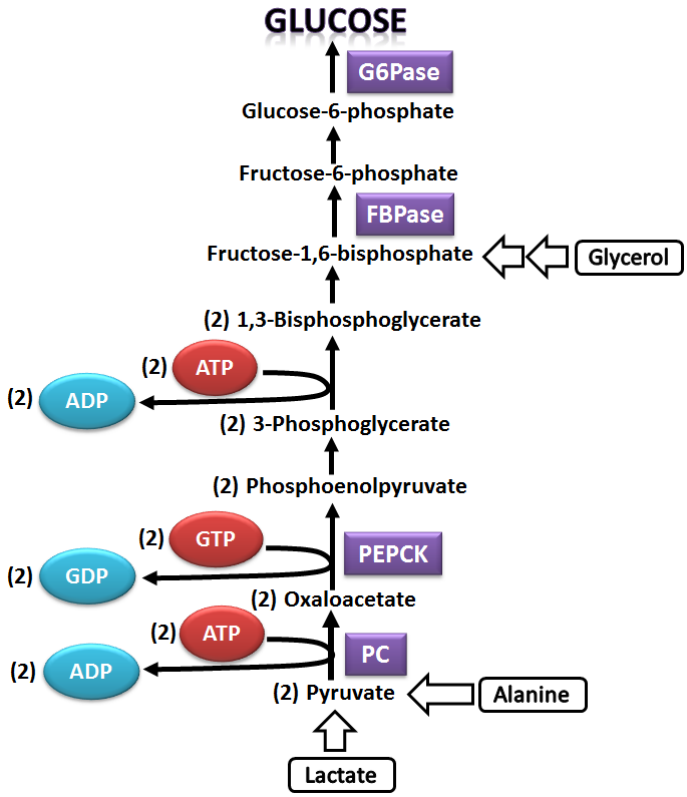

Figure 1-3: Pathway of hepatic gluconeogenesis. The rate of gluconeogenesis is regulated by the rate-limiting enzymes: PC, PEPCK, FBPase, and G6Pase. During gluconeogenesis, 2 moles of pyruvate are used to produce 1 mole of glucose, and in the process, consumes 6 moles of ATP; making the gluconeogenic process very costly from an energetic point-of-view, since glycolysis yields only 2 moles of ATP. FBPase: fructose-1,6-bisphosphate; G6Pase: glucose-6-phosphatase; PEPCK: phosphoenolpyruvate carboxykinase; PC: pyruvate carboxylase.

1.2 Pathophysiology of glucose metabolism

1.2.1 Insulin resistance and uncontrolled glucose production

1.2.1.1 Metabolic syndrome

The metabolic syndrome represents a cluster of abnormalities that together greatly increases one's risk of developing cardiovascular diseases and T2DM. The most widely accepted definition of the metabolic syndrome is provided by the International Diabetes Federation (12). This federation suggests that if a person is to be diagnosed with metabolic syndrome, the individual must have central obesity (waist circumference is greater than 88 cm or 35 inches for women or 102 cm or 40 inches for men), and any two of the following abnormalities: increased triglycerides; reduced high-density lipoprotein (HDL) cholesterol; elevated blood pressure (BP), and/or elevated fasting plasma glucose level.

Central obesity is a fundamental feature of the metabolic syndrome; due to the strength of the evidence linking waist circumference with cardiovascular disease and T2DM development. Since the metabolic syndrome is made up of a cluster of different types of pathologies, there is no single treatment available as of yet; however, therapies that address several of the risk factors concurrently are being researched and provides hope for the future.

1.2.1.1.1 T2DM

Canadians are aging, and the obesity rates are rising. In 2015, one in four Canadians, roughly over 9 million people, lives with diabetes or prediabetes (a condition known as "borderline diabetes;" classified when an individual has abnormally high fasted blood sugar level, 5.6-6.9 mM, but not as high as a diabetic, >7 mM) (13). If nothing is done to curve this trend, by 2020, it will be one in three (13). Consequently, this poses a serious burden on Canada's publicly

funded health care system and economy. In 2015, diabetes would cost Canada almost $14 billion, whereby in 2020, it would cost the Canadian health care system and the economy almost $16 billion (13). Clearly, diabetes prevalence is growing at epidemic levels across Canada, and urgent action is needed to reduce the cost pressure on the Canadian health care system and economy.

Diabetes mellitus, also known as "starvation in the midst of plenty," is a chronic metabolic disorder characterized by hyperglycemia (chronic high blood sugar level). Hyperglycemia occurs either because pancreatic β-cells are unable to produce insulin (type 1 diabetes mellitus; T1DM), or because peripheral tissues (i.e. white adipose tissue, skeletal muscle, and liver) no longer responds effectively to insulin signaling (T2DM).

Hyperglycemia is the root cause of clinical diabetic complications. Prolonged exposure to hyperglycemia eventually leads to microvascular complications such as damage to the eyes (retinopathy), kidney (nephropathy), and nerves (neuropathy) (14). Hyperglycemia may also lead to macrovascular complications (large vessel diseases) such as heart disease and stroke (14). Proper management of blood sugar level is critical. One of the major metabolic defects that contribute to hyperglycemia is uncontrolled glucose production (gluconeogenesis) from the insulin-resistant liver.

1.2.1.1.2 Obesity

Obesity is the sixth most influential risk factor contributing to the overall burden of disease worldwide (15). In fact, roughly 1.4 billion adults, 20 years and older, are overweight, and these numbers are only increasing (16). Being overweight is a medical concern because it can seriously affect a person's health. Obesity can increase the risk of developing cardiovascular

diseases (i.e. hypertension, atherosclerosis, ischemic heart disease) as well as cancer (i.e. liver, pancreas, gall bladder, and prostate cancer) (15).

2.0 Hydrogen sulfide (H_2S)

Hydrogen sulfide (H_2S) is the most recent addition to the gasotransmitter family, including nitric oxide (NO) and carbon monoxide (CO). These gasotransmitters are small molecules of gas that has the remarkable ability to freely diffuse through a cell membrane to induce an array of intracellular signaling responses (17-19). Their production and metabolism are enzymatically regulated, and chemical donors can duplicate the effects of the gasotransmitters.

H_2S is regarded to have physiological importance in the cardiovascular, neuronal, immune, renal, respiratory, gastrointestinal, reproductive, and endocrine systems. H_2S carries out its physiological function by targeting membrane ion channels, proteins, enzymes, and transcription factors (17; 18; 20). The key mechanism by which H_2S may carry out these effects is through the *S*-sulfhydration of proteins by converting cysteine-SH groups to –SSH (20). Indeed, H_2S can *S*-sulfhydrate about 10-25% of liver proteins, including actin, tubulin, and glyceraldehyde-3-phosphate dehydrogenase, under physiological conditions (20). This suggests that post-translational modification by H_2S may be an important signaling mechanism in the cardiovascular system (18).

The pursuit of determining the endogenous level of H_2S is by far one of the most controversial issues in the H_2S field. In the blood or plasma, H_2S level has been reported to be above 35 μM in several species, such as rat, mouse, or human (21-23). In brain tissue, H_2S was detected in the range of 50–160 μM. These measurements of detecting H_2S are based upon the methylene blue method; this is most common assay used that relies on trapping H_2S with zinc

followed by acidification, which is then measured spectrophotometrically. However, this method of H_2S detection involves harsh conditions that release bound sulfide from proteins and amino acids; hence, caution should be used when interpreting these results. Thankfully, advancements have been made where more sensitive methods (gas chromatography and polarographic H_2S sensor) can accurately measure free H_2S concentrations (as low as 14 nM), without releasing stored sulfide (24-26). Despite this, there is still uncertainty about the exact level of endogenous H_2S level in mammalian biological tissues.

2.1 Biochemistry of H_2S

H_2S is a colorless, flammable gas with the classic odor of rotten eggs. Our nose is so sensitive to the smell of H_2S that we can detect it as low as 0.02 ppm (27). H_2S has a small molecular weight of 34.08 and is highly lipophilic; because of this, H_2S easily diffuses through the phospholipid bilayer of a cell membrane to carry out its signaling effects. Once in solution, H_2S can dissociate into H^+ and hydrosulfide anion (HS^-), which can further dissociate to H^+ and sulfide anion (S_2^-) as demonstrated by the following reaction: $H_2S \leftrightarrow H^+ + HS- \leftrightarrow 2H + S_2^-$. The pKa_1 is sensitive to both temperature and ionic strength. Essentially, there is no S_2^- in biological tissues, only H_2S and HS^-, due to a pKa_1 6.5 and a pKa_2 >17. Approximately 20% H_2S/80% HS^- exists in the extracellular fluid and plasma at 37˚C and pH 7.4. Since all three chemical species of dissolved H_2S are present in an aqueous solution, it is difficult to assess which is the biologically active one. Therefore, it is a common practice to associate the sum of all free sulfide concentrations as H_2S.

Not only is H_2S highly lipophilic, but it is also very volatile. With a vapor pressure of 18.75 x 10^5 Pa, H_2S evaporates relatively easy from water into air. Therefore, once in contact

with air, biological samples will begin to lose free H_2S. In fact, it was determined that the sulfide concentration in cell culture medium exhibits a signal exponential decay with a halftime of 6.2 minutes (28; 29).

2.2 Formation of H_2S

Mammalian cells generate H_2S either through enzymatic or non-enzymatic production. The non-enzymatic pathway accounts for a small portion of H_2S production (~10%). The majority of H_2S is synthesized by four enzymes that endogenously produce H_2S under tightly regulated conditions. They are cystathionine γ-lyase (CSE; EC 4.4.1.1), cystathionine β-synthase (CBS; EC 4.2.1.22), cysteine aminotransferase (CAT: EC 2.6.1.3) and β-mercaptopyruvate sulfurtransferase (MST; EC 2.8.1.2) (Figure 1-4). All four enzymes are involved in the reverse transsulfuration pathway.

2.2.1 Enzymatic synthesis of H_2S

2.2.1.1 The pyridoxal-5´-phosphate-dependent enzymes

2.2.1.1.1 CSE

CSE is a pyridoxal 5'-phosphate (PLP; the active form of vitamin B_6)-dependent enzyme that catalyzes the conversion of cystathionine to cysteine in the reverse transsulfuration pathway (Figure 1-4). The main substrate of CSE is $_L$-cysteine, which is made available from alimentary sources or endogenous proteins (30). This non-essential amino acid can also be synthesized from $_L$-methionine through the reverse transsulfuration pathway, which uses homocysteine (Hcy) as an intermediate (30).

Interestingly, CSE is expressed in a tissue-specific manner. For example, CSE is the dominate H_2S-producing enzyme in the liver and kidney (22; 31; 32), pancreas (33), as well as in vascular smooth muscle cells (VSMCs) (23; 34; 35). CSE is also expressed in the respiratory system (36; 37). Whereas CSE is mainly expressed in the cardiovascular system, small amounts of CSE mRNA have been found in the brain (38). The CSE inhibitors, $_{D,L}$-propargylglycine (PPG) and β-cyano-L-alanine, had no effect on the production rate of H_2S in the brain (39), but were able to suppress H_2S generation in the liver and kidney (40). Thus far, CSE is the dominant H_2S-producing enzyme in the peripheral nervous system, but not the central nervous system (CNS) (38; 41).

To date, CSE activity has only been detected in the cell cytosol. Ogasawara *et al.* (1994) (42) reported that CSE activity was mainly detected in the cytosolic fractions of both liver and kidney. Fu *et al.* (2012) (43) also showed that CSE is localized only in the cytosol in VSMCs under resting conditions; however, once the VSMCs were exposed to hypoxic conditions, CSE translocated from the cytosol to the mitochondria, thus increasing ATP production. Thus, under specific stimulations, CSE can translocate from the cytosol to the mitochondria to help the body cope under stressful conditions.

Human mutations in the CSE gene may increase the development of certain metabolic disorders such as hypercystathioninemia, bladder cancer, and atherosclerosis (44).

2.2.1.1.2 CBS

Like CSE, CBS is also PLP-dependent enzyme and is the predominant H_2S-producing enzyme in the CNS, and it too is localized in the cytosol (45). Recently, our laboratory has shown that CBS is also located in hepatocyte mitochondria under physiological conditions; whereby,

ischemia/hypoxia conditions increased the accumulation of CBS proteins in mitochondria (46). CBS generates H_2S through the condensation of Hcy and serine in the following well-known reaction: $_L$-serine + $_L$-Hcy ↔ $_L$-cystathionine + H_2O (Figure 1-4). Additionally, CBS catalyzes the condensation of cysteine with Hcy to produce cystathionine and H_2S (47). As such, CBS overwhelmingly catalyzes the formation of H_2S from cysteine + Hcy (~96%), whereas cysteine alone accounts for only 1-3% (48).

CBS is the major H_2S-generating enzyme in the CNS where its protein is highly expressed in the hippocampus and cerebellum in the brain (39; 49). Studies have also shown that CBS is expressed in astrocytes (50) and neurons (51). In the cardiovascular and respiratory system, CBS expression is either rare or absent (18).

2.2.1.1.3 CAT/MST

Recently, a new H_2S-generating enzymatic system has been identified as CAT/MST, which was shown to generate H_2S in both the brain (52) and endothelium (53). This unique pathway requires 3-mercaptopyruvate, which is produced by CAT from cysteine and α-ketoglutarate, as a precursor for MST-generated H_2S production (Figure 1-4). Both CAT and MST have been detected in the cytosol and mitochondria (18). However, only under high alkaline conditions (pH 9.7) and high cysteine concentration is the CAT/MST system observed, whereas under more physiologically relevant conditions (2 mM cysteine and pH 7.4), the CAT/MST system failed to produce H_2S in rat liver and kidney (40). Moreover, the existence of 3-mercaptopyruvate has yet to be determined in cells. How the CAT/MST system contributes to the physiological regulation of H_2S remains to be determined.

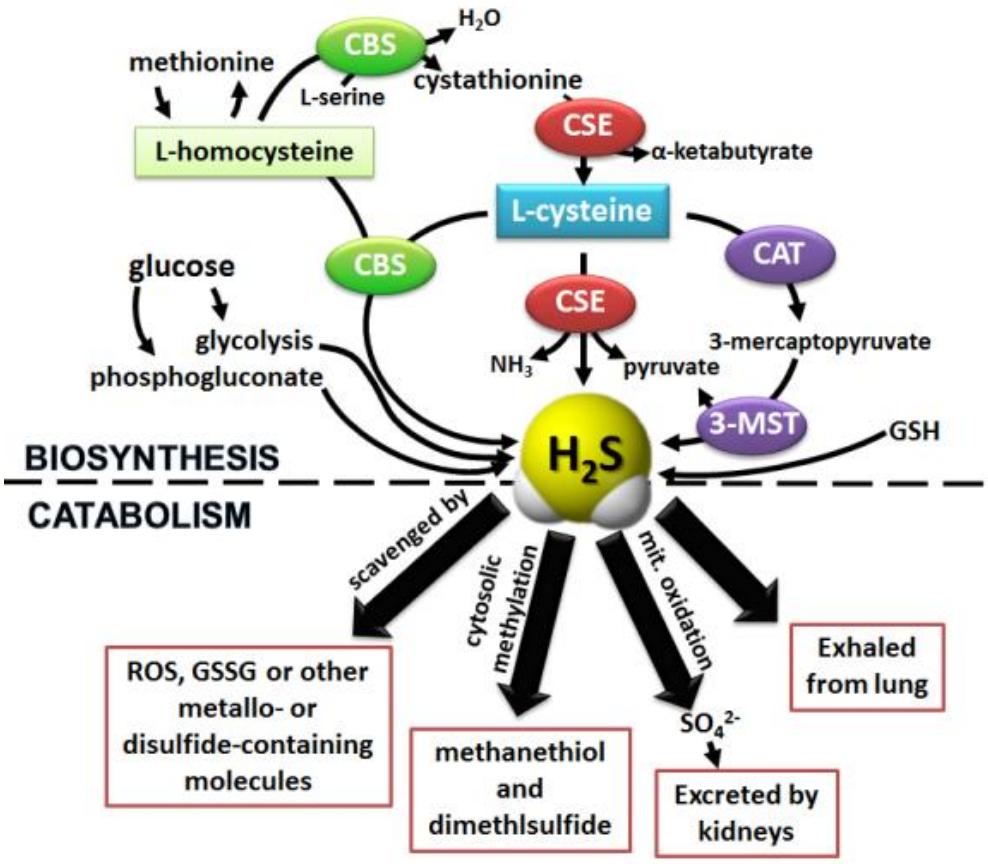

Figure 1-4: Biosynthesis and catabolism of H_2S. Two mechanisms endogenously synthesize the gasotransmitter H_2S: enzymatically *via* CSE, CBS, and CAT/MST; and non-enzymatically *via* reducing equivalents of glucose. The intracellular level of H_2S is maintained by H_2S scavenging, cytosolic methylation, mitochondrial oxidation, and/or exhalation from lungs. Adopted and modified from Mani *et al.* (2014) (54).

2.2.2 Non-enzymatic synthesis of H_2S

The non-enzymatic generation of H_2S is a less significant source of H_2S, but nonetheless, it is an area of fascination (55). This pathway generates H_2S *via* the reduction of elemental sulfur produced from the reducing equivalents of oxidized glucose that occurs during glycolysis (55). Moreover, to a lesser extent of H_2S production, the phosphogluconate pathway was also observed to produce H_2S through a non-enzymatic mechanism in erythrocytes (55). How these

pathways are influenced under physiological and pathophysiological conditions remains to be seen.

2.3 Catabolism of H_2S

To maintain proper physiological balance of H_2S, the mammalian system has developed four major routes of H_2S elimination. These elimination mechanisms include oxidation, methylation, scavenging, and expiration and excretion as described below and depicted in Figure 1-4.

2.3.1 Oxidation

Oxidation is the most important mechanism by which the body rids itself of excess H_2S (Curtis (24; 56; 57). The oxidation of H_2S mainly occurs in the liver; however, all cells in the body are capable of this process (24; 58). Indeed, even plasma can oxidize H_2S (56). The mitochondria are very effective in oxidizing sulfides with the help of reduced glutathione (GSH) acting as an intermediate. The mitochondrion first oxidizes H_2S to thiosulfate, which is later converted to sulfite and sulfate by sulfite oxidase (58). Finally, the metabolized sulfates are excreted in the urine as either free or conjugated sulfates.

2.3.2 Methylation

As oxidation occurs in mitochondria, methylation of H_2S happens in the cytosol. This catabolic pathway methylates H_2S to methanethiol and dimethyl sulfide by S-methyltransferase in the cytosol (59). In comparison to oxidation, H_2S methylation is slow. For example, in colonic mucosa, sulfide methylation is ~10,000 times slower than the oxidation rate of H_2S (60).

2.3.3 Scavenging

H_2S can be scavenged by methemoglobin (17), as well as metallo- or disulfide-containing molecules including horseradish peroxidase-catalase and oxidized glutathione (GSSG) (61; 62). Hemoglobin acts as a "sink" for H_2S in the blood stream, which may compete with the other gasotransmitters, NO and CO, for binding (17). The binding of one gasotransmitter to hemoglobin could affect the binding probability of other gasses, thus affecting their bioavailability (17). These three gasses not only compete with each other for binding sites on hemoglobin but also with oxygen, thus contributing to their toxicity on high exposure.

2.3.4 Expiration and Excretion

Occasionally, the lungs provide an elimination route for H_2S. In healthy individuals, very little H_2S is eliminated through the lungs, likely because alveolar air (end expiration) only contains 25–50 ppb H_2S (63; 64). Insko *et al.* (2009) (65) demonstrated that when rats received intravenous injections of sodium sulfide (Na_2S), an H_2S donor, a significant amount of exhaled H_2S was detected.

3.0 Physiological properties of H_2S

The effects of H_2S are well documented to be biphasic, mainly due to the wide range of H_2S concentrations used. At low concentrations (nM to ~<100 μM), H_2S was demonstrated to be cytoprotective *via* acting as an antioxidant and anti-inflammatory agent, whereas at high concentrations (~>100 μM to mM) H_2S becomes an oxidant and a pro-inflammatory agent, as well as an inhibitor of insulin secretion from pancreatic β-cells.

3.1 Cytoprotective effects of H_2S

3.1.1 Vasorelaxant

For more than a decade, there have been numerous findings linking H_2S to BP regulation (17; 23; 66; 67). The first experimental evidence that suggests H_2S to be a vasorelaxant was demonstrated by Zhao *et al.* (2001) (23). These authors showed that i.p. injections of H_2S produced a concentration-dependent decrease in the arterial BP in anesthetized Sprague-Dawley (SD) rats. This vasorelaxant effect of H_2S was likely due to the opening of K^+-dependent-ATP (K_{ATP}) channels. The K_{ATP} channels are inward rectifying channels and composed of two types of subunits, such as the inwardly rectifying K^+ channel subunits (Kir6.1 or Kir6.2) and the larger regulatory sulfonylurea receptors (SUR1, SUR2A, and SUR2B). The opening of the K_{ATP} channels hyperpolarizes the cell membrane that closes the voltage-dependent Ca^{2+} channels and reduces intracellular Ca^{2+} levels. Ca^{2+} plays a fundamental role in the contractile responses of VSMCs, where a low Ca^{2+} level results in vasodilation. Zhao *et al.* (2001) reported that H_2S was mimicked by pinacidil (a K_{ATP} channel opener) and attenuated by glibenclamide (a K_{ATP} channel blocker) in SD rats (23), which was consistent with other findings (68; 69). Other molecular mechanisms that H_2S was shown to induce vasorelaxation included induction of intracellular acidosis (70), depletion of intracellular ATP levels (71; 72), inhibition of phosphodiesterase (PDE) (73) and modulation of intracellular Ca^{2+} levels (74; 75).

More conclusive evidence was brought forth when Rui Wang and associates (2008) (41) generated mice with the knockout of the gene encoding CSE, which resulted in these mice becoming hypertensive (41). At seven weeks of age, both male and female CSE knockout (KO) mice exhibited significantly higher BP readings than their age-matched WT counterparts, which increased further in an age-dependent fashion (41). At twelve weeks of age, male CSE-KO mice

exhibited 135 mm Hg, which was about 18 mm Hg higher than the WT mice (41). Furthermore, intravenous bolus injections of sodium hydrosulfide (NaHS; an H_2S donor) decreased systolic BP in both CSE-KO and WT; however, the magnitude of decrease was greater in the CSE-KO mice, suggesting enhanced sensitivity of H_2S stimulation (41). The H_2S/CSE system was likely responsible for the age-dependent increase in BP in the CSE-KO mice because H_2S level in the brain and endothelial NO synthase (eNOS) protein was unchanged, administration of $_L$-methionine did not increase BP, and the kidney architecture was preserved (41). These CSE-KO mice also developed impaired endothelium-dependent vasorelaxation upon methacholine (an endothelium-dependent vasorelaxant) administration in mesenteric arteries, which were pre-constricted with phenylephrine (41). These exciting observations points to the possibility that H_2S may be the next endothelium-derived relaxing factor (EDRF) in the cardiovascular system (41; 76).

3.1.2 Antioxidant

Excessive reactive oxygen species (ROS) promotes oxidative stress in the cell. H_2S is a strong reducing agent, giving it the capacity to interact with ROS. Numerous studies have shown that low concentrations of exogenously applied H_2S (approximately 10-100 μM) can have antioxidant properties (34; 69; 77-80). H_2S was demonstrated to increase intracellular levels of the potent antioxidant GSH in VSMCs (34), primary cortical neurons (79) and in HT22 immortalized hippocampal cells (78). H_2S increases GSH level *via* enhancing the enzymatic activity of γ-glutamylcysteine synthetase, leading to increased cellular γ-glutamylcysteine level; the latter being a precursor for $_L$-cysteine production and thus GSH production (78; 79). Studies also

showed that H_2S can increase cysteine/glutamate antiporter (xc-system) activity, thereby increasing available cysteine for glutamate production.

By either increasing GSH levels or directly scavenging ROS, NaHS (30 and 50 μM) was shown to ameliorate Hcy-induced peroxynitrite ($ONOO^-$), hydrogen peroxide (H_2O_2) or superoxide anion (O_2^-) generation in rat VSMCs (77). The same authors showed that NaHS enhanced the inhibitory effects of various antioxidants, including GSH, $_L$-NAME, and superoxide dismutase (SOD) on Hcy-induced ROS production. In a subsequent study, NaHS (50 μM) attenuated methionine-induced cell death, and decreased both Hcy level and ROS production in bEnd3 (a mouse brain endothelial cell line) (81). This group also showed that NaHS enhanced the antioxidant effects of GSH, SOD, and catalase on methionine-induced ROS production in bEnd3 cells.

3.1.3 Anti-inflammatory

The response and effect of inflammation and its regulators are complex in nature. Activated endothelial cells that line the arteries release pro-inflammatory cytokines into the bloodstream (54). These pro-inflammatory cytokines promote the attachment, adherence, and spreading of mononuclear cells (i.e. macrophages, neutrophils) onto the luminal surface of the arterial walls, allowing their infiltration into the VSMC mass and to the source of infection/aggravation (54).

H_2S has been shown to reduce inflammation by acting through various pathways. Sulfide-releasing diclofenac derivative decreased tissue neutrophil infiltration and interleukin (IL)-1β levels, upregulated IL-10 level, and suppressed the activation of NF-κB in an endotoxin-induced lung and liver inflammation model (82). In fact, many studies suggest that the anti-inflammatory effects of H_2S are mediated *via* downregulating the expression of pro-

inflammatory cytokines (i.e. tumor necrosis factor (TNF)-α, interferon-γ, IL-12, and IL-23) (83; 84). Additionally, H_2S was shown to decrease leukocytes rolling velocity (85) as well as to induce the apoptosis of neutrophils and promote macrophage differentiation toward an anti-inflammatory phenotype (86). Subsequently, H_2S was shown to exert protective effects in animal models of inflammation and inflammation-generated pain (30; 85).

3.2 Deleterious effects of H_2S

3.2.1 Inhibition of cellular respiration

H_2S has a strong affinity for cytochrome c oxidase, a key factor in the electron transport chain (ETC) in the mitochondrion. Due to its high chemical reactivity, H_2S inhibits cellular respiration *via* binding to the copper center of cytochrome c oxidase (a fundamental component of mitochondrial respiratory chain complex IV); resulting in the attenuation of cellular oxygen consumption (87) (the subunits and complexes of the ETC are discussed below in section 3.4.2). Once the catalytic activity of cytochrome c oxidase is blocked, aerobic metabolism is arrested (88). In the extreme case, if an individual inhales a fatally high dose of H_2S (500-1000 ppm), cytochrome c oxidase will be inhibited in the brain, reducing oxygen uptake into cells and inhibiting the reuptake of $_L$-glutamate (an excitatory neurotransmitter), ultimately leading to death (89).

3.2.2 Pro-inflammatory

Although H_2S was shown to exert anti-inflammatory effects in models of inflammation and inflammation-related pain, other studies have contradicted these observations. One study demonstrated that H_2S injection upregulated leukocyte attachment and rolling blood vessels as

well as increased the intercellular adhesion molecule-1 expression level in sepsis mice, an effect that was attenuated by PPG supplementation (82). Also, H_2S administration increased the production of the pro-inflammatory cytokines, TNF-α, IL-1β, and IL-6, *via* activating ERK-NF-κB signaling pathway in human monocytes (90). Another group showed that NaHS (500-1000 μM) increased the generation of pro-inflammatory cytokines (i.e. TNF-α, IL-1β, and prostaglandin E_2); however, when macrophages were treated with lower concentrations of NaHS (100-500 μM) anti-inflammatory cytokines were upregulated. The authors of this study suggest that the effects of H_2S on inflammation are dependent on the H_2S concentrations used and the rate of H_2S generation within the macrophages (91).

3.2.3 Inhibition of insulin secretion

3.2.3.1 Activation of K_{ATP} channels in pancreatic β-cells

A large body of evidence suggests that H_2S is an endogenous modulator of insulin secretion from pancreatic β-cells (33; 92-96). This phenomenon is mainly due to H_2S-stimulated activation of K_{ATP} channels on the insulin-secreting cells, including INS-1E (100 μM NaHS) (92) and HIT-T15 (100 μM H_2S) (93). H_2S interrupts insulin secretion by activating K_{ATP} channels, which prevents depolarization of the plasma membrane and the entry of Ca^{2+} into pancreatic β-cell. For instance, 10 μM glibenclamide (a K_{ATP} channel blocker) prevented 100 μM NaHS-induced inhibition of insulin secretion from HIT-T15 cells (93). Another study demonstrated that $_L$-cysteine and NaHS reduced the intracellular Ca^{2+} level and ATP generation, which consequently attenuated insulin release in both isolated mouse islets and MIN6 cells (a mouse pancreatic β-cell line) (97).

3.2.3.2 Induced apoptosis of pancreatic β-cells

Another mechanism by which H_2S blocks glucose-stimulated insulin secretion is by inducing apoptosis of β-cells. For example, Yang *et al.* (2007) (96) showed that by activating the p38 MAPK pathway and upregulating BiP and CHOP (both indicators of ER stress), overexpression of CSE induced apoptosis of INS-1E cells. Furthermore, knocking down CHOP ameliorated H_2S-induced apoptosis of INS-1E cells (96). Cao and colleagues (2006) (98) reported that supplementation of 10 μM NaHS for 3 hours induced phosphatidylserine externalization (an indicator of the early stages of apoptosis) in isolated pancreatic acinar cells (exocrine cells that aids in digestion) (98). This group also demonstrated that H_2S-induced apoptosis of acinar cells occurred mainly *via* activation of both the mitochondrial and death receptor pathways.

However, similar to the controversial effects of H_2S on inflammation, one group showed that H_2S treatment prevented apoptosis and, in fact, protect insulin-secreting cells from oxidative stress. Kaneko *et al.* (2009) (95) reported that 3 mM $_L$-cysteine and 100 μM NaHS prevented glucose-induced apoptosis of isolated mouse pancreatic β-cells and increased total glutathione level. Pancreatic β-cells are highly susceptible to glucotoxicity due to their weak antioxidant defense mechanisms (99). Therefore, an increase in total glutathione levels would assist in preserving β-cell function. Treatment with 2 mM $_{DL}$-propargylglycine (PAG; a CSE inhibitor) abrogated the cytoprotective effects of $_L$-cysteine against glucose-induced apoptosis of β-cells (95). These discrepancies of the effects of H_2S on apoptosis could be due to different treatments used; for instance, $_L$-cysteine (95) is known to upregulate GSH, a well-known antioxidant, whereas the direct effects of H_2S could be toxic (96; 98). Also, due to the biphasic nature of H_2S, the effects of low concentrations (50 μM) *vs.* high concentrations (100 μM) of H_2S on pancreatic β-cells need to be elucidated. Data obtained from experiments using 100 μM or

higher of NaHS/H_2S must be viewed with caution and their pathophysiological implications questioned.

3.3 H_2S-releasing drugs

In response to the biological importance of H_2S, novel therapeutics aimed to deliver H_2S or to suppress its endogenous production are currently being investigated on a world-wide scale. For stance, ATB-346 (produced by Antibe Therapeutics) is an H_2S-releasing nonsteroidal anti-inflammatory drug (NSAID) derivative and is currently being studied in the treatment of osteoarthritis (86; 100). Its Phase I clinical trials was recently completed in healthy volunteers (100). NBS-1120 (patented by a group at the City University of New York, USA) is an NSAID linked to both NO- and H_2S-releasing moieties and is currently in preclinical trials to test its effectiveness in various animal models of cancer (101; 102). Moreover, preclinical studies have confirmed that SG-1002 (developed by SulfaGENIX in New Orleans, Louisiana, USA) decreased infarct size, improved cardiac function, increased angiogenesis, decreased inflammation, and downregulated oxidative stress after infarction in animal models of heart failure (ClinicalTrails.gov identifier: NCT02278276). Lastly, the most widely studied H_2S-releasing drug is GYY4137 (produced by Moore *et al.* at the National University of Singapore). GYY4137 is a valuable tool to measure the effects of H_2S because it allows the slow release of H_2S. GYY4137 was demonstrated to exhibit antihypertensive action in spontaneously hypertensive rats (SHRs) (103) as well as reduce inflammation *via* reducing circulating levels of various pro-inflammatory cytokines and mediators (104). Needless to say, H_2S-based therapies have a promising future due to the success seen in preclinical and early clinical testing.

3.4 H_2S and glucose regulation

3.4.1 H_2S-regulated induction of hepatic glucose output and utilization

Among many endogenous substances that regulate glucose production is H_2S (22; 105; 106). Only recently was the role of H_2S in hepatic glucose production explored in detail by our laboratory. Zhang *et al.* (2013) (105) demonstrated that both exogenous and endogenous H_2S inhibited glucose uptake and utilization in $HepG_2$ cells and primary hepatocytes isolated from WT and CSE-KO mice, respectively. H_2S-mediated impairment of glucose uptake was dependent upon its ability to attenuate AMP-activated protein kinase (AMPK) phosphorylation (Thr172), which was reversed *via* treatment of an AMPK activation reagent in $HepG_2$ cells (105). AMPK is a pivotal regulator of energy homeostasis, whereby its stimulation hampers hepatic glycogenolysis and gluconeogenesis and induces the uptake and utilization of glucose in liver cells (6; 107; 108). Lower AMPK activity likely contributed to higher hepatic glycogen content in CSE-KO liver tissues compared to WT liver tissues in the fed state. Furthermore, we found that primary liver cells isolated from CSE-KO mice produced less glucose compared to isolated WT hepatocytes, a phenomenon that may be dependent on H_2S-mediated increase in PEPCK activity (105). Lastly, we observed that insulin inhibited CSE expression, and exogenous H_2S decreased insulin-stimulated phosphorylation of Akt in $HepG_2$ cells. Overall, this study was the first to suggest that H_2S plays a pivotal role in regulating insulin sensitivity and glucose metabolism in liver cells.

In another study, we found that PC, one of the rate-limiting gluconeogenic enzymes, is also involved in H_2S-mediated glucose production in liver cells (109). Supplementation of NaHS or CSE overexpression increased PC activity (*via* *S*-sulfhydration) in $HepG_2$ cells and mouse primary liver cells. In fact, mutation of PC (Cys 265) diminished H_2S-induced PC *S*-

sulfhydration, and thus its activity, in $HepG_2$ cells. In agreement, PC overexpression increased glucose production, whereas its knockdown abolished H_2S-simtulated glucose production in $HepG_2$.

Taken together, it is clear that H_2S plays a fundamental role in hepatic glucose regulation. Knowing that H_2S stimulates *pgc-1α* gene expression (22), and the role PGC-1α has in regulating both hepatic gluconeogenesis (105; 109) and mitochondrial homeostasis, implies that H_2S may stimulate hepatic glucose production through other mechanisms. It seems we are merely scratching the surface of fully understanding the role H_2S plays in regulating hepatic glucose production

3.4.2 H_2S-mediated induction of hepatic mitochondrial energy production

Mitochondria are unique organelles in the cell where they are surrounded by a double-layer membrane and retain their own small genome (mtDNA). The majority of mitochondrial proteins are encoded in the nucleus, synthesized in the cytosol and then transported into the mitochondrion for mitochondrial biogenesis. There are roughly 300-400 mitochondria in a cell (110). Mitochondria produce the bulk of cellular energy by coupling cellular respiration to the production of ATP (also known as oxidative phosphorylation) (Figure 1-5).

For years, the toxic biological actions of H_2S have been known (62). At toxic concentrations, H_2S binds to cytochrome c oxidase, thus preventing the binding of oxygen and inhibiting the ETC (as mentioned in section 3.2.1) (111). However, recent research suggests that low concentrations of H_2S may, in fact, hold a physiological role in normal mitochondrial function, for example, to serve as an inorganic electron donor to promote ATP production.

H_2S is endogenously produced in the mitochondrion by all known H_2S-generating enzymes, CSE (43), CBS (46; 112), and MST (40; 52; 113; 114). In 2007, Goubern *et al.* (115) suggested that exogenously applied H_2S can act as an electron donor as well as an inorganic source of energy in mammalian cells. Treatment with chemical H_2S donors of Chinese hamster ovary cells overexpressing sulfide:quinone oxidoreductase (SQR), a complex II-related protein, resulted in increased cellular oxygen utilization and ATP production (115-117). Additionally, Módis *et al.* (2013a) (113) demonstrated that SQR has the capacity of oxidizing H_2S (Figure 1-5). Oxidation of two H_2S molecules leads to the donation of two electrons to SQR, whereby the electron travels to complex II and passed through the ETC. As a result, this fosters mitochondrial ATP generation, supporting cellular bioenergetics, and maintaining cellular viability. In fact, H_2S demonstrates a biphasic effect here, where low concentrations of H_2S (0.1–1 μM) increase mitochondrial function (i.e. ATP production, oxygen consumption rate) in isolated murine liver mitochondria while higher concentrations (3–30 μM) were inhibitory (113). Silencing MST or SQR reduced mitochondrial function and ATP production in murine hepatocytes (113). In fact, the functional effect of H_2S just may be comparable to tricarboxylic acid cycle (TCA)-derived electron donors, such as NADH or $FADH_2$ (113; 118). Additionally, Fu and colleagues (2012) (43) demonstrated that by sensing mitochondrial oxygen level, cytosolic CSE translocates into the mitochondria to promote H_2S generation, which increases mitochondrial ATP production under hypoxic conditions in VSMCs. Therefore, on the basis of the results of Fu *et al.* (2013) (43) and from previous studies (113; 115-117), endogenous H_2S plays a physiological role in the maintenance of cellular bioenergetics (Figure 1-5). Indeed, the functional importance of H_2S may become ever greater as a backup source of electrons under conditions in which TCA-derived electron donors are diminished (113).

3.4.3 H_2S, insulin resistance, and diabetes

The pathophysiological role of H_2S has been extensively studied in both high-fat diet (HFD)-induced insulin resistance and T1DM and T2DM animal models. Expression levels of both CSE and CBS are higher in the liver (119-122) and pancreas (33; 119) of streptozotocin (STZ)-induced rats (119-122), or Zucker diabetic fatty (ZDF) rats (33). For instance, Yusuf *et al.* (2005) (119) showed that both CSE- and CBS-H_2S generating enzymes were elevated in liver and pancreas tissues from STZ-treated rats, abnormalities that were later reversed with insulin treatment (8 U/kg, subcutaneously for 5 days). Jacobs *et al.* (1998) (122) also demonstrated that the activities of both CBS and CSE

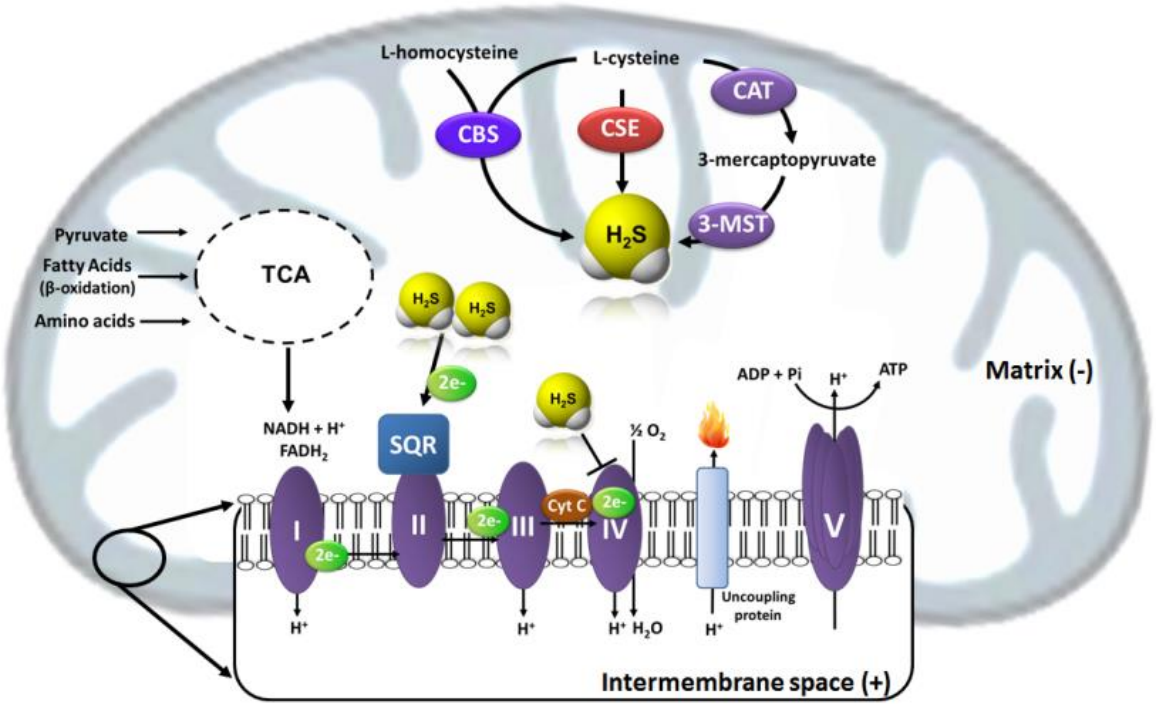

Figure 1-5: The ETC and the regulatory role H_2S plays in maintaining cellular bioenergetics. The ETC consists of complexes I-IV and it exists in the inner mitochondrial membrane. NADH and $FADH_2$, acquired from the tricarboxylic acid cycle, TCA, donate high energy electrons to pass along the ETC. The purpose of the ETC is to pump H^+ protons from the mitochondrial matrix into the intermembrane space to generate a chemiosmotic gradient across

the inner membrane. This electrochemical gradient is what powers complex V, also known as ATP synthase, to catalyze the synthesis of ATP from ADP + Pi. At the end of the ETC, the final electron acceptor is oxygen, and this ultimately forms water. Low concentrations of H_2S aids in the production of ATP *via* donating electrons to SQR localized on complex II, whereas high concentrations inhibit Cyt C in complex IV thus obviating ATP generation. Cyt C: cytochrome c oxidase; e-: electron; ETC: electron transport chain; SQR: sulfide:quinone oxidoreductase; TCA: tricarboxylic acid cycle. Modified from Módis *et al*. (2015) (110) and Módis *et al.* (2013a) (113).

were significantly higher in the liver of STZ-treated rats; whereby insulin treatment also normalized the activities of these enzymes. On the contrary, Manna *et al.* (2014) (123) reported that CSE protein expression and its activity were both reduced in livers of STZ-treated rats, which was associated with higher ROS generation.

In regards to insulin resistance in the liver, Hwang *et al.* (2013) reported that the mRNA and protein levels of CBS and CSE are significantly higher in livers of mice fed with a high-fat diet (HFD), which resulted in a significant elevation of hepatic H_2S production (124). In agreement, Zhang *et al.* (2013) (105) showed that CSE expression was significantly upregulated in insulin-resistant $HepG_2$ cells (engineered *via* treatment with high levels of insulin (500 nM) and glucose (33 mM) for 24 hours) (105). However, Yu *et al.* (2015) demonstrated that both CSE expression and H_2S-mediated sulfhydration of PC were reduced in livers of mice fed with HFD (109). Additionally, other studies have found that H_2S biosynthesis is decreased in both liver (125; 126) and adipose tissue (127) of HFD-fed mice. These contradictory results may be due to different experimental conditions, severity of the disease, as well as different types of mouse genetic background, fat contents, the age of the animals, feeding periods, etc.

Numerous lines of research show a strong correlation between a high H_2S level and the deterioration of insulin secretion in pancreatic β-cells (33; 92; 93; 96; 97). As discussed in section 3.2.3.1, H_2S-mediated inhibition of insulin secretion is mainly accredited to its capability

to activate K_{ATP} channels in the insulin-secreting cell. Intriguingly, the biosynthesis of H_2S was shown to be upregulated in pancreas tissues from ZDF rats (33) and STZ-treated rats (119). Wu and colleagues (2009) (33) demonstrated that inhibition of pancreatic H_2S production in ZDF rats (*via* daily PAG i.p. injections for 4 weeks) significantly elevated serum insulin level and reduced hyperglycemia. Also, another study showed 10 μM of glibenclamide, an antidiabetic drug which inhibits K_{ATP} channels, abrogated 100 μM NaHS-mediated inhibition of insulin secretion from pancreatic β-cells (93). These data suggest that elevated levels of H_2S in pancreatic β-cells could be involved in a maladaptive mechanism of impaired insulin secretion. Interestingly, pancreatic CSE expression and H_2S production were significantly greater in ZDF rat than in Zucker fatty (ZF) or Zucker lean (ZL) rats (33). ZDF rats also had reduced serum insulin levels, hyperglycemia, and insulin resistance. On the other hand, serum insulin levels were much higher in ZF rats than in ZL rats, which may indicate lower pancreatic H_2S production. However, no difference was observed in H_2S production in pancreatic tissues from ZF and ZL rats (33). Therefore, the relationship between circulating insulin and glucose, and pancreatic H_2S production in the early or late stage of insulin resistance should be investigated further in different models of diabetes.

Contrary to an elevated H_2S level in the pancreas under diabetic conditions, H_2S level was shown to be lower in the circulation and endothelium layer. In fact, changes in H_2S homeostasis has been suggested to play a role in the pathogenesis of endothelial injury. Endothelial dysfunction is a well-documented complication of various forms of diabetes, prediabetes, as well as in atherosclerosis. Recently, Suzuki and colleagues (128) suggested that H_2S plays a protective role against hyperglycemic-induced endothelial dysfunction by attenuating mitochondrial-derived ROS production. Endothelial cells placed in elevated glucose conditions

exhibited accelerated H_2S consumption, which was attenuated by treatment with ROS scavengers or with mitochondrial uncoupling agents (128). Inhibition of H_2S production (by CSE siRNA silencing) exacerbated ROS production, whereas supplementation or overexpression of CSE reduced mitochondrial ROS production and protected endothelium cells from hyperglycemic-induced cell dysfunction (128). Moreover, supplementation of H_2S, *via* H_2S-releasing minipump, improved the endothelium-dependent relaxant responses of the thoracic aorta *ex vivo*, without affecting the degree of hyperglycemia in STZ-induced rats (128). A similar study also showed that H_2S treatment protected human umbilical vein endothelial cells against high glucose-induced apoptosis (129). Therefore, these observations indicate that supplementation/donation of H_2S may be used as a therapeutic approach to maintain diabetic blood vessel patency and to protect against the development of diabetic complications.

4.0 The PGC family

The PGC family consists of three members, PGC-1α, PGC-1β, and the most distant cousin, peroxisome proliferator-activated receptor γ coactivator-related protein (PPRC). PGC-1α is by far the most studied and well-known coactivator, whereas PPRC is the least understood. These coactivators are involved in regulating thermogenesis, gluconeogenesis, mitochondrial biogenesis, and cellular growth (130-132). All three PGC proteins contain leucine-rich motifs (133-135) and a conserved tetrapeptide motif (DHDY) (136-138) that enables interaction with two critical regulators of mitochondrial biogenesis, such as nuclear respiratory factor-1 (NRF-1) and NRF-2, respectively. Emphasis of this literature review will be placed on the ability of the PGC family to stimulate gluconeogenesis and mitochondrial biogenesis (Figure 1-6).

4.1 PGC-1α

As mentioned in section 1.1.2, in the fasted stated, glucagon and glucocorticoid are released into the bloodstream from pancreatic α-cells and the adrenal cortex, respectively, where these endocrine hormones act on hepatocytes to replenish the falling blood glucose level. Stimulation of the glucagon receptor results in the activation of adenylyl cyclase, an enzyme that catalyzes the conversion of ATP to cAMP. This secondary messenger activates protein kinase A (PKA) which then phosphorylates the cAMP response element binding protein (CREB; at Ser133). The latter enters the nucleus and binds to the consensus cAMP response element (CRE) site on the PGC-1α promoter (139; 140), thus increasing its transcription. Glucocorticoid also upregulates PGC-1α expression level *via* entering the hepatocyte and binding to its cytosolic receptor, whereby the glucocorticoid and glucocorticoid receptor (GR) complex enters the nucleus (141). Once inside the nucleus, the complex binds to the promoter region of the *pgc-1α* gene to induce transcription. Glucocorticoid and the cAMP/PKA pathways work synchronically to increase the expression level of PGC-1α in hepatocytes (Figure 1-6).

PGC-1α activity is regulated posttranscriptionally by sirtuin (SIRT) 1. During the fasting state, pyruvate and NAD^+ levels increase that lead to elevated SIRT1 protein level as well as its activity (142; 143). SIRT1 activates PGC-1α *via* deacetylation (142). It was suggested that PGC-1α undergoes cycles of acetylation and deacetylation during the fed and fasted states, which are dependent on SIRT1 activity (143). Little is known about the posttranslational modification of PGC-1β and PPRC, but it was speculated to also occur (144).

Recently, our laboratory has shown a link between endogenous and exogenous H_2S and PGC-1α expression level. Renal extracts from CSE-KO mice had decreased PGC-1α mRNA level compared to their respective WT controls (22). Treatment with 30 and 50 μM NaHS

significantly upregulated PGC-1α mRNA expression level, along with its downstream target, *fbpase*, in A-10 cells (a rat vascular smooth muscle cell line) (22). Interestingly, NO (145) and CO (146) were also shown to increase PGC-1α expression level in brown adipose tissues (145) and cardiac tissues (146). How this relationship between H_2S and PGC-1α correlates to hepatic glucose production remains to be seen.

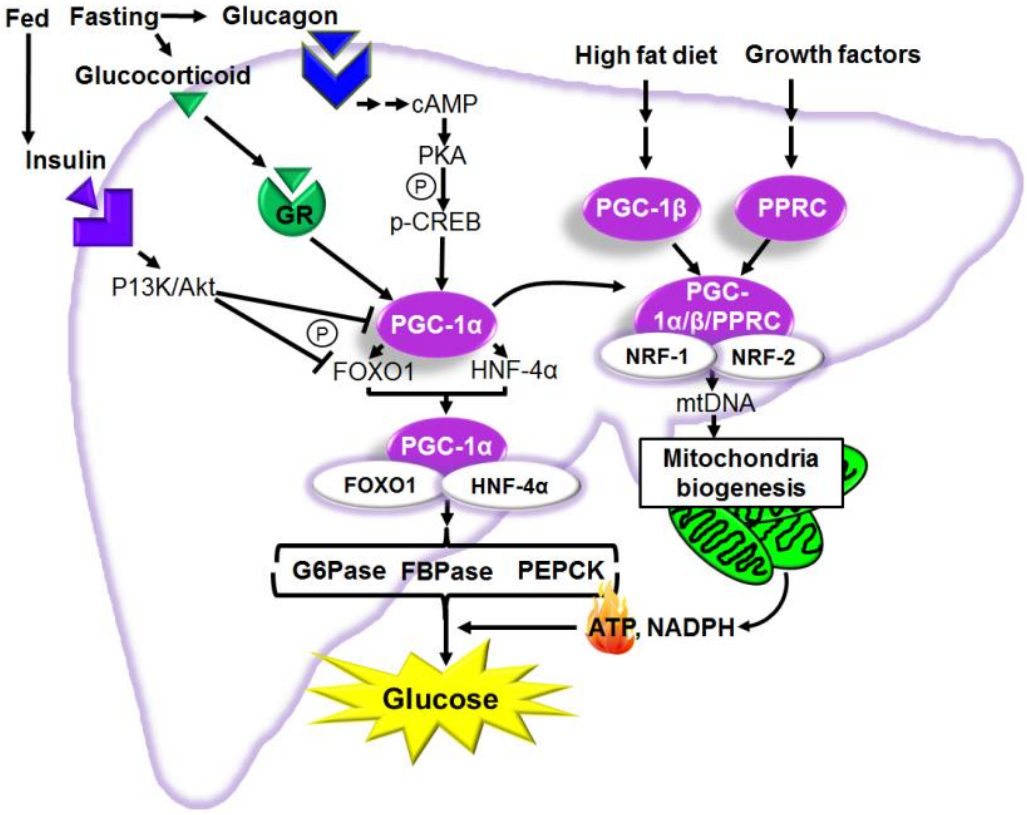

Figure 1-6: General overview of the PGC family in hepatic glucose production. PGC-1α induces the gene transcription of the rate-limiting gluconeogenic enzymes *via* coactivating and binding to specific transcription factors, FOXO1 and HNF-4α, in hepatocytes. All three members of the PGC family, PGC-1α, PGC-1β, and PPRC, stimulate mitochondrial biogenesis with help from NRF-1 and NRF-2. CREB: cAMP response element-binding protein; FOXO1: forkhead box protein O1; G6Pase: glucose-6-phosphatase; GR: glucocorticoid receptor; H_2S: hydrogen sulphide; HNF: hepatocyte nuclear factor; mtDNA: mitochondrial DNA; NRF: nuclear respiratory factor; P: phosphorylation; P13K/Akt: phosphatidylinositide 3-kinases/Akt signaling pathway; PKA: protein kinase A; PEPCK: phosphoenolpyruvate carboxykinase; PGC: peroxisome proliferator-activated receptor-γ coactivator; PPRC: peroxisome proliferator-activated receptor-γ coactivator related protein. Modified from Finck and Kelly (2006) (130).

4.1.1 PGC-1α stimulates hepatic gluconeogenesis

PGC-1α fires up hepatic gluconeogenesis in two ways: it directly upregulates the gene expression levels of the main rate-limiting gluconeogenic enzymes, *pepck*, *fbpase*, and *g6pase*; and it stimulates mitochondrial biogenesis and mitochondrial energy production to fuel the high energy demand of this pathway.

To upregulate the expression levels of the aforementioned genes, PGC-1α first coactivates hepatic nuclear factor (HNF)-4α and forkhead box protein O1 (FOXO1), by binding to their respective promoter regions and increasing their gene transcripts. Once the proteins of HNF-4α and FOXO1 are synthesized and are translocated back into the nucleus, PGC-1α protein then binds to these cognate transcription factors, producing a unique protein tirade. This protein complex has high specificity to bind to the promoter regions of *pepck*, *fbpase*, and *g6pase*, thus stimulating their gene transcription (132; 140; 147). Indeed, Yoon *et al.* (2001) (140) demonstrated that PGC-1α physically interacts with HNF-4α, specifically at the amino-terminal 190 amino acid of PGC-1α. Substitution of Leu 145 to Ala in the GST-PGC-1 (1-190 amino acids) eliminated the binding of PGC-1α to HNF-4α (140). Puigserver *et al.* (2003) (148) demonstrated that PGC-1α induction of gluconeogenic genes was blocked by a dominant-negative effect of FOXO1 in Fao hepatocytes (a rat hepatoma cell line); whereas transfection of a functional FOXO1 yielded opposite results. Also, through binding experiments, this group of researchers showed that FOXO1 binds to the carboxy-terminal part of PGC-1α (551-635 amino acids) and that PGC-1α interacts with the amino-terminal part of FOXO1 (1-300 amino acids) (148).

The production of glucose for systemic consumption requires ATP, and PGC-1α regulates this process with the aid of certain coactivators. Wu *et al.* (1999) (149) showed that

PGC-1α coactivates NRF-1 and NRF-2. These transcription factors regulate the expression of mitochondrial transcription factor A (Tfam), which is a nuclear-encoded transcription factor crucial for the replication, maintenance, and transcription of mitochondrial DNA (150; 151). This role for PGC-1α in mitochondrial biogenesis is supported by gain/loss of function studies in cells (149) and in mice (152-154). In fact, PGC-1α function is critical for the normal expression of mitochondrial genes; where the mRNA level of mitochondrial genes were dramatically reduced in skeletal muscle, heart, liver, brown fat, and brain of mice lacking the *pgc-1α* gene (153; 154). Leone *et al.* (2005) (153) demonstrated that the loss of PGC-1α function resulted in significant functional deficits in the oxidative metabolism in multiples tissues (i.e. skeletal muscle, heart, liver) and rendered PGC-1α KO mice exercise intolerant.

4.1.2 PGC-1α, insulin resistance, and T2DM

Abnormal PGC-1α function has been implicated in the pathophysiological development of glucose intolerance, insulin resistance, and T2DM in both human and animal studies. From human genetic variant studies, scientists have identified a polymorphism in the coding region of the *pgc-1α* gene (Gly482Ser) which is associated with an increased risk of T2DM (155-158). The Gly482Ser gene variant showed a 1.34-fold increase risk of T2DM development among Danish Caucasians (158) and a significant association among middle-aged Japanese men (155). In contrast, other groups dispute this claim (159; 160) in that the Gly482Ser variant did not predict diabetes in French Caucasians (159) nor in Pima Indians (161). However, these studies were carried out in single populations. The most compelling evidence came from Andrulionytè *et al.* (2004) (157) when they used a mixed population of 770 participants (387 men and 383 women) with prediabetes enrolled in STOP-NIDDM (Study To Prevent Non-Insulin Dependent

Diabetes Mellitus). This group found that the Gly482Ser variant in the *pgc-1α* gene was associated with a 1.6-fold higher risk for diabetes. The authors also found a correlation between treatment with the anti-diabetic drug, acarbose (acts by slowing the conversion of carbohydrates into glucose in the GI tract) and genetic variation. For instance, Andrulionytè *et al.* (2004) (157) showed that acarbose treatment significantly reduced the risk of T2DM development among prediabetic carriers of the Gly482Ser variant.

In animal studies, PGC-1α activity was abnormally upregulated in the diabetic liver, potentially contributing to increased hepatic glucose production and thus hyperglycemia (140; 148; 162-164). Liver-specific overexpression and knockdown strategies showed that PGC-1α orchestrates hepatic glucose production, hepatic insulin resistance, and glucose overproduction (139; 140; 148; 162). In fact, Koo *et al.* (2004) (162) proposed that PGC-1α induced hepatic insulin resistance by stimulating TRB-3 activity, a potent inhibitor of Akt signaling, thus interfering with insulin signaling in hepatocytes. This group found that PGC-1α and TRB-3 protein expression levels were upregulated in liver tissues from both *db/db* and liver-specific insulin receptor knockdown (LIRKO) mice. Injection of an adenovirus expressing PGC-1α iRNA decreased both PGC-1α and TRB-3 expression levels in *db/db* and LIRKO mice, as well as improved glucose tolerance in *db/db* mice (162). Lastly, normal mice transduced with the adenovirus encoding TRB-3 iRNA showed improved glucose tolerance, whereas hepatic overexpression of TRB-3 reversed this effect (162).

Currently, little is known about the potential effects PGC-1β and PPRC may have in the development of hepatic insulin resistance or T2DM.

4.2 PGC-1β

In contrast to PGC-1α, PGC-1β has little to no effect on the expression of hepatic gluconeogenic genes; it is not upregulated by cold exposure in brown fat, nor is it upregulated in skeletal muscle in response to exercise (165). PGC-1β is, however, upregulated by high-fat feeding (166) and consequently was shown to induce the expression of genes related to fatty acid oxidation (167), hepatic lipid synthesis (166) as well as to mitochondrial biogenesis (167). In fact, PGC-1β targets the same mitochondrial transcription factors as PGC-1α (132). For example, PGC-1β upregulates and bind to NRF-1 and NRF-2, thus increasing the gene levels of *tfam* and ultimately the expression levels of nuclear respiratory genes, the latter leading to increased mitochondrial mass (130; 149; 165; 167; 168). Moreover, studies found that PGC-1β null mice exhibited decreased mitochondrial gene expression (169; 170). Despite this, one group showed that PGC-1β was unable to compensate for the loss of PGC-1α as seen in PGC-1α null mice (154). In fact, *pgc-1β* mRNA level remained unchanged in several energy demanding tissues (i.e. heart, liver, brown fat) in *pgc-1α* deficient mice (154).

Both PGC-1α and PGC-β stimulate mitochondrial biogenesis but with different metabolic characteristics, suggesting that these two coactivators regulate the expression of overlapping but distinct set of mitochondrial genes. For instance, mitochondrial respiration stimulated by PGC-1β is tightly coupled than PGC-1α-mediated stimulation (171), indicating that fewer protons (H^+) leak across the inner mitochondrial membrane and into the intermembrane space (*via* uncoupling proteins), and thereby generating heat instead of ATP (Figure 1-5). PGC-1β appears to serve, more than PGC-1α, as a molecular machine committed to promoting cellular energy *via* fuel oxidation in hepatocytes (167; 171). The differential effects of PGC-1α and PGC-1β may be due to their selective preferences to DNA-binding transcription factors and/or their ability to

communicate differently with the general mitochondrial transcription machinery (172). Therefore, modulating the cellular activity of PGC-1α and PGC-1β may lead to fine-tuning of mitochondrial function to meet the energetic demands of the cell in response to certain environmental conditions.

4.3 PPRC

PPRC was discovered by Andersson *et al.* (2001) (133) by a database search for sequences similar to PGC-1α. This group found that PPRC was ubiquitously expressed in murine, human tissues, and various cell lines. Similar to PGC-1α and PGC-1β, PPRC binds to nuclear transcription factors implicated in the expression of mitochondrial function, such as NRF-1 and NRF-2 (138; 173; 174). Knockdown of PPRC in *in vitro* resulted in reduced respiratory chain expression and ATP production along with abundant abnormal mitochondria that lacked organized cristae and exhibited severe membrane abnormalities (133; 175; 176). Unlike PGC-1α and PGC-1β, PPRC expression is rapidly induced by the introduction of serum (133). In fact, its function has been widely implicated as an important cellular growth factor (133; 174; 177; 178).

PPRC activity was shown to correlate with the cell proliferative cycle (133). The steady-state expression of PPRC mRNA and protein is remarkably high in growing cells but rapidly diminishes upon exit from the cell cycle as a consequence of treatment with cell-cycle inhibitors or from serum withdrawal (133). Andersson *et al.* (2001) (133) demonstrated that PPRC protein was rapidly induced when quiescent fibroblasts re-entered the cell cycle in response to serum stimulation (133). This group proposed that PPRC activity may be essential for mitochondrial maintenance and respiratory function in growing cells.

Cell growth and proliferation requires mitochondrial respiratory for its high energy needs. Goto *et al.* (1997) (179) showed that PPRC binds to host cell factor (HCF)-1(138), a chromatin-associated protein required for progression through G_1 of the cell cycle phase (179). HCF-1 also functions as an NRF-2 coactivator (180), a component demonstrated to be critical for PPRC to bind to and *trans*-active NRF-2 (138). Therefore, HCF-1 serves as a platform for PPRC transcription factor interactions *via* promoting the expression of genes needed not only for cell growth but also for mitochondrial biogenesis and respiratory function. Needless to say, PPRC helps to integrate the expression of respiratory apparatus and mitochondrial biogenesis with the cell proliferative program.

Interestingly, a member of the gasotransmitter family, NO, was shown to modulated the gene expression of *pprc*. Raharijaona *et al.* (2009) (176) demonstrated that NO rapidly induced *pprc* expression in two human cell models of oncocytic thyroid tumours (XTC.UC1 and B-CPAP cell lines). Not only did it increase PPRC mRNA level, but 100 μM SNAP (an NO donor) also elevated PPRC-mediated mitochondrial biogenesis (*via* NRF-1, Tfam) and respiration (*via* COX5B; a subunit of complex IV, also known as cytochrome c oxidase) (176). Treatment with a PKG inhibitor (KT5823), an inhibitor of the NO/cGMP pathway, blocked this upregulation of the aforementioned genes (176). Because NO upregulates PPRC expression as well as PPRC-mediated induction of mitochondrial biogenesis and respiration, preludes to the possibility that H_2S may regulate PPRC expression and mitochondrial biogenesis

5.0 C/EBP-β, gluconeogenesis, and diabetes

CCAAT-enhancer-binding proteins (C/EBP)-β belongs to the leucine zipper family of transcription factors from which other members have been characterized (i.e. C/EBP-α and

C/EBP-γ) (181; 182). Due to its high expression in hepatocytes (183), C/EBP-β has been linked to hepatocyte-specific gene regulation (184). For instance, C/EBP-β contributes to regulating the acute-phase response of the liver in inflammation (185; 186), liver regeneration (187; 188), as well as liver gluconeogenesis (154; 189).

C/EBP-β is another important transcription factor that regulates glucose homeostasis through the induction of PEPCK and G6Pase (154; 189). In fact, C/EBP-β aids in cAMP/PKA-induced glucose production *via* inhibiting PDE, thus increasing PKA activity (190). Similar to PGC-1α, C/EBP-β gene expression level was also shown to increase in the fasted mouse liver (154) or in the liver of rats that received injections of a chemical analog of cAMP (191). C/EBP-β transcription is stimulated by cAMP/PKA in response to fasting-induced glucagon release (139; 192). After its activation by cAMP, PKA phosphorylates CREB (Ser133). The latter enters the nucleus and binds to the CRE site in the promoter region of the c*/ebp-β* gene (192), thus increasing its transcription. C/EBP-β can be induced by the activation of the cAMP/PKA pathway as well as the GR pathway (193). Similar to PGC-1α, insulin downregulates the expression level of C/EBP-β, thus inhibiting C/EBP-β-mediated induction of gluconeogenesis (194).

Interestingly, C/EBP-β was shown to directly induce *pgc-1α* transcription *via* binding to its specific promoter region in both hamster kidney cells (187) and in mouse brown fat cells (195). Wang *et al.* (2008) (187) characterized C/EBP-β binding sites in the promoter region of *pgc-1α* (-765/-752), which was shown to increase *pgc-1α* promoter activity by ~7 fold; an observation that was later confirmed by Kajimura *et al.* (2009) (195). Mutation at *pgc-1α* (-765/-752) binding site blocked C/EBP-β-induced *pgc-1α* promoter activity (187).

C/EBP-β is significantly upregulated in livers of STZ-induced diabetic rats (194) and mice (189). One study showed that livers from STZ-treated rats exhibited a 3-fold increase in C/EBP-β mRNA level (194). Subsequently, Arizmendi *et al.* (1999) (189) found that C/EBP-β deletion in mice delayed the status of hyperglycemia, prevented the increase in plasma free fatty acids, limited the full induction of *pepck* and *g6pase* genes, and reduced the gluconeogenic rate all in comparison to STZ-treated WT mice. Since C/EBP-β regulates both glucose and lipid concentrations, the authors suggest that C/EBP-β may be used as a therapeutic target to treat multiple metabolic disorders (i.e. diabetes, obesity).

6.0 Rationale and hypothesis

Recent work from our group has clearly shown that H_2S regulates glucose production (22; 105; 106). Studies done on CSE-KO mice revealed that isolated KO liver cells produced less glucose compared to isolated WT liver cells (105). We further showed that PGC-1α mRNA level was lower in CSE-KO renal tissues and that it was upregulated by exogenous H_2S in A-10 cells (22). Identifying that H_2S stimulates the regulation of PGC-1α holds exciting prospects for this protein as it regulates an array of energy-consuming metabolism pathways, namely mitochondrial biogenesis and gluconeogenesis (5; 130; 142; 143; 154; 170; 196; 197). Another important transcription factor, C/EBP-β, also regulates glucose homeostasis through the induction of PEPCK and G6Pase (154; 189), enhancing the activity of PKA (190) as well as upregulating PGC-1α expression level (187; 195). Interestingly, CSE (119; 120), PGC-1α (139; 140; 162), and C/EBP-β (189; 194) are significantly upregulated in livers of streptozotocin-induced diabetic rats (119; 120; 194) and mice (140; 189), *db*/*db* (139; 162) and *ob*/*ob* mice (140), as well as in liver-specific insulin-receptor knockout mice (140). These altered gene expression profiles

suggest a linkage between CSE/H_2S system and PGC-1α and C/EBP-β in the context of gluconeogenesis regulation in the liver. Additionally, since H_2S was shown to upregulate *pgc-1α* expression level (22), suggests that it may also upregulate the expression levels of PGC-1β and PPRC. Indeed, NO was shown to upregulate PPRC-mediated induction of mitochondrial biogenesis and respiration (176). **Therefore, my hypothesis is that endogenous H_2S is an important regulator of hepatic glucose production; it does this by upregulating the major gluconeogenic enzymes (i.e. PEPCK, FBPase, and G6Pase) as well as mitochondrial biogenesis to fuel hepatic glucose production.**

7.0 Objectives and experimental approaches

This thesis focuses on the relationship between H_2S and hepatic glucose production and has been divided into two consecutive studies.

7.1 Study 1: Decreased gluconeogenesis in the absence of cystathionine γ-lyase and the underlying mechanisms

Currently, the role of endogenous H_2S availability in gluconeogenesis is unknown. Therefore, we focused on the crucial role of CSE-generated H_2S in hepatic glucose production under physiological conditions. How H_2S enhanced gluconeogenesis, and the roles of PGC-1α and C/EBP-β play in H_2S-mediated glucose production were investigated (Figure 1-7). Our objectives are as follows:

1.0 To determine the *in vivo* effects of endogenous and exogenous H_2S on the rate of gluconeogenesis *via* pyruvate tolerance test in both WT and CSE-KO mice.

2.0 To investigate the stimulatory effect of H_2S on glucose production as well as changes in gluconeogenic factors (i.e. PGC-1α, C/EBP-β, PEPCK, etc.) in isolated primary liver cells from overnight fasted WT and CSE-KO mice. Also, whether or not H_2S increases the protein and *S*-sulfhydration levels of PEPCK, FBPase, and G6Pase, will be analyzed.

3.0 To study the stimulatory effect of the cAMP/PKA and GR pathways on glucose production and protein expression levels of major gluconeogenic factors (i.e. PGC-1α, C/EBP-β, FBPase, etc.) *via* 8-Br-cAMP and dexamethasone treatment, respectively, in isolated hepatocytes.

4.0 To analyze the signaling pathway(s) H_2S mediates to induce hepatic glucose production in the primary liver cells (i.e. cAMP/PKA and/or glucocorticoid signaling pathway[s]). Inhibitors selective to the cAMP/PKA (KT5720) and GR (RU-486) pathway will be used.

5.0 Lastly, we intend to determine if H_2S-induced hepatic glucose production is dependent, or not, on PGC-1α and/or C/EBP-β signaling pathway(s) in both CSE-KO and WT hepatocytes.

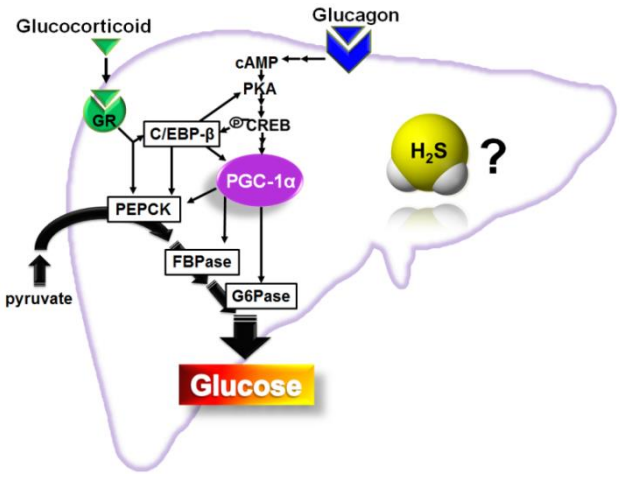

Figure 1-7: Schematic diagram of the layout of Study 1.

7.2 Study 2: Stimulatory effect of the CSE/H_2S system on hepatic mitochondrial biogenesis and the underlying mechanisms

After determining that H_2S stimulates hepatic glucose production through the PGC-1α signaling pathway, we turned our attention to determine whether or not H_2S induced mitochondrial biogenesis. As mentioned earlier, it was shown that the other gasotransmitters, NO (145) and CO (146), are involved in adaptive oxidative metabolism by ameliorating mitochondrial biogenesis in brown adipocytes (145) and cardiac tissues (146). In fact, both of these gasotransmitters use PGC-1α activity to induce mitochondrial biogenesis. Therefore, since H_2S increases PGC-1α protein expression as well as its activity (*via S*-sulfhydration) in primary hepatocytes, we investigated whether it could also induce mitochondrial biogenesis in liver cells (Figure 1-8). To carry out this study, we wanted to determine the following:

1. The endogenous mtDNA copy number in primary hepatocytes isolated from both WT and CSE-KO mice.
2. The effect of endogenous and exogenous H_2S has on mitochondrial biogenesis gene transcripts (i.e. *nrf-1*, *nrf-2*, *tfam*), as well as on the expression levels of PGC-1β and PPRC. Furthermore, it would be necessary to determine if H_2S sulfhydrates PGC-1β and PPRC in primary hepatocytes.
3. The ability of endogenous and exogenous H_2S to induce mitochondrial biogenesis in primary liver cells by using a fluorescence probe.
4. Lastly, to investigate if H_2S-induced mitochondrial biogenesis is dependent on PGC-1α signaling activity, or the activity of other mitochondrial biogenesis coactivators (i.e.

PGC-1β, PPRC) to stimulate mitochondrial content and distribution in primary hepatocytes.

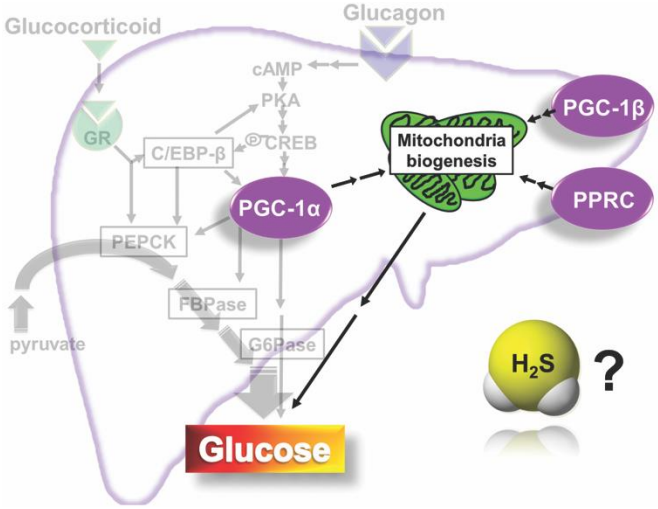

Figure 1-8: Schematic diagram of the layout of Study 2.

CHAPTER 2

GENERAL METHODOLOGY

MOUSE PRIMARY LIVER CELL ISOLATION

Mouse primary hepatocytes were chosen as the ideal experimental model to study glucose metabolism due to their metabolic competence, practicality, cost, and due to our unique access to CSE-KO mice (discussed in Chapter 5). Prior to cell isolation, mice (8-12 weeks) were starved for 16 h where glycogen content of hepatocytes was virtually depleted as shown in our previous study (105). Hepatocytes were isolated from CSE-KO and WT mice as described previously (105) with modification. In brief, mice livers were perfused through the inferior vena cava with a buffer consisting of the following: 140 mM NaCl, 2.6 mM KCl, 0.28 mM Na_2HPO_4, 5 mM glucose, and 10 mM HEPES (pH 7.4). The perfusion was first for 7 min with the buffer supplemented with 0.5 mM EGTA and then for 10 min with the buffer containing 5 mM $CaCl_2$ and 100 U/ml collagenase type IV (Worthington, Lakewood, NJ). The isolated hepatocytes were filtered on nylon mesh (100 μm pore size), and selected by centrifugation in a 26% percoll isodensity gradient and then seeded in DMEM (5.5 mM glucose) containing 10% fetal bovine serum and 1X penicillin-streptomycin-neomycin. After 2 h at 37ºC in a humidified atmosphere of 5% CO_2, the medium was removed and replaced with DMEM (5.5 mM glucose) supplemented with only 1X penicillin-streptomycin-neomycin. Cell viability was measured by trypan blue staining (method described below). The viability of all preparations was above 95%.

TRYPAN BLUE STAINING

Trypan blue method was used to detect cell viability of primary liver cells after isolation. Freshly isolated primary liver cells were resuspended in low-glucose DMEM (5.5 mM glucose) supplemented with 10% FBS and 1X penicillin-streptomycin-neomycin (10^6 cells/mL). A 1:1 ratio of 0.4% trypan blue and cell suspension (dilution of cells) were constituted and mixed

thoroughly *via* pipetting up and down. Approximately 10 μL of the trypan blue/cell mixture was applied to a hemacytometer. The unstained (viable) and stained (nonviable) cells were counted separately in the hemacytometer to obtain the total number of viable cells. Isolated mouse hepatocytes with cell viability at or above 95% were used for experiments.

ENDOGENOUS H_2S MEASUREMENT

The endogenous H_2S level was determined by the zinc-agar trap method as described elsewhere (198). Primary liver cells were cultured in 50 mL cell culture flasks with a preset monolayer of zinc-agar (1% agar, 9 mM zinc). After 24 h in cell culture, the medium was carefully aspirated, and the trapped H_2S in the zinc-agar layer was liberated and quantified *in situ via* the methylene blue reaction. Accordingly, 2 mL of *N, N*-dimethyl-*p*-phenylenediamine chloride (40 mM in 7.2 M HCl) was added, and the flasks were incubated at room temperature for 10 min followed by the addition of 400 μL $FeCl_3$ (30 mM in 1.2 M HCl). After 20 min incubation, the absorbance was measured at 670 nm in a Multiskan Spectrum (Thermo Labsystems, Altrincham, CH, UK). Endogenous H_2S released from the cells was quantified by a NaHS standard curve and normalized to total protein content that was determined by the Bradford method (Bio-Rad Laboratories, Inc., Mississauga, ON, Canada).

GLUCOSE PRODUCTION ASSAY

The glucose production assay was carried out as described previously (105; 109). Primary hepatocytes isolated from WT or CSE-KO mice were plated onto 12-well tissue culture plates at a density of 5×10^4 cells per well and maintained in low-glucose (5.5 mM), serum- and insulin-free DMEM (containing 1.25 mM pyruvic acid). This maintenance medium prevents the

replenishment of glycogen stores in the isolated hepatocytes (199; 200). Cells were treated with either NaHS (10 or 30 μM) for 6 h or with 8-Br-cAMP/Dex (1 mM/1 μM) for 3 h or 6 h. For the PKA and glucocorticoid inhibitor studies, cells were pretreated for 1 h with 5 μM KT5720 or 5 μM RU-486. The medium was aspirated, and cells were washed with PBS before a 6 h treatment with NaHS (30 μM) or 8-Br-cAMP/Dex (1 mM/1 μM). After treatment, the medium was removed, and cells were washed with PBS and incubated for 3 h in glucose-free DMEM. Thereafter, the medium was collected, and glucose concentration was determined using a glucose assay kit II (Biovision, Mountain View, CA). The effects of KT5720 and RU-486 on cell viability was assessed by the trypan blue assay (201).

SULFHYDRATION ASSAY

The assay was conducted as described elsewhere (20; 109) with modifications. Briefly, primary liver cells were sonicated three times (10 s/each) on ice using a cell sonicator (Sonic Dismembrator Model 100; Fisher Scientific) in HEN buffer [250 mM Hepes (pH 7.7), 1 mM EDTA, and 0.1 mM neocuproine] supplemented with 100 μM deferoxamine, 1:100 protease inhibitors, and 1% NP-40. Samples were centrifuged at 14,000 rpm for 20 min at 4°C. Blocking buffer (HEN buffer adjusted to 2.5% SDS and 20 mM MMTS) was added to the samples, which were then incubated at 50°C for 20 min with frequent shaking. After the addition of acetone, proteins were precipitated at -20°C for 20 min. Next, acetone was removed, and proteins were resuspended in HENS buffer (HEN buffer adjusted to 1% SDS) with the addition of biotin-HPDP. After incubation at 25°C for 3 h, the biotinylated proteins were precipitated by streptavidin agarose beads and washed 5X with HENS buffer. The biotinylated proteins were eluted by 5X loading buffer, and samples were subjected to Western blot analysis. The total

targeted protein (i.e. total FBPase) was used as the normalizing control to quantify the densitometry of the *S*-sulfhydrated level of a targeted protein (i.e. SSH-FBPase).

WESTERN BLOT ANALYSIS

Cultured cells or liver tissue extracts were harvested in PBS supplemented with protease cocktail solution (1:100). Samples were sonicated three times (10 s/each) on ice using a cell sonicator (Sonic Dismembrator Model 100) and were centrifuged at 14,000 rpm for 15 mins at 4ºC. Protein was determined *via* BCA method. Equal amount of proteins were boiled in 1 X SDS sample buffer (62.5 mM Tris-HCl, pH 6.8, 2% SDS, 10% glycerol, 50 mM DTT, and 0.01% bromophenol blue). Total cell lysates or liver tissue extracts (30-50 μg per lane) were separated by standard 10% SDS/PAGE and then transferred onto PVDF membranes (Millipore) and probed with selected primary antibodies. The primary antibody dilutions were 1:1,000 for anti-PGC-1α (Novus Biologicals, Oakville, ON, Canada), anti-PEPCK, anti-CSE (Abnova, Walnut, USA), anti-C/EBP-β, anti-G6Pase-α antibodies (Novus Biologicals); and 1:10,000 for anti-β-actin antibody (Santa Cruz Biotechnology, Santa Cruz, CA). HRF-conjugated secondary antibodies were used at either 1:10,000 or 1:5,000. Immunoreactions visualised by enhanced chemiluminescence (ECL) and exposed to X-ray film (Kodak Scientific Imaging Film). Densitometric quantification was performed using ImageJ Software (National Institutes of Health).

SHORT INTERFERING RNA (siRNA) TRANSFECTION

All siRNAs were designed by and purchased from Santa Cruz Biotechnology. Isolated primary liver cells were seeded in six-well plates at a density of 1×10^5 cells per well. Transfection of siRNA into primary liver cells was achieved using Lipofectamine® RNAi/MAX Reagent

(Invitrogen, Burlington, ON, USA). Briefly, mouse primary liver cells were transfected with (70-100 nM) of targeting (siPGC-1α, siC/EBP-β, siPPRC) or non-targeting (control-siRNA-A) siRNA in Opti-MEM I culture medium (Invitrogen) without antibiotics for 4 h. Afterwards, the transfection medium was removed, primary liver cells were washed with PBS, and fresh DMEM (5 mM glucose) supplemented with 1X penicillin-streptomycin-neomycin with or without 10% FBS was added to the cells. Hepatocytes were incubated for another 56 h prior to their respective treatments.

REAL-TIME PCR

Total cellular RNA was isolated using TRIzol (Sigma), and treated with RNase-free DNase (New England BioLabs, Pickering, ON, Canada). RNA quantity and purity was verified by A260/A280 measurements (Agilent 2100 Biosystem, Mississauga, Ontario, Canada). The integrity of the extracted RNA was determined by running a 1% agarose-formaldehyde denaturing gel stained with ethidium bromide to check the 2:1 ratio of the 28S and 18S bands (densitometric quantification was determined *via* ImageJ Software). Only RNA samples with no RNA smearing below the 18S band and with a 2:1 ratio of the 28S and 18S bands were used for experiments.

First-strand cDNA was prepared by reverse transcription using M-MuLV reverse transcriptase and random hexamer primers from a ProtoScript II RT-PCR Kit (New England Biolabs) according to the manufacturer's protocol. The relative abundance of mRNA in each sample was measured by real-time PCR in a fluorescent temperature cycler (iQ5 Real-Time PCR Detection System, Bio-Rad, Mississauga, ON, Canada) with SYBR Green PCR Master Mix (Qiagen), as described previously (22; 34). Controls containing no reverse transcriptase were used to safeguard for genomic DNA contamination in each sample. Primer sequences specific for

either human $HepG_2$ cells or primary mouse hepatocytes are listed in Tables 2-1 and 2-2, respectively. All pre-designed primers were synthesized and supplied by Sigma-Aldrich (Oakville, ON, Canada). β-actin was chosen as the reference gene as its mRNA level remained unchanged throughout various sample treatments. As β-actin mRNA levels fluctuate between different mouse tissues (202), comparisons were only made from samples derived from the same experimental model (i.e. $HepG_2$ cells or mouse primary liver cells). The PCR conditions were as follows: denaturation at 95°C for 3 min, followed by 40 cycles of denaturation at 95°C for 30 s, annealing at 55°C for 1 min, and extension at 72°C for 30 s as described (22; 34). The specificity of PCR was determined by melt-curve analysis for each reaction. The relative difference in mRNA between samples was calculated using the arithmetic formula $2^{-\Delta\Delta CT}$. ΔCT is the difference between the threshold cycle of a given target mRNA and an endogenous reference β-actin mRNA. Based on the calculated ΔCT value, the target mRNA level in the treated group was subsequently expressed as the percentage of that in the control group.

STATISTICAL ANALYSIS

All data sets are presented as mean ± S.E.M. For primary liver cell experiments, *n* value designates the number of mice used in the experiments. Results were analyzed using Student's *t* test, or one-way ANOVA followed by a *post hoc* analysis (Tukey's test) when applicable. Statistical significance was considered at $P < 0.05$.

Table 2-1: Real-time PCR primer sequences for gene targets in mouse hepatocytes

Short name	Forward primer 5´-3´	Reverse primer 5´-3´
PPRC	GGTTTCAGTGGTCAGATGC	CAGCCTGTCCCTCAAGTTC
PGC-1β	CTGGATGAAGGCGACACAC	CTGGAACTGAGGCTGGTCTG
NRF-1	CAGCACCTTTGGAGAATG	CGACCTGTGGAATACTTG
NRF-2	CTCACAGATGAAACAGGAG	GTCACAATGATGGGCTGA
Tfam	CGTCTATCAGTCTTGTCTG	GTATGCTTTCCACTCAGC
ATP1a5	GCCTTACCAGTCATTGAAAC	CACCCGCATAGATAACAG
β-actin	CCCATCTACGAGGGCTAT	TGTCACGCACGATTTCC

Table 2-2: Real-time PCR primer sequences for gene targets in human $HepG_2$ cells

Short name	Forward primer 5´-3´	Reverse primer 5´-3´
PGC-1α	GTCAAGCCACTACAGACACC	CCGACATAAATCACACGG
HNF-4α	GTACTCCTGCAGATTTAGCC	CTCATAGCTTGACCTTCGAG
FOXO1	CCTCGAACTAGCTCAAATGC	GGGATTGCTTATCTCAGAC
PEPCK	GGTGCTGGAGTGGATGTTC	GGAGGTCGGCATTGACTTG
FBPase	CGATTGCCTTGTGTCCGTTG	GACCAGAGTGCGATGAAC
G6Pase	CCTTCACAGGAATGGAGTGC	CTGAGTTTCTTGGACCCACC
β-actin	GGACATCCGCAAAGACCTG	GGACTCGTCATACTCCTGC

CHAPTER 3

DECREASED GLUCONEOGENESIS IN THE ABSENCE OF CYSTATHIONINE γ-LYASE AND THE UNDERLYING MECHANISMS

Ashley A. Untereiner,[1,2,3] Rui Wang,[1,4] YoungJun Ju,[1,5] and Lingyun Wu[1,2,3,*]

[1] The Cardiovascular and Metabolic Research Unit, Lakehead University, ON, Canada

[2]Department of Health Sciences, Lakehead University, ON, Canada

[3]Thunder Bay Regional Research Institute, ON, Canada

[4]Department of Biology, Laurentian University, ON, Canada

[5]Department of Kinesiology, Lakehead University, ON, Canada

This chapter has been published as an article in *Antioxidant and Redox Signaling* (I.F: 7.40).

Contents of this chapter have been adapted/reproduced from the published article with permission from *Antioxidant and Redox Signaling*. The references for this chapter are separately listed at the end of this chapter.

ABSTRACT

Aims: To investigate the regulation of hepatic glucose production by cystathionine γ-lyase (CSE)-generated hydrogen sulfide (H_2S) in hepatic glucose production under physiological conditions.

Results: We found that CSE-knockout (KO) mice had a reduced rate of gluconeogenesis, which was reversed by administration of NaHS (an H_2S donor) (i.p.). Interestingly, isolated CSE-KO hepatocytes exhibited a reduced glycemic response to chemical-induced activation of the cAMP/PKA and glucocorticoid pathways compared to wild-type (WT) hepatocytes. Treatment with the inhibitors for PKA (KT5720) or glucocorticoid receptor (RU-486) significantly reduced H_2S-stimulated glucose production from both WT and CSE-KO mouse hepatocytes. NaHS treatment upregulated the protein levels of key gluconeogenic transcription factors, such as peroxisome proliferator-activated receptor-γ coactivator-1α (PGC-1α) and CCAAT-enhancer-binding proteins-β (C/EBP-β). Moreover, exogenous H_2S augmented the S-sulfhydration of the rate-limiting gluconeogenic enzymes and PGC-1α and increased their activities, which were lower in untreated CSE-KO hepatocytes. Finally, knockdown of PGC-1α, but not C/EBP-β, significantly decreased NaHS-induced glucose production from the primary hepatocytes.

Conclusion: This study demonstrates the stimulatory effect of endogenous H_2S on liver glucose production and reveals three underlying mechanisms; i.e. H_2S upregulates the expression levels of PGC-1α and PEPCK *via* glucocorticoid receptor pathway; H_2S upregulates the expression level of PGC-1α through the activation of the cAMP/PKA pathway, as well as PGC-1α activity *via S*-sulfhydration; and H_2S upregulates the expression and the activities (by *S*-sulfhydration) of G6Pase and FBPase. This study may offer clues for the homeostatic regulation of glucose metabolism under physiological conditions and its dysregulation in metabolic syndrome.

Keywords: H_2S ● PGC-1α ● gluconeogenesis ● cAMP/PKA pathway ● glucocorticoid

INTRODUCTION

Glucose is the most efficient and abundant energy substrate for mammalian cells, fueling numerous physiological functions, including cell proliferation and growth, protein and nucleic acid synthesis, fatty acid and cholesterol synthesis, etc. Glucose is converted to ATP, the energy currency of the cell, *via* oxidative phosphorylation mostly and anaerobic glycolysis to a lesser degree. Thus, glucose homeostasis is critical for maintaining physiological function of our body, whereby its sustained disturbance may lead to metabolic syndrome.

Fasting induces the release of glucagon and glucocorticoid from pancreatic α-cells and the adrenal cortex, respectively, into the bloodstream through which these endocrine hormones act on the liver. The liver is the major glucose-producing organ, whereby the breakdown of glycogen produces glucose (glycogenolysis) and the *de novo* synthesis of glucose (gluconeogenesis) occurs within this organ. Both glycogenolysis and gluconeogenesis are activated by glucagon signaling *via* increasing intracellular cAMP level, eventually leading to glycogen breakdown and the transcription of gluconeogenic genes. Glucocorticoid, on the other hand, initiates only the gluconeogenic process *via* binding to its cytosolic receptor to activate the transcription of gluconeogenic genes. The glucagon and glucocorticoid signaling pathways synergistically work together to enhance hepatic glucose production.

Among many endogenous substances that regulate glucose production is hydrogen sulfide (H_2S) (27,35,40). H_2S is a gasotransmitter with the ability to freely diffuse through cell membranes and elicit physiological responses (17,31,36,41). In the liver, H_2S production is largely catalyzed by cystathionine γ-lyase (CSE) and, to a lesser degree, by cystathionine β-synthase (11). Recently, we showed that liver cells isolated from mice lacking the *cse* gene (CSE-KO) have significantly lower basal glucose level compared to their wild-type (WT)

counterparts (40). In subsequent studies, we discovered that NaHS (an H_2S donor) upregulated the expression of peroxisome proliferator-activated receptor-γ coactivator-1α (PGC-1α) in rat vascular smooth muscle cells, A-10 cells (27). PGC-1α is a major transcription factor involved in an array of energy-consuming metabolism pathways, such as cholesterol synthesis, fatty acid oxidation, mitochondria biogenesis, and gluconeogenesis (6). As an important gluconeogenic regulator, PGC-1α upregulates the expression of gluconeogenic rate-limiting enzymes, such as phosphoenolpyruvate carboxykinase (PEPCK), fructose-1,6-bisphosphatase (FBPase), and glucose-6-phosphatase (G6Pase) (6).

CCAAT-enhancer-binding proteins-β (C/EBP-β), another important transcription factor, also regulates glucose homeostasis through the induction of PEPCK and G6Pase (1,15). Interestingly, CSE (8,39), PGC-1α (10,14,38), and C/EBP-β (1,2) are significantly upregulated in livers of streptozotocin-induced diabetic rats (2,8,39) and mice (1,38), *db*/*db* (10,14) and *ob*/*ob* mice (38), as well as in liver-specific insulin-receptor knockout mice (38). These altered gene expression profiles suggest a linkage between CSE/H_2S system and PGC-1α and C/EBP-β in the context of gluconeogenesis regulation in the liver. We hypothesized that endogenous H_2S is an important regulator for liver glucose production. How H_2S enhanced gluconeogenesis and the roles of PGC-1α and C/EBP-β play in H_2S-mediated glucose production were investigated in the present study.

MATERIALS and METHODS

Animal and Tissue Preparation

CSE-KO mice were generated and home-bred as previously described (36). Eight to twelve-week-old male CSE-KO mice and age-matched male WT littermates were used. All animal experiments were conducted in compliance with the Guide for the Care and Use of Laboratory Animals published by the US National Institutes of Health (NIH Publication no. 85-23, revised 1996) and approved by the Animal Care Committee of Lakehead University, Canada. Mice were maintained on standard rodent chow with free access to food and water. Liver tissues were isolated in ice-cold PBS, cleaned, and snap-frozen in liquid nitrogen immediately and stored at -80°C until processing.

Hepatocyte Preparation

Prior to cell isolation, mice (8-12 weeks) were starved for 16 h where glycogen content of hepatocytes was virtually depleted as shown in our previous study (40). Hepatocytes were isolated from CSE-KO and WT mice as described elsewhere (40) (please see Chapter 2 for method details).

Pyruvate Tolerance Test

Mice were starved overnight and injected i.p. with 2 g/kg pyruvate. The animals received NaHS or saline (i.p.) 10 min prior to pyruvate injection. Blood glucose level was measured using blood glucose strips (One-Touch Glucometer, Johnson, local pharmacy).

Hepatocyte Glucose Production Assay

Primary hepatocytes isolated from WT or CSE-KO mice were plated onto 12-well tissue culture plates at a density of 5 x 10^4 cells per well and maintained in low-glucose (5.5 mM), serum- and insulin-free DMEM (containing 1.25 mM pyruvic acid). This maintenance medium prevents the replenishment of glycogen stores in the isolated hepatocytes (28,29). Cells were treated with either NaHS (10 or 30 μM) for 6 h or with 8-Br-cAMP/Dex (1 mM/1 μM) for 3 h or 6 h. For the PKA and glucocorticoid inhibitor studies, cells were pretreated for 1 h with 5 μM KT5720 or 5 μM RU-486. The medium was aspirated and cells were washed with PBS prior to a 6 h treatment with NaHS (30 μM) or 8-Br-cAMP/Dex (1 mM/1 μM). After treatment, the medium was removed and cells were washed with PBS, and incubated for 3 h in glucose-free DMEM. Thereafter, the medium was collected and glucose concentration was determined using a glucose assay kit II (Biovision, Mountain View, CA). The effects of KT5720 and RU-486 on cell viability were assessed by the trypan blue assay (16).

Endogenous H_2S Measurement

The endogenous H_2S level was determined by the *in situ* methylene blue assay as described elsewhere (13) (please see Chapter 2 for details on method).

Gene Silencing with siRNA

Primary liver cells were transfected with 70 nM siRNA-A (control), siPGC-1α, siC/EBP-β, or both siPGC-1α and siC/EBP-β for 60 h. The siRNA complexes were diluted in Opti-MEM media (Invitrogen, Burlington, ON, Canada) and Lipofectamine® RNAi/MAX Reagent (Invitrogen) was used as the transfection reagent.

Intracellular cAMP Levels

Endogenous cAMP levels in primary mouse hepatocytes were determined by Cyclic AMP Select EIA Kit (Cayman Chemicals, Burlington, ON, Canada) according to the manufacturer's instructions. Briefly, after liver cells were treated for 6 h with NaHS (30 μM), cells were washed 3X with ice-cold PBS and 1.657 mL of 0.1 M HCl was added to the 100 mm plates. Plates were incubated at room temperature for 20 min and cells were scraped off and centrifuged at 1,000 *g* for 10 min. The supernatant was diluted 1:2 with the supplied EIA buffer. Thereafter, 50 uL of sample was added to the coated 96-well plate which also contained the appropriate amounts of the supplied EIA buffer, AChE tracer, and EIA antiserum. The plate was incubated at 4°C for 18 h, where after the wells were washed 5X with the supplied Wash buffer and 200 uL of Ellman's Reagent was added to each well. The plate was incubated in the dark for 90 min on a shaker. Thereafter, the absorbance was measured at 410 nm in a Multiskan Spectrum (Thermo Labsystems) and data was analyzed using the online Cayman spreadsheet program (www.caymanchem.com/analysis/eia). Only sample values within the accepted $\%B/B_0$ range were used for statistical analysis. Ultrapure water (Cayman Chemical) was used to make up the working solutions from the supplied concentrated stock solutions.

Plasma Hormone Analysis

Blood samples for glucagon measurement were collected in heparin-coated tubes (to prevent interference with the EIA assay) supplemented with aprotinin (20 mg/L) to prevent proteolysis (21). Bloods samples for corticosterone were collected in EDTA-coated tubes. Plasma was collected by centrifuging whole blood at 3,000 *g* for 10 min at 4ºC. Plasma glucagon was measured *via* Glucagon (human/mouse/rat) EIA kit (Biovision) and corticosterone by

Corticosterone ELISA (Abcam, Toronto, ON, Canada). Analyzes were performed according to the respective manufacturer's protocols.

Immunoblot Analysis

Western blotting was performed as described before (7). The primary antibody dilutions were 1:1,000 for anti-PGC-1α, anti-C/EBP-β (Novus biologicals, Oakville, ON, Canada), anti-PEPCK, and anti-CSE (Abnova, Walnut, USA) antibodies; 1:100 for anti-FBPase, anti-G6Pase, and anti-FOXO1 antibody (Santa Cruz Biotechnology, Santa Cruz, CA); and 1:10,000 for anti-β-actin antibody (Santa Cruz Biotechnology).

Sulfhydration Assay

The assay was conducted as described elsewhere (22) with modifications. Briefly, primary liver cells were sonicated three times (10 s/each) on ice using a cell sonicator (Sonic Dismembrator Model 100; Fisher Scientific) in HEN buffer [250 mM Hepes (pH 7.7), 1 mM EDTA, and 0.1 mM neocuproine] supplemented with 100 μM deferoxamine, 1:100 protease inhibitors, and 1% NP-40. Samples were centrifuged at 14,000 rpm for 20 min at 4°C. Blocking buffer (HEN buffer adjusted to 2.5% SDS and 20 mM MMTS) was added to the samples, which were then incubated at 50°C for 20 min with frequent shaking. After the addition of acetone, proteins were precipitated at -20°C for 20 min. Next, acetone was removed and proteins were resuspended in HENS buffer (HEN buffer adjusted to 1% SDS) with the addition of biotin-HPDP. After incubation at 25°C for 3 h, the biotinylated proteins were precipitated by streptavidin agarose beads and washed 5X with HENS buffer. The biotinylated proteins were eluted by 5X loading buffer and samples were subjected to Western blot analysis.

Gluconeogenic Enzyme Assays

FBPase enzyme activity was assayed as described elsewhere (27). Briefly, total cell lysates were added to an assay mixture that contained 40 mM glycine buffer (pH 9.1), 2.0 mM $MgCl_2$, 1.0 mM EDTA, 0.6 mM $NADP^+$, and 1.2 U/mL of both glucose-6-phosphate dehydrogenase and phosphoglucose isomerase. The reaction mixture was equilibrated for 10 min at 37°C and initiated by the addition of 70 µM fructose-1,6-bisphosphate. The increase in absorbance was measured at 340 nm *via* a Multiskan Spectrum. Ultrapure water (Cayman Chemical) was used to make up the solutions. FBPase activity was calculated by subtracting the content of cell lysates incubated in the absence of fructose-1,6-bisphosphate from that of a complete system incubated in the presence of the substrate.

G6Pase activity was assayed as described elsewhere (9) with modifications. Briefly, the assay was conducted at 37°C for 15 min in 100 mM cacodylate buffer (pH 6.5). Hydrolytic activity was initiated with 100 µL of 100 mM glucose-6-phosphate mixed with 100 µL cell lysates. After 15 min at 37°C, 1.8 mL of 10% trichloroacetic acid was added, and samples were centrifuged at 4,000 *g* for 10 min. Afterwards, 1.0 mL of supernatant was added to 5.0 mL of 0.25% ammonium molybdate and 1.0 mL 0.2% 1-amino-2-naphthol-4-sulfonic acid (EMD Millipore Chemicals, Chemicals, Billerica, MA). The amount of liberated phosphate was measured at 700 nm *via* a Multiskan Spectrum. Ultrapure water (Cayman Chemical) was used to make up the solutions. G6Pase activity was calculated by subtracting the inorganic phosphorus content of cell lysates incubated in the absence of glucose-6-phosphate from that of a complete system incubated in the presence of the substrate. A blank containing all reagents except cell lysates revealed no free inorganic phosphorus.

Chemicals and Statistical Analysis

All chemicals and enzymes used in this study were obtained from Sigma-Aldrich (Oakville, ON, Canada) unless otherwise stated. siRNA products were obtained from Santa Cruz Biotechnology (Santa Cruz, CA) and antibodies were purchased from Abcam unless otherwise specified. All data sets are presented as mean ± S.E.M. For primary liver cell experiments, *n* value designates the number of mice used in the experiments. Results were analyzed using Student's *t* test, or one-way ANOVA followed by a *post hoc* analysis (Tukey's test) when applicable. Statistical significance was considered at $P < 0.05$.

RESULTS

Impaired gluconeogenic system in CSE-KO mice

The pyruvate tolerance test (PTT) is an estimation of the rate of gluconeogenesis, reflected by the time the liver takes to generate glucose from pyruvate. The injection of pyruvate to overnight fasted mice elicited a rapid glycemic response, where glucose level peaked 20 min after the injection and gradually declined over 2 h (Figure 3-1A). The amplitude of glycemic response was significantly lower in CSE-KO mice than in WT mice (Figure 3-1A). To determine if exogenous H_2S can restore gluconeogenesis in CSE-KO mice, the KO mice were given i.p. injections of NaHS or saline 10 min prior to pyruvate injection. NaHS pretreatment significantly increased basal plasma glucose level in CSE-KO mice before pyruvate stimulation (Fig. 1B). The pyruvate-stimulated gluconeogenesis in CSE-KO mice was rescued by NaHS pretreatment at 39 μmol/kg and restored it to the same level as WT mice (Figure 3-1B). NaHS pretreatment at a higher concentration of 63 μmol/kg resulted in significantly greater pyruvate-stimulated glycemic response than other treatments (Figure 3-1B).

To investigate specifically the stimulatory effect of H_2S on glucose production in the liver, we isolated primary liver cells from overnight fasted WT and CSE-KO mice. As expected, endogenous H_2S level in cultured CSE-KO liver cells was about 39% of that in WT liver cells (Figure 3-2A). To observe hepatocytes' response to chemical-induced activation of the cAMP/PKA and glucocorticoid pathways, we treated the cultured liver cells with 8-Br-cAMP and dexamethasone (Dex), which are synthetic analogs for cAMP (38) and glucocorticoid (20), respectively. Treatment with 8-Br-cAMP/Dex for 3 h and 6 h increased glucose production in WT cells by 87% and 246%, respectively (Figure 3-2B). Interestingly, 8-Br-cAMP/Dex treatment for 3 h and 6 h elicited a higher percentile increase in glucose production response in

CSE-KO cells by 215% and 329%, respectively, compared to untreated CSE-KO liver cells (Figure 3-2B). However, the actual glucose levels in CSE-KO cells were 54% and 40% of those in WT cells with 3 h and 6 h 8-Br-cAMP/Dex treatment, respectively.

The changed gluconeogenic proteins levels followed the same trend as the glucose production level in 8-Br-cAMP/Dex-treated WT cells. For instance, the protein levels of PGC-1α, PEPCK, FBPase, G6Pase, and C/EBP-β (also known as LAP) were significantly increased in WT liver cells after 3 or 6 h treatment with 8-Br-cAMP/Dex (Figure 3-2C-H). A similar increase in the protein level of forkhead box protein O1 (FOXO1; a PGC-1α co-activator (6)) was also observed in WT hepatocytes with 8-Br-cAMP/Dex treatment (Supplementary Figure 3-1A and B). Interestingly, the basal levels of these proteins were significantly higher in CSE-KO liver cells than those of WT liver cells (Figure 3-2C-E, G and H, and Supplementary Figure 3-1), with the exception to FBPase (Figure 3-2C and F). CSE-KO liver cells exhibited a moderate increase in PGC-1α expression level by 34% and PEPCK by 48% after treatment with 8-Br-cAMP/Dex for 6 h (Figure 3-2D and E). Moreover, CSE expression level significantly decreased in WT hepatocytes with 8-Br-cAMP/Dex treatment (Figure 3-2C and I). This downregulation suggests hormonal control of CSE protein expression by glucagon-stimulated cAMP signaling or/and by glucocorticoid signaling.

It has been reported that under starvation conditions, PGC-1α and PEPCK are significantly upregulated in mouse liver (15,38). C/EBP-β gene expression level was also shown to increase in the fasted mouse liver (15) or in the liver of rats that received injections of a chemical analogue of cAMP (24). How these key gluconeogenic proteins are regulated by H_2S under different nutritional states was unknown. Here, we found a significant increase in PGC-1α, PEPCK, and C/EBP-β expression levels in non-fasted CSE-KO livers compared to WT livers

(Figure 3-3A-D). In agreement with Fig. 2I, CSE expression was decreased in fasted WT livers in comparison with the level in non-fasted WT livers (Figure 3-3A and E). Furthermore, plasma levels of glucagon and corticosterone (a major glucocorticoid) were significantly elevated in non-fasted and fasted CSE-KO mice compared to the respective WT groups (Figure 3-3F and G).

NaHS enhances glucose production, protein level and induces *S*-sulfhydration of major gluconeogenic factors

Based on our previous study (40), it came to no surprise when we found that NaHS treatment significantly increased glucose production in primary cultured WT and CSE-KO liver cells (Figure 3-4A). To dig further into this mechanism, we discovered that 30 μM NaHS increased the enzymatic activities of total FBPase and G6Pase in isolated hepatocytes (Figure 3-4B and C). Since H_2S-indued *S*-sulfhydration was shown to enhance enzymatic activity (22), we determined it necessary to measure the sulfhydrated levels of these gluconeogenic proteins. In fact, all three gluconeogenic enzymes: PEPCK, FBPase, and G6Pase, showed elevated levels of their sulfhydrated forms with NaHS treatment in both WT and CSE-KO hepatocytes (Figure 3-4D-I).

Bucci *et al.* (2010) (3) demonstrated the ability of H_2S to enhance endogenous cAMP in vascular smooth muscle cells. Indeed, we found this similar phenomenon to also occur in primary hepatocytes treated with NaHS (Figure 3-5A). Like its effect on the major gluconeogenic enzymes (Figure 3-4D-I), exogenous H_2S also enhanced the *S*-sulfhydration level of PGC-1α by approximately 1 fold in both WT and CSE-KO liver cells with comparison to their respective control groups (Figure 3-5B and C). Furthermore, NaHS treatment increased the protein expression levels of PGC-1α, PEPCK, FBPase, G6Pase, and C/EBP-β in WT and CSE-KO hepatocytes (Figure 3-5D-I). For example, NaHS at 10 μM and 30 μM increased the levels

of PGC-1α by 35% and 69% in WT cells, respectively (Figure 3-5D and E). Contrary to 30 μM NaHS treatment, 5 mM $_L$-cysteine (a major precursor for H_2S biosynthesis) failed to induce glucose production and PGC-1α, FBPase, and G6Pase protein expression levels in isolated CSE-KO hepatocytes (Supplementary Figure 3-2).

H_2S induces glucose production through the cAMP/PKA and glucocorticoid pathways

To determine the signaling pathways for H_2S-induced glucose production, we used 5 μM KT5720 to inhibit PKA and 5 μM RU-486 to inhibit glucocorticoid receptor (GR) in primary cultured WT and CSE-KO liver cells. Pretreatment with KT5720 or RU-486 for 1 h did not affect cell viability as tested with trypan blue assay (data not shown), but the inhibitors significantly attenuated the gluconeogenic effect of 8-Br-cAMP/Dex (Figure 3-6A and B). Pretreatment of WT and CSE-KO liver cells with KT5720 or RU-486 also significantly suppressed NaHS-induced glucose production (Figure 3-6C and D). The gluconeogenic effects of 8-Br-cAMP/Dex and NaHS on WT and CSE-KO liver cells were completely abolished by the co-treatment with both KT5720 and RU-486 (Figure 3-6).

H_2S-induced glucose production is dependent on PGC-1α in WT and CSE-KO primary liver cells

To determine whether H_2S-stimulated hepatic glucose production was mediated by PGC-1α and/or C/EBP-β, we transfected WT and CSE-KO primary liver cells with siPGC-1α, siC/EBP-β, or both siPGC-1α and siC/EBP-β for 60 h. These maneuvers significantly knocked down the expression of the respective proteins (Figure 3-7A and B). Transfection with siC/EBP-β had no effect on NaHS-induced glucose production in both WT and CSE-KO primary liver cells (Figure

3-7C). However, glucose production induced by NaHS at 30 μM was completely abolished by siPGC-1α transfection in both WT and CSE-KO liver cells (Figure 3-7C). In agreement, co-transfection of both PGC-1α and C/EBP-β also abolished NaHS-induced glucose production in WT and CSE-KO liver cells (Figure 3-7C).

DISCUSSION

We previously showed that exogenous H_2S increased glucose production in cloned liver carcinoma $HepG_2$ cells (40). In the present study, we focused on the crucial role of endogenous H_2S in hepatic glucose production under physiological conditions as well as under fasting conditions. CSE-KO mice, with diminished hepatic H_2S production, displayed significantly reduced glucose production after pyruvate supplementation. Cultured primary liver cells isolated from CSE-KO mice produced significantly lower glucose and exhibited a reduced glycemic response to chemical-induced activation of the cAMP/PKA and glucocorticoid pathways compared to WT liver cells. Endogenous H_2S was also responsible for increased enzymatic activity and sulfhydration levels of major gluconeogenic factors. Thus, we demonstrated that endogenous H_2S stimulates gluconeogenesis in mouse liver, leading to increased net glucose production. Our results also reveal the critical roles of PKA and glucocorticoid receptor (GR) in H_2S-induced glucose production and that of PGC-1α in H_2S-induced gluconeogenesis. One very intriguing discovery from our study is the differential responses of endogenous H_2S on the gluconeogenic proteins. In comparison with WT liver cells, we observed higher levels of PGC-1α, PEPCK, G6Pase, and C/EBP-β in untreated CSE-KO liver cells (Figure 3-2 and 3-5), thus indicating that endogenous H_2S inhibited the gene expression of PGC-1α, PEPCK, and G6Pase (Figure 3-2 and 3-5). On the other hand, NaHS treatment upregulated the expression of these gluconeogenic proteins (Figure 3-5). In the case of FBPase, both endogenous and exogenous H_2S increased its expression (Figure 3-2 and 3-5). It seems that endogenous and exogenous H_2S plays differential roles in the regulation of this protein.

The stimulatory effect of endogenous H_2S on gluconeogenesis was demonstrated in the present study with the pyruvate tolerance test (PTT) (Figure 3-1). PTT measures net glucose

level, a balance between glucose production and its utilization. The systemic utilization of hepatic glucose produced through pyruvate metabolism is dependent on glucose-stimulated insulin secretion and insulin sensitivity of peripheral tissues. High endogenous H_2S level in the pancreas of Zucker diabetic rats inhibits insulin synthesis and release (34). By the same token, low endogenous H_2S level in CSE-KO mice may lead to increased insulin release (35). In fact, we previously showed that CSE-KO mice have an improved glucose tolerance compared to the WT control (35). That unique metabolic feature of the CSE-KO mice was likely due to a higher level of glucose-stimulated insulin release (35), considering that H_2S inhibits insulin release (*via* activating K_{ATP} channels) from pancreatic β-cells (37). Therefore, these previously published results support the notion that more insulin is released in response to glucose stimulation in CSE-KO mice, leading to a faster clearance of glucose from the bloodstream. Our previous study also showed no difference in the insulin tolerance test results between CSE-KO and WT mice (35), suggesting that endogenous H_2S has no effect on peripheral insulin sensitivity. On the contrary, other studies have reported that NaHS supplementation inhibits insulin-stimulated glucose uptake into both fat (5) and liver (40) cells, implying that exogenous H_2S reduces insulin sensitivity. The discrepancy between Yang *et al*. (2011) (35) and the aforementioned studies (5,40) was due to the use of different preparations, i.e., whole animal *in vivo* study (35) *vs.* isolated rat adipocytes (5) and cultured $HepG_2$ cells (40). It may also reflect the difference in the effects of endogenous H_2S (35) and exogenously applied H_2S donors (5,40). On another note, our present study shows that H_2S enhances the rate of gluconeogenesis through PGC-1α signaling and by directly increasing the activities of FBPase and G6Pase. Taking these current and previously published results into consideration, the decreased glycemic response to pyruvate stimulation in CSE-KO mice can be explained by the lack of endogenous H_2S so that two effects

of H_2S, i.e. the upregulation of gluconeogenesis in the liver and inhibition of insulin secretion from pancreatic β-cells, cannot be realized. Future studies to compare the glucose levels, with pyruvate added to and insulin removed from the culture medium and vice versa, in cultured WT and CSE-KO liver cells will help differentiate H_2S-induced gluconeogenesis from H_2S-inhibited glucose utilization.

To study the liver-specific effect of H_2S on glucose production, we isolated and cultured primary hepatocytes from CSE-KO and WT mice. The mice were starved overnight to deplete hepatic glycogen (40) prior to liver cell isolation. Overnight starvation of rodents suppresses the ability of isolated primary liver cells to synthesize and accumulate glycogen (28). To further prevent the replenishment of glycogen stores, primary liver cells were cultured in glucose (5.5 mM), insulin- and FBS-free medium (28,29). Under these conditions, we found that CSE-KO liver cells produced significantly lesser glucose than WT liver cells with the activation of the cAMP/PKA and glucocorticoid pathways by 8-Br-cAMP/Dex treatment. The expression levels of PGC-1α, PEPCK, FBPase, G6Pase, and C/EBP-β proteins were increased in both WT and CSE-KO liver cells with the 8-Br-cAMP/Dex treatment; however, with the exception for FBPase, no significant difference was observed in these protein levels after 3 h of treatment in CSE-KO liver cells. Thus, this diverse pattern of protein upregulation along with lower glucose levels suggests an impaired gluconeogenic system in the CSE-KO liver cells. Moreover, the inability of supplemented $_L$-cysteine to increase gluconeogenesis in CSE-KO liver cells (Supplementary Figure 3-2A-E) supports the notion that CSE is the dominative H_2S-producing enzyme in the liver (11). During starvation, gluconeogenesis is 'switched on', meaning that PGC-1α, PEPCK, FBPase, and G6Pase are upregulated to increase hepatic glucose output. Interestingly, CSE protein was downregulated upon starvation (Figure 3-3) and also in 8-Br-

cAMP/Dex-treated WT hepatocytes (Figure 3-2), suggesting these gluconeogenic factors were upregulated in the presence of low endogenous H_2S. We assume that this fasting-induced downregulation of CSE is metabolically advantageous for two reasons: 1) It will prevent a massive outburst of hepatic glucose production into the circulation. H_2S is a potent stimulator of hepatic glucose production, *via* activating the cAMP/PKA and glucocorticoid pathways (Figure 3-6) as well as increasing the activities of the rate-limiting gluconeogenic enzymes, FBPase and G6Pase (Figure 3-4). Intermitted bursts of high amount of plasma glucose could lead to elevated levels of reactive oxygen species (ROS) and advanced glycation end-products (AGEs) in peripheral tissues (4). The deleterious effects of elevated ROS and AGEs levels have been implicated in the development of hypertension (32) and insulin-resistance (4). Additionally, the pancreas would have to respond to the high plasma glucose level by producing more insulin. This would put tremendous strain on the pancreas, which may eventually lead to pancreatic β-cell failure, as seen in the late stages of T2DM (4). 2) The hepatocytes would be more sensitive to insulin signaling under fasting conditions, where the downregulation of CSE expression would enable an immediate "turned-off" of gluconeogenesis. We recently showed that exogenous H_2S blocked insulin-induced phosphorylation of Akt at Ser^{473} in $HepG_2$ cells, which abolished the uptake and utilization of glucose (40). Coincident or not, upregulation of CSE has been reported in livers of streptozotocin-induced diabetic rats (8,39) and in insulin-resistant $HepG_2$ cells (40). Thus, it is metabolically beneficial to down-regulate the CSE/H_2S system in hepatocytes during fasting in order to preserve glucose homeostasis and possibly prevent the development of metabolic diseases.

We recently reported that hepatic lipolysis was reduced in CSE-KO mice (17,18). Liver tissues from fasted CSE-KO mice had lower mRNA levels of *pparα* and *pparγ*, two critical

regulators of lipid metabolism (17). FGF21, another important mediator of hepatic lipid metabolism, induced by fasting, is upregulated by PPARα (33). With lower *pparα* mRNA expression level, FGF21 expression may also be decreased in fasted CSE-KO livers. In fact, CSE-KO mice fed with a high fat diet (HFD) for 12 weeks developed severe dyslipidemia, hepatic injury (i.e. higher aspartate aminotransferase, alanine aminotransferase, and alkaline phosphatase levels), and fatty liver with comparison to the HFD-fed WT mice (17). This observation suggests the defect in the clearance of excess dietary fat from CSE-KO mouse liver. Clearly, not only is the gluconeogenic system impaired, but lipid metabolism as well in these CSE-KO mice. The impact of the impaired lipolysis system on the impaired hepatic gluconeogenic system in CSE-KO mice needs to be further clarified.

PGC-1α and C/EBP-β transcriptions are stimulated by cAMP/PKA in response to fasting-induced glucagon release (10,23). After its activation by cAMP, PKA phosphorylates the cAMP response element binding protein (CREB). The latter enters the nucleus and binds to the consensus cAMP response element (CRE) site on the PGC-1α promoter (10) or to the promoter region of the c*/ebp-β* gene (23), thus increasing their transcriptions. It is possible that exogenous H_2S increases PGC-1α and C/EBP-β expressions through the inhibition of AMP-activated protein kinase (AMPK) (40) and/or through the inhibition of phosphodiesterase (PDE) (3). Intriguingly, not only did H_2S increase PGC-1α protein level but also its activity *via S*-sulfhydration (Figure 3-5). Mustafa *et al.* (2010) (22) describes protein sulfhydration as a physiological post-transcriptional modification of cysteine residues in the target protein that leads to enhanced protein function. Sirtuin 1 activates PGC-1α *via* deacetylation (25); however, no deacetylation of PGC-1α was observed in primary hepatocytes treated with NaHS (data not

shown). Thus, we propose a novel mechanism by which PGC-1α activity is also regulated by S-sulfhydration in primary hepatocytes, leading to an enhanced gluconeogenic system.

PGC-1α is crucial for NaHS-induced glucose production because siPGC-1α transfection significantly abolished NaHS-stimulated glucose output from both WT and CSE-KO primary liver cells (Figure 3-7). The present study also demonstrates that both cAMP/PKA and glucocorticoid pathways are involved in NaHS-induced glucose production (Figure 3-6C and D). Preincubation with either PKA or GR inhibitor significantly reduced, and the co-treatment with both inhibitors completely abolished, NaHS-stimulated glucose production in both WT and CSE-KO liver cells (Figure 3-6C and D). PGC-1α can be activated by cAMP in primary rat (19,38) and mouse hepatocytes (19) and synergistically by both cAMP and Dex (19,38). NaHS may increase endogenous cAMP level (Figure 3-5A) through the inhibition of PDE (3), leading to CREB activation and thus *pgc-1α* transcription (10). C/EBP-β was shown to directly induce *pgc-1α* transcription, *via* binding to its specific promoter region in both hamster kidney cells (30) and in mouse brown fat cells (12). C/EBP-β can be induced by the activation of the cAMP/PKA pathway as well as the GR pathway (1,20). Therefore, when the cAMP/PKA pathway was inhibited, NaHS could still stimulate PGC-1α expression *via* GR pathway-mediated C/EBP-β induction. Furthermore, C/EBP-β can directly up-regulate *pepck* and *g6pase* gene expression levels (1,15). In fact, GR is capable of directly inducing *pepck* transcription (1), thus increasing glucose production. Clearly, the cAMP/PKA and GR pathways work as an interconnected network to regulate PGC-1α expression. Maximal induction of NaHS-stimulated glucose production requires functional cAMP/PKA and GR pathways, whereby PGC-1α is the center piece of this signaling web. Therefore, we propose H_2S may increase gluconeogenesis through three main mechanisms. 1) H_2S upregulates the expression levels of PGC-1α and PEPCK *via*

glucocorticoid receptor pathway. 2) H_2S upregulates the expression level of PGC-1α through the activation of the cAMP/PKA pathway, as well as PGC-1α activity *via S*-sulfhydration. 3) H_2S upregulates the expression and the activities (by *S*-sulfhydration) of G6Pase and FBPase (Fig. 8).

A balanced and functionally intact CSE/H_2S system is important for the homeostasis of adaptive energy metabolism. A pathophysiologically over-activated CSE/H_2S system in the liver could pre-dispose an individual to metabolic syndrome because H_2S blocks insulin release from pancreatic β-cells (26,34) and inhibits insulin-stimulated glucose uptake into both fat (5) and liver (40) cells. In this regard, it has been reported that both CSE (8,39) and PGC-1α (10,14,38) are robustly upregulated in the liver under diabetic conditions. Correspondingly, it was demonstrated that the CSE protein is upregulated in insulin-resistant $HepG_2$ cells where $_{DL}$-propargylglycine treatment (a potent inhibitor of CSE activity) improved glucose consumption in these cells (40). In agreement, we previously reported that streptozotocin-induced diabetic CSE-KO mice exhibited a delayed onset to diabetic status (hyperglycemic, hypoinsulinemia, and insulin resistance) (35). Overall, these findings stress the importance of targeting an over-activated CSE/H_2S system in the insulin-resistance liver to prevent or attenuate the progress of metabolic syndrome.

The present study identifies key targets of the CSE/H_2S system in liver gluconeogenesis, deepening insight on hepatic glucose metabolism under physiological conditions and shedding light on the potential impact of endogenous H_2S on the dysregulated gluconeogenesis in metabolic syndrome.

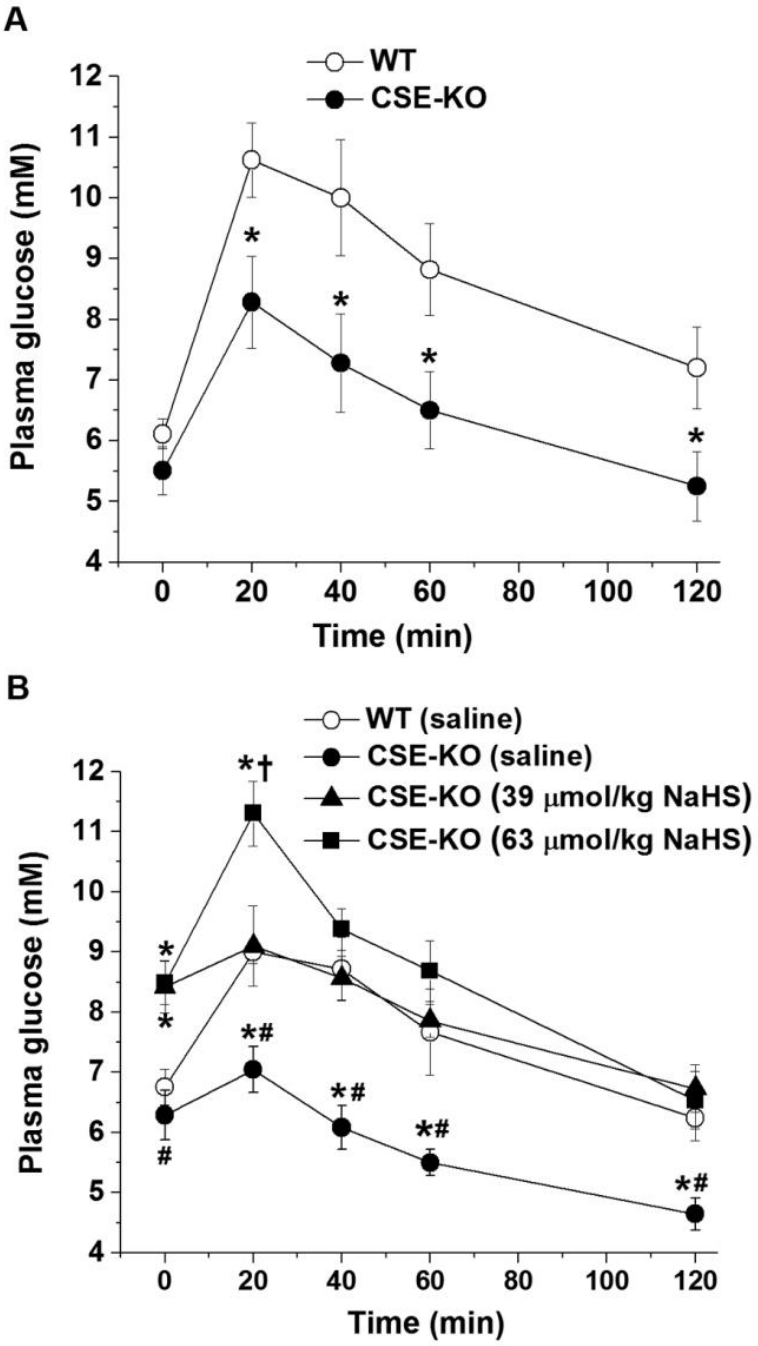
A
WT
CSE-KO
Plasma glucose (mM)
Time (min)
B
WT (saline)
CSE-KO (saline)
CSE-KO (39 μmol/kg NaHS)
CSE-KO (63 μmol/kg NaHS)
Plasma glucose (mM)
Time (min)

Figure 3-1. Gluconeogenesis in WT and CSE-KO mice. The rate of gluconeogenesis was determined *via* pyruvate tolerance test on overnight-fasted mice. **(A)** Mice were injected i.p. with 2 g/kg pyruvate at time 0. n = 7-11 for each group. **(B)** Mice were injected with NaHS or saline 10 min before pyruvate injection. Pyruvate injection was given at time 0. Blood glucose was measured with a One-Touch Glucometer. n = 5-9 for each group. Statistical analyses performed were: Student's *t*-test **(A)** and one-way ANOVA followed by a *post hoc* analysis (Tukey's test) **(B)**. $^{*}P < 0.05$ *vs.* respective WT group with or without saline injection; $^{\#}P < 0.05$ *vs*. respective CSE-KO (39 μmol/kg NaHS) group; $^{\dagger}P < 0.05$ *vs.* respective CSE-KO (39 μmol/kg NaHS) group.

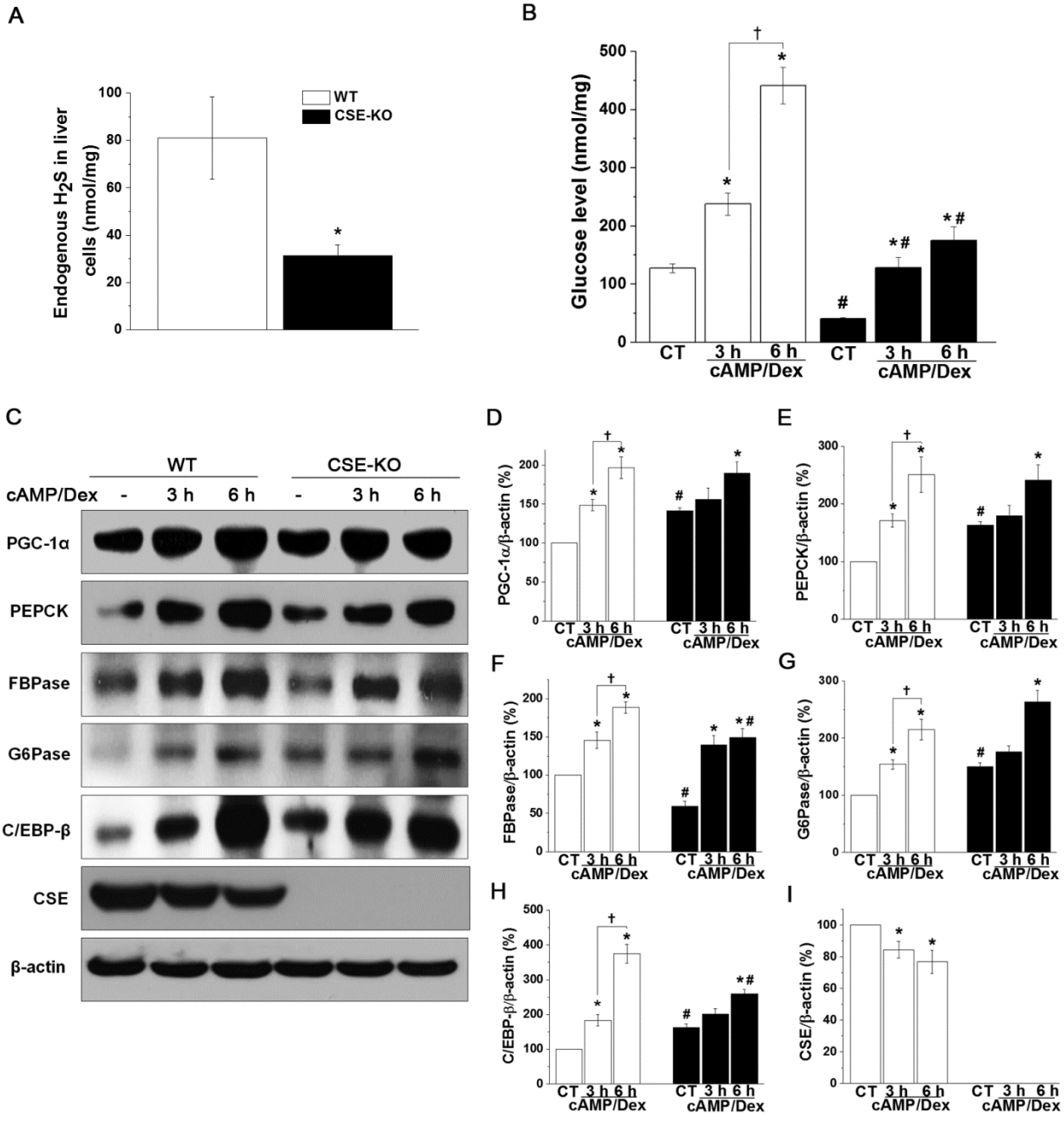
A
Endogenous H_2S in liver cells (nmol/mg)
WT
CSE-KO
B
Glucose level (nmol/mg)
CT
3 h
6 h
cAMP/Dex
C
WT
CSE-KO
cAMP/Dex
PGC-1α
PEPCK
FBPase
G6Pase
C/EBP-β
CSE
β-actin
D
PGC-1α/β-actin (%)
E
PEPCK/β-actin (%)
F
FBPase/β-actin (%)
G
G6Pase/β-actin (%)
H
C/EBP-β/β-actin (%)
I
CSE/β-actin (%)

Figure 3-2. Reduced glycemic response in CSE-KO liver cells treated with cAMP/Dex. Primary liver cells were isolated from overnight fasted 8-12 week-old WT and CSE-KO mice. **(A)** Endogenous H_2S level in WT and CSE-KO liver cells were determined *via in situ* methylene blue assay. n = 6-7 for each group. **(B)** Liver cells were treated with 1 mM 8-Br-cAMP and 1 μM Dex (dexamethasone) for 3 h or 6 h. Thereafter, the glucose level in these cells was measured with a glucose assay kit. n = 5-8 for each group. **(C)** Representative Western blot results of the changed expression levels of selective proteins in WT and CSE-KO liver cells with 8-Br-cAMP/Dex treatment. **(D-I)** Summary of the changed expression levels of selective proteins in WT and CSE-KO liver cells with 8-Br-cAMP/Dex treatment. The densities of selective proteins were normalized to that of β-actin and expressed as a percentage of untreated WT cells. PGC-1α: n = 6-9 for each group; PEPCK: n = 7-12 for each group; FBPase: n = 6-8 for each group; G6Pase: n = 7-9 for each group; C/EBP-β: n = 7-8 for each group; CSE: n = 5-6 for each group. Statistical analyses performed were: Student's t-test **(A and I)** and one-way ANOVA followed by a *post hoc* analysis (Tukey's test) **(B and D-H)**. $^{*}P < 0.05$ *vs*. corresponding control (CT) group; $^{\#}P < 0.05$ *vs*. corresponding WT group; $^{\dagger}P < 0.05$.

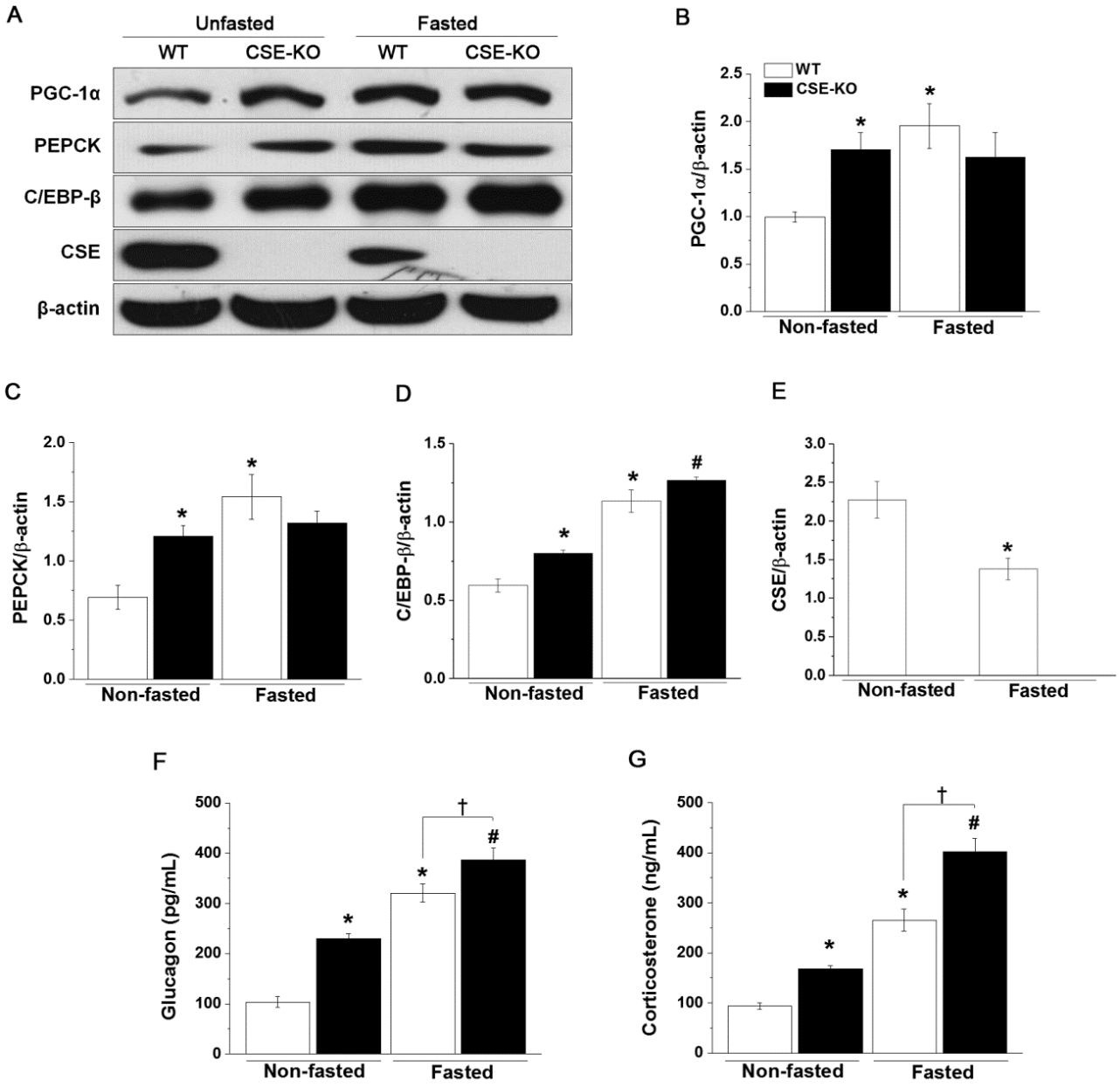
A
Unfasted
Fasted
WT
CSE-KO
WT
CSE-KO
PGC-1α
PEPCK
C/EBP-β
CSE
β-actin
B
WT
CSE-KO
PGC-1α/β-actin
Non-fasted
Fasted
C
PEPCK/β-actin
Non-fasted
Fasted
D
C/EBP-β/β-actin
Non-fasted
Fasted
E
CSE/β-actin
Non-fasted
Fasted
F
Glucagon (pg/mL)
Non-fasted
Fasted
G
Corticosterone (ng/mL)
Non-fasted
Fasted

Figure 3-3. Downregulation of CSE in fasted WT livers along with upregulation of gluconeogenic factors in livers and plasma in non-fasted CSE-KO mice. Liver extracts were harvested from non-fasted or 24 h fasted WT and CSE-KO mice. **(A)** Representative Western blot results of the changed expression levels of selective proteins in liver tissues from non-fasted and fasted WT and CSE-KO mice. **(B-E)** Summary of the changed expression levels of selective proteins in liver tissues from non-fasted and fasted WT and CSE-KO mice. Plasma glucagon **(F)** and corticosterone **(G)** levels were analyzed from mice after a 16 h fast. Glucagon: $n = 7$; corticosterone: $n = 6$. PGC-1α: $n = 6$-8 for each group; PEPCK: $n = 6$-7 for each group; C/EBP-β: $n = 9$ for each group; CSE: $n = 8$ for each group. Statistical analyses performed were: one-way ANOVA followed by a *post hoc* analysis (Tukey's test) **(B-D, F and G)** and Student's *t*-test **(E)**. $^{*}P < 0.05$ *vs.* non-fasted WT group; $^{\#}P < 0.05$ *vs.* non-fasted CSE-KO group.

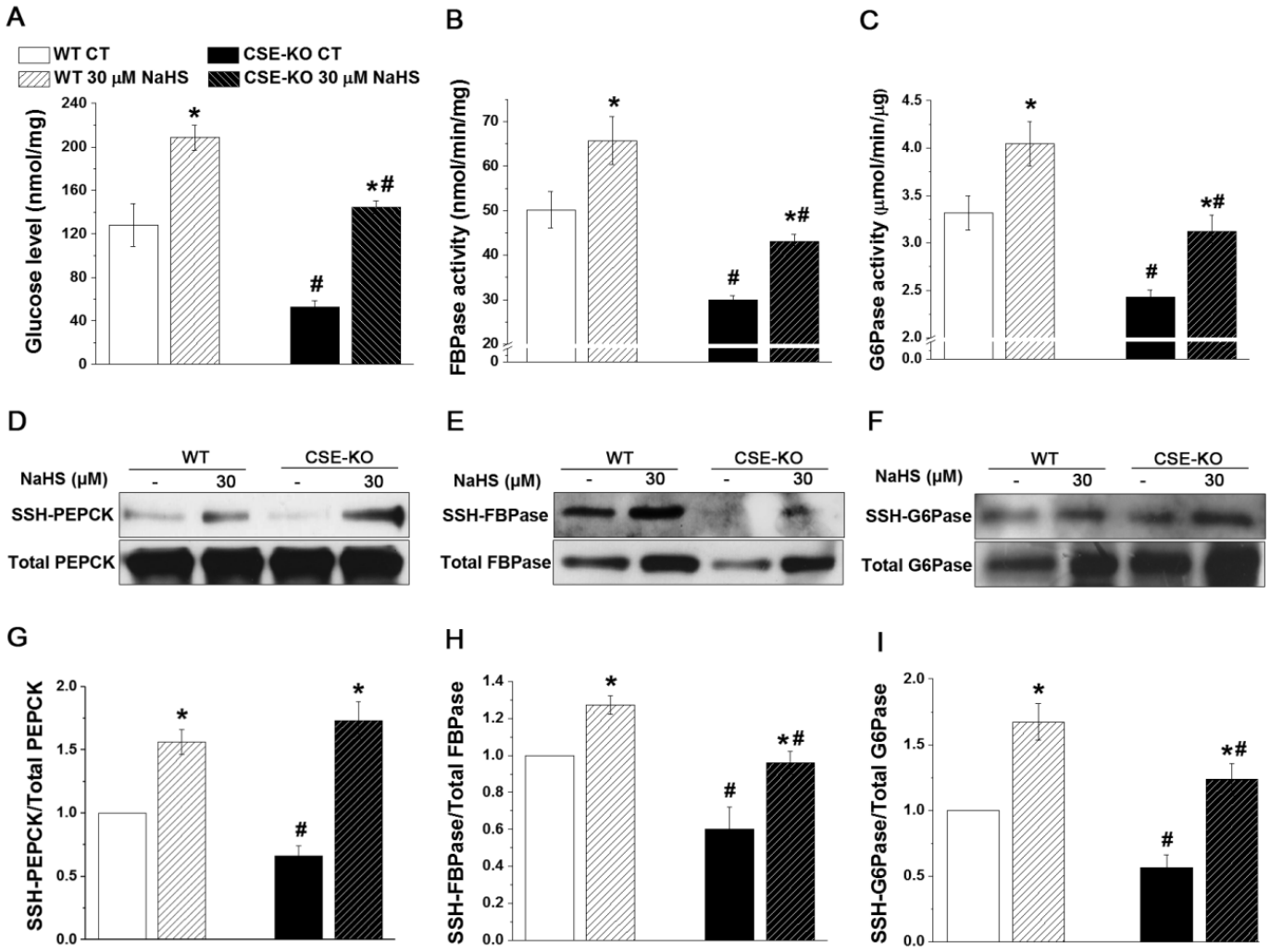
A
WT CT
WT 30 μM NaHS
CSE-KO CT
CSE-KO 30 μM NaHS
Glucose level (nmol/mg)
B
FBPase activity (nmol/min/mg)
C
G6Pase activity (μmol/min/μg)
D
NaHS (μM)
WT
CSE-KO
SSH-PEPCK
Total PEPCK
E
SSH-FBPase
Total FBPase
F
SSH-G6Pase
Total G6Pase
G
SSH-PEPCK/Total PEPCK
H
SSH-FBPase/Total FBPase
I
SSH-G6Pase/Total G6Pase

Figure 3-4. Exogenous H_2S enhanced glucose production and gluconeogenic enzyme activities, as well as *S*-sulfhydrated PEPCK, FBPase, and G6Pase in primary hepatocytes. Primary liver cells isolated from overnight fasted WT and CSE-KO mice were treated with 30 μM NaHS for 6 h. **(A)** Glucose levels in liver cells. n = 6-10 for each group. **(B, C)** The enzymatic activities of total FBPase and G6Pase, respectively, in whole cell lysates. For FBPase, n = 8 for each group. For G6Pase, n = 10-12 for each group. **(D-F)** Representative Western blot results of the *S*-sulfhydration (SSH) of selective proteins in WT and CSE-KO liver cells. **(G-I)** Summary of changed SSH expression levels of selective proteins in primary hepatocytes. The densities of selective SSH proteins were normalized to total selected protein and expressed as a fold change to that of untreated WT cells. PEPCK: n = 10 for each group; FBPase: n = 7-8 for each group; G6Pase: n = 6-7 for each group. Statistical analysis was performed using the one-way ANOVA followed by a *post hoc* analysis (Tukey's test). $^{*}P < 0.05$ *vs*. corresponding control (CT) group; $^{\#}P < 0.05$ *vs*. corresponding WT group.

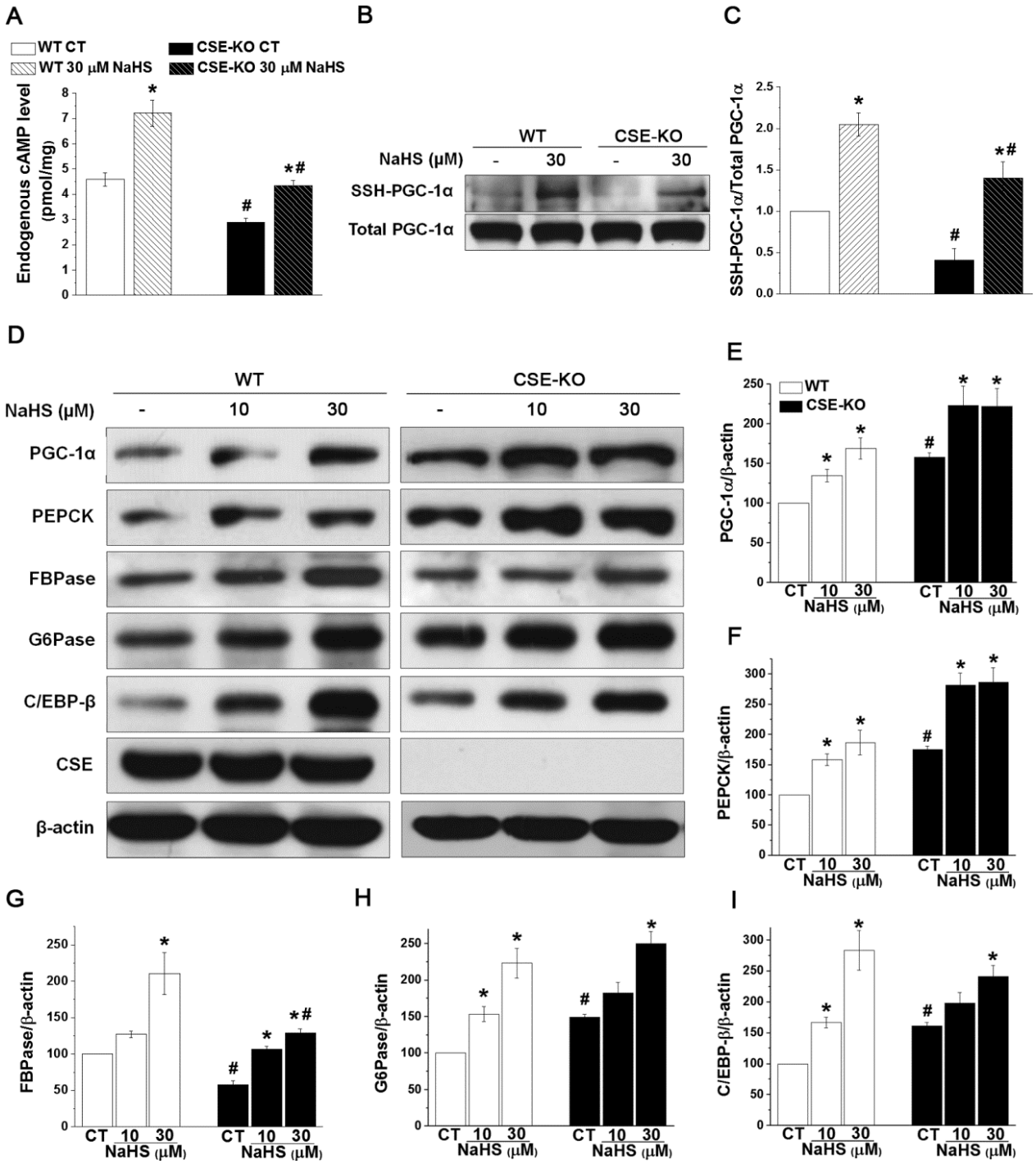
A
WT CT
WT 30 μM NaHS
CSE-KO CT
CSE-KO 30 μM NaHS
Endogenous cAMP level (pmol/mg)
B
WT
CSE-KO
NaHS (μM)
SSH-PGC-1α
Total PGC-1α
C
SSH-PGC-1α/Total PGC-1α
D
WT
CSE-KO
NaHS (μM)
PGC-1α
PEPCK
FBPase
G6Pase
C/EBP-β
CSE
β-actin
E
PGC-1α/β-actin
F
PEPCK/β-actin
G
FBPase/β-actin
H
G6Pase/β-actin
I
C/EBP-β/β-actin
CT 10 30
NaHS (μM)

Figure 3-5. Exogenous H_2S upregulated cAMP levels, induced PGC-1α *S*-sulfhydration, and increased protein levels of key gluconeogenic factors in isolated WT and CSE-KO hepatocytes. Primary liver cells isolated from fasted WT and CSE-KO mice were treated with 10 or 30 μM NaHS for 6 h. **(A)** Endogenous cAMP levels in whole cell lysates. n = 8-12 for each group. **(B)** Representative Western Blot result of SSH-PGC-1α in whole cell lysates. **(C)** Summary of the changed SSH expression level of PGC-1α in primary hepatocytes. The density of SSH-PGC-1α was normalized to total PGC-1α protein and expressed as a fold change to that of untreated WT cells. n = 5-7 for each group. **(D)** Representative Western blot results of the changed expression levels of selective proteins. **(E-I)** Summary of the changed expression levels of selective proteins. The densities of selective proteins were normalized to that of β-actin and expressed as a percentage of untreated WT cells. PGC-1α: n = 6-9 for each group; PEPCK: n = 8-12 for each group; FBPase: n = 6-8 for each group; G6Pase: n = 7-9 for each group; C/EBP-β: n = 7-9 for each group. Statistical analysis was performed using the one-way ANOVA followed by a *post hoc* analysis (Tukey's test). $^{*}P < 0.05$ *vs*. corresponding control (CT) group; $^{\#}P < 0.05$ *vs*. corresponding WT group.

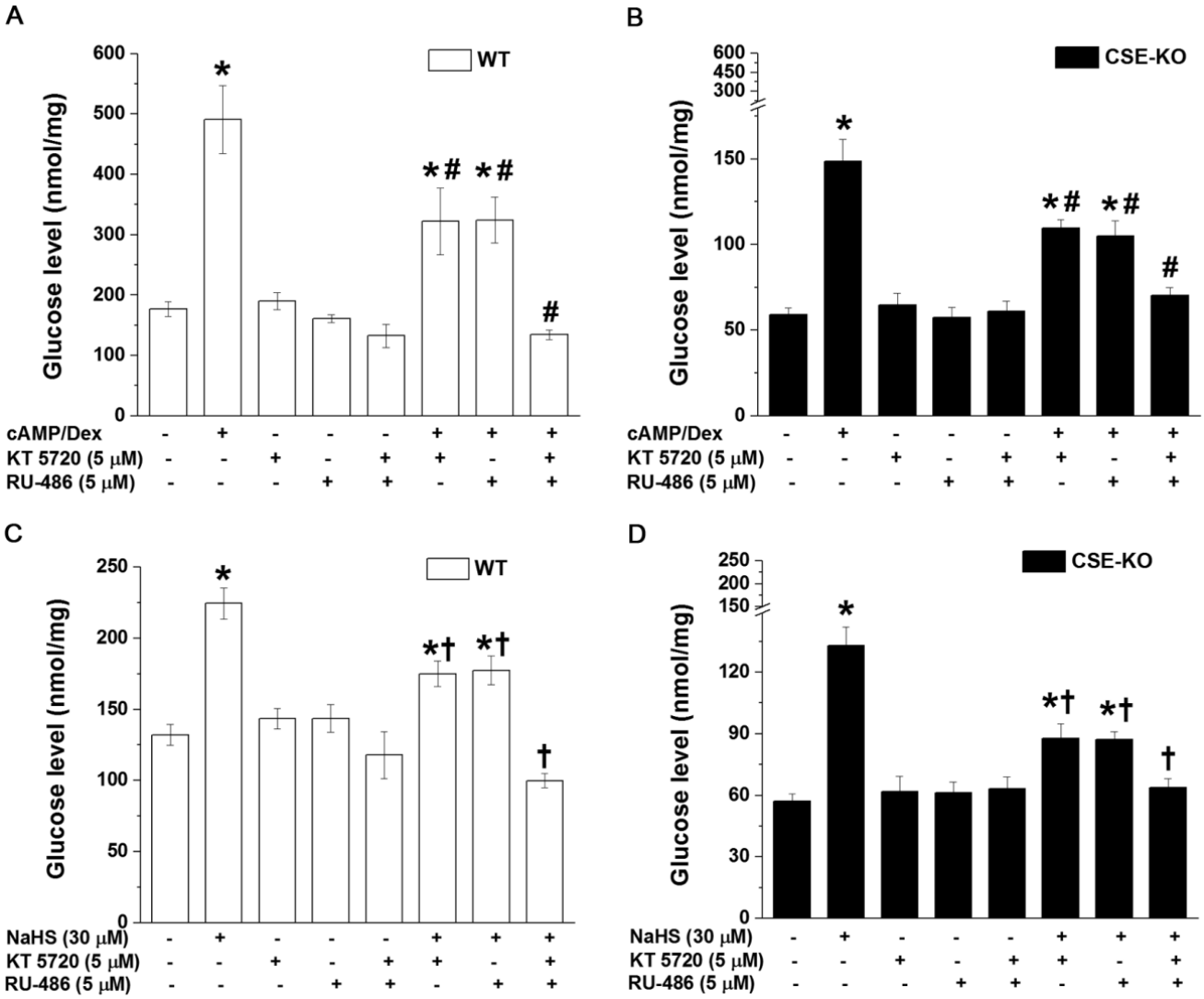
A
WT
Glucose level (nmol/mg)
600
500
400
300
200
100
0
*
*#
*#
#
cAMP/Dex - + - - - + + +
KT 5720 (5 μM) - - + - + + - +
RU-486 (5 μM) - - - + + - + +
B
CSE-KO
Glucose level (nmol/mg)
600
450
300
150
100
50
0
*
*#
*#
#
cAMP/Dex - + - - - + + +
KT 5720 (5 μM) - - + - + + - +
RU-486 (5 μM) - - - + + - + +
C
WT
Glucose level (nmol/mg)
250
200
150
100
50
0
*
*†
*†
†
NaHS (30 μM) - + - - - + + +
KT 5720 (5 μM) - - + - + + - +
RU-486 (5 μM) - - - + + - + +
D
CSE-KO
Glucose level (nmol/mg)
250
200
150
120
90
60
30
0
*
*†
*†
†
NaHS (30 μM) - + - - - + + +
KT 5720 (5 μM) - - + - + + - +
RU-486 (5 μM) - - - + + - + +

Figure 3-6. The roles of cAMP/PKA and glucocorticoid receptor in NaHS-induced glucose production in WT and CSE-KO liver cells. Primarily cultured liver cells were pretreated for 1 h with 5 μM KT 5720 (a PKA inhibitor) or 5 μM RU-486 (a glucocorticoid receptor inhibitor) prior to a 6 h treatment with 8-Br-cAMP/Dex (1 mM/1 μM) or NaHS (30 μM). The roles of cAMP/PKA and glucocorticoid receptor in 8-Br-cAMP/Dex-induced glucose production in WT **(A)** (n = 4-8 for each group) and CSE-KO **(B)** (n = 7-9 for each group) hepatocytes. The roles of cAMP/PKA and glucocorticoid receptor in NaHS-induced glucose production in WT **(C)** (n = 6-10 for each group) and CSE-KO **(D)** (n = 6-10 for each group) hepatocytes. Statistical analysis was performed using the one-way ANOVA followed by a *post hoc* analysis (Tukey's test). $^{*}P < 0.05$ *vs.* untreated cells; $^{\#}P < 0.05$ *vs.* cAMP/Dex-treated group; $^{\dagger}P < 0.05$ *vs.* 30 μM NaHS-treated group.

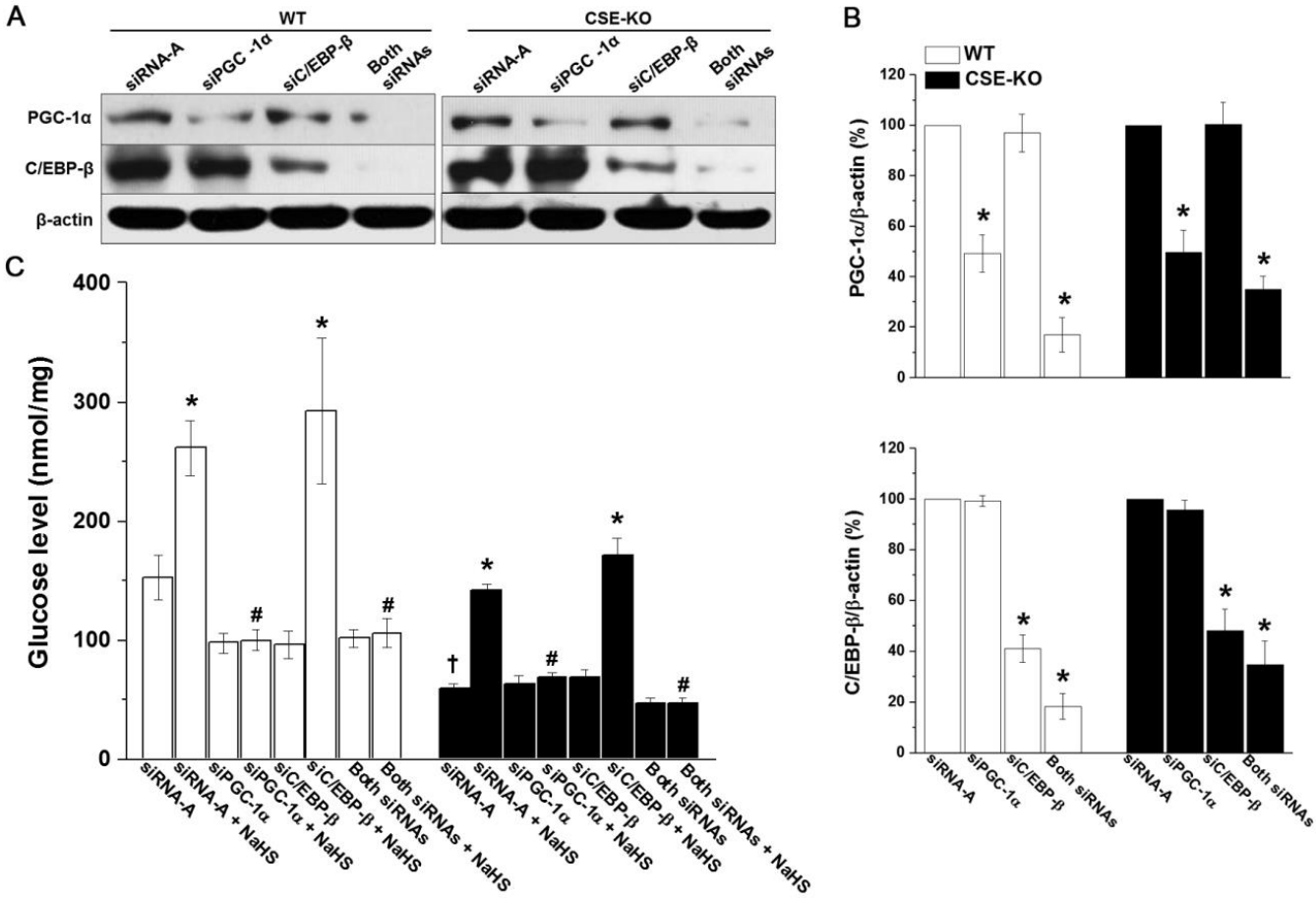
A
WT
CSE-KO
siRNA-A
siPGC -1α
siC/EBP-β
Both siRNAs
PGC-1α
C/EBP-β
β-actin
B
WT
CSE-KO
PGC-1α/β-actin (%)
C/EBP-β/β-actin (%)
C
Glucose level (nmol/mg)
siRNA-A
siRNA-A + NaHS
siPGC-1α
siPGC-1α + NaHS
siC/EBP-β
siC/EBP-β + NaHS
Both siRNAs
Both siRNAs + NaHS

Figure 3-7. NaHS-induced glucose production is dependent on PGC-1α in primary liver cells from WT and CSE-KO mice. Primary liver cells isolated from 8-12 week-old WT and CSE-KO mice were transfected with siRNA-A (control), siPGC-1α, siC/EBP-β, or both siPGC-1α and siC/EBP-β for 60 h. Lipofectamine RNAiMAX was used as the transfection reagent. **(A)** Representative Western blot results of the selected proteins in WT and CSE-KO liver cells. **(B)** Summary of the changes in the selected proteins in WT and CSE-KO liver cells with different treatments. The densities of the selected proteins were normalized to that of β-actin and expressed as a percentage of the corresponding siRNA-A transfected WT or CSE-KO liver cells. PGC-1α: n = 4-6 for each group; C/EBP-β: n = 4-6 for each group. **(C)** Glucose production in transfected liver cells. NaHS at 30 μM was used to treat the cells for 6 h and glucose production was measured *via* a glucose assay kit. n = 7-14 for each group. Statistical analyses performed were: Student's *t*-test **(B)** and one-way ANOVA followed by a *post hoc* analysis (Tukey's test) **(C)**. $^{*}P < 0.05$ *vs*. respective siRNA-A group; $^{\#}P < 0.05$ *vs*. respective 30 μM NaHS-treated group; $^{\dagger}P < 0.05$ *vs*. WT siRNA-A group. Both siRNAs: siPGC-1α and siC/EBP-β.

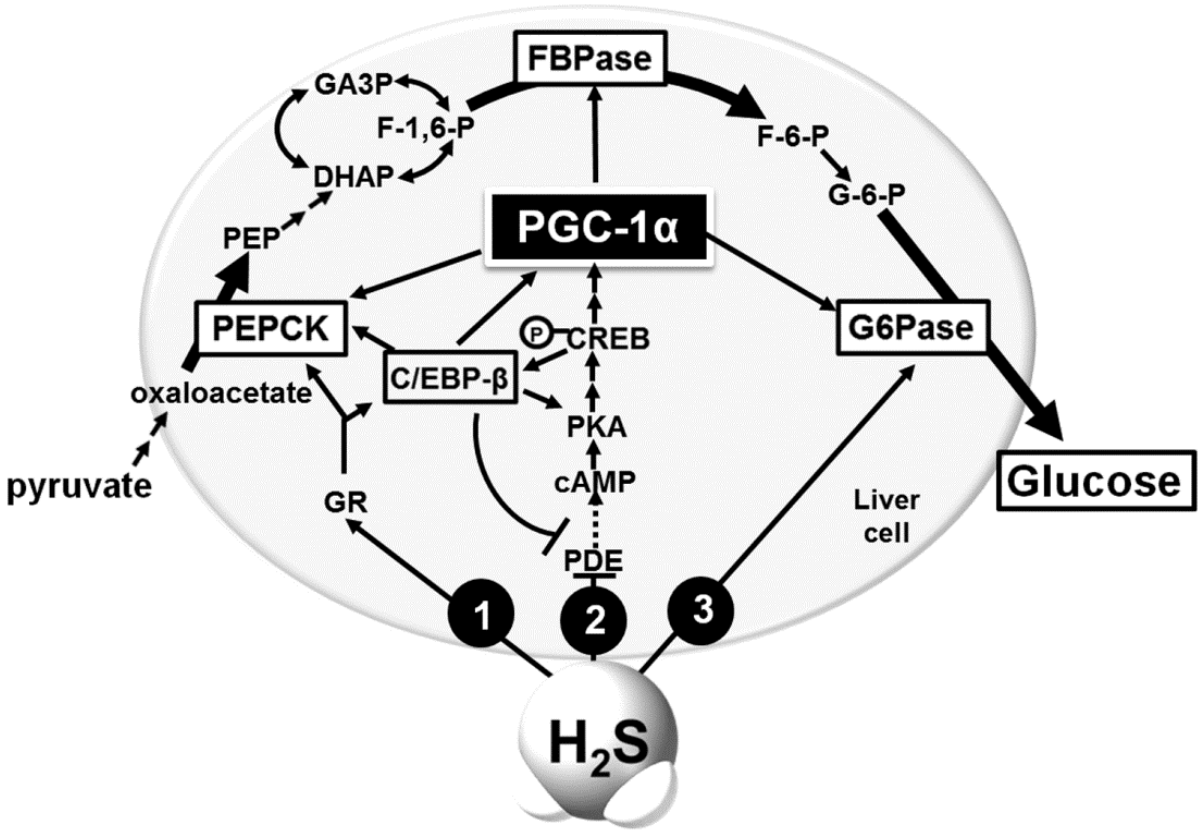
FBPase
GA3P
F-1,6-P
F-6-P
DHAP
G-6-P
PEP
PGC-1α
PEPCK
CREB
G6Pase
C/EBP-β
oxaloacetate
PKA
pyruvate
cAMP
Glucose
GR
Liver
cell
PDE
1
2
3
H2S

Figure 3-8. Schematic representation of H_2S-induced glucose production and the proposed underlying mechanisms. Endogenous H_2S stimulates liver glucose production *via* three underlying mechanisms: 1) the glucocorticoid receptor-mediated upregulation of PGC-1α and PEPCK; 2) the cAMP/PKA-mediated upregulation of PGC-1α, as well as PGC-1α activity *via* S-sulfhydration; and 3) the increased expression and activities (*via* S-sulfhydration) of FBPase and G6Pase. Solid arrows represent either stimulation or the direction of the metabolic reactions. Dotted arrows represent degradation reactions. C/EBP-β: CCAAT-enhancer-binding proteins-β; P-CREB: phosphorylated cAMP response element binding protein; DHAP: dihydroxyacetone phosphate; F-1,6-P: fructose-1,6-bisphosphate; F-6-P: fructose-6-phosphate; FBPase: fructose-1,6-bisphosphatase; G-6-P: glucose-6-phosphate, G6Pase: glucose-6-phosphatase; GA3P: glyceraldehyde 3-phosphate; H_2S: hydrogen sulfide; PDE: phosphodiesterase; PEP: phosphoenolpyruvate; PEPCK: phosphoenolpyruvate carboxykinase; PGC-1α: peroxisome proliferator-activated receptor-γ coactivator-1α; PKA: protein kinase A.

SUPPLEMENTARY DATA

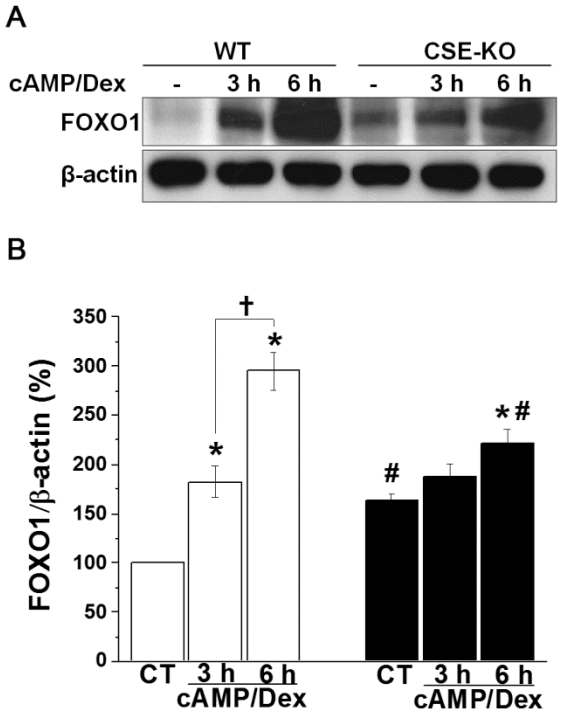

Supplementary Figure 3-1. Impaired glycemic response to cAMP/Dex-stimulated FOXO1 upregulation in primary CSE-KO hepatocytes. Primary liver cells isolated from overnight fasted 8-12 week-old WT and CSE-KO mice were treated with 1 mM 8-Br-cAMP and 1 μM Dex (dexamethasone) for 3 h or 6 h. **(A)** Representative Western blot result of the changed expression level of FOXO1 in WT and CSE-KO liver cells with 8-Br-cAMP/Dex treatment. **(B)** Summary of the changed expression level of FOXO1 in WT and CSE-KO liver cells. The density of FOXO1 was normalized to that of β-actin and expressed as a percentage to that of untreated WT cells. n = 8-9 for each group. Statistical analysis was performed using the one-way ANOVA followed by a *post hoc* analysis (Tukey's test). $^{*}P < 0.05$ *vs*. corresponding control (CT) group; $^{\#}P < 0.05$ *vs*. corresponding WT group; $^{\dagger}P < 0.05$.

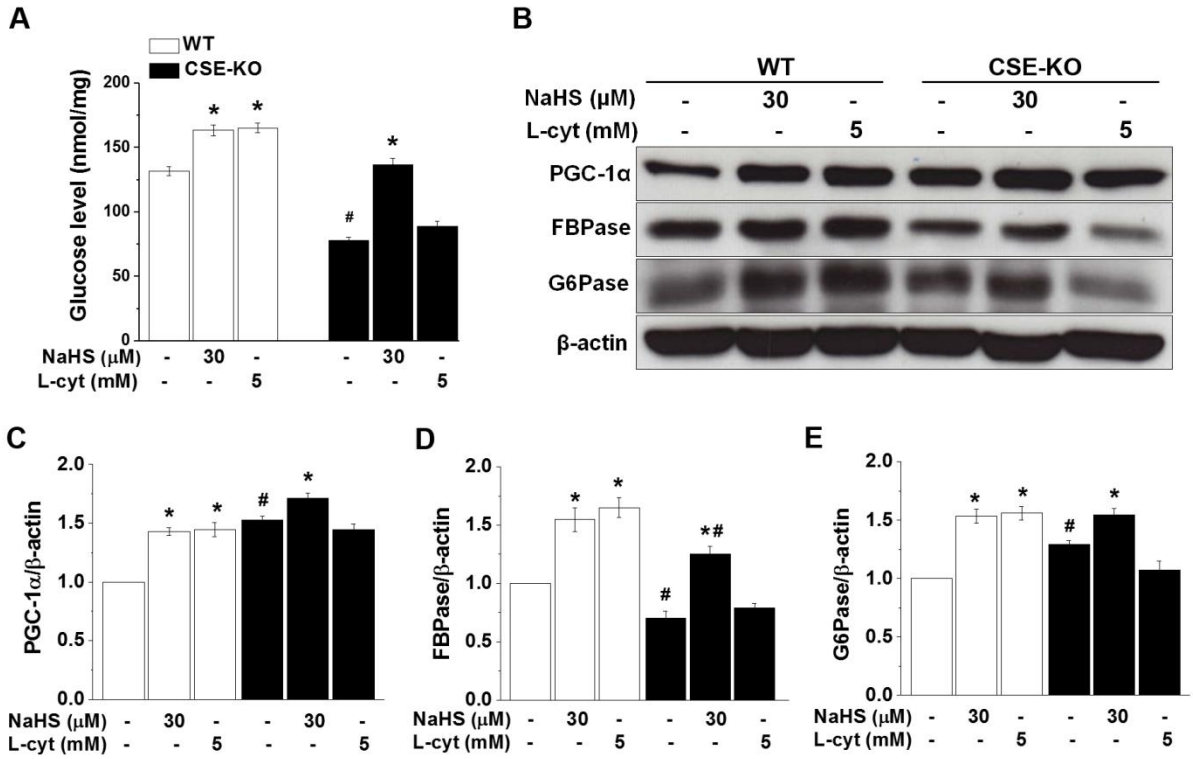

Supplementary Figure 3-2. Exogenous $_{L}$-cysteine has no effect on gluconeogenesis in primary CSE-KO hepatocytes. Primary liver cells isolated from overnight fasted WT and CSE-KO mice were treated with 30 μM NaHS or 5 mM $_{L}$-cysteine for 24 h. **(A)** Glucose level in liver cells. n = 12 for each group. **(B)** Representative Western blot results of the changed expression levels of selective proteins. **(C)** Summary of the changed expression levels. The densities of the selected proteins were normalized to that of β-actin and expressed as a percentage to that of untreated WT cells. PGC-1α: n = 11-9 for each group; FBPase and G6Pase: n = 7-8 for each group. Statistical analysis was performed using the one-way ANOVA followed by a *post hoc* analysis (Tukey's test). *$P < 0.05$ *vs*. corresponding control (CT) group; $^{\#}P < 0.05$ *vs*. corresponding WT group. $_{L}$-cyt: $_{L}$-cysteine.

REFERENCES

1. Arizmendi C, Liu S, Croniger C, Poli V, Friedman JE. The transcription factor CCAAT/enhancer-binding protein beta regulates gluconeogenesis and phosphoenolpyruvate carboxykinase (GTP) gene transcription during diabetes. *J Biol Chem* 274: 13033-40, 1999.
2. Bosch F, Sabater J, Valera A. Insulin inhibits liver expression of the CCAAT/enhancer-binding protein beta. *Diabetes* 44: 267-71, 1995.
3. Bucci M, Papapetropoulos A, Vellecco V, Zhou Z, Pyriochou A, Roussos C, Roviezzo F, Brancaleone V, Cirino G. Hydrogen sulfide is an endogenous inhibitor of phosphodiesterase activity. *Arterioscler Thromb Vasc Biol* 30: 1998-2004, 2010.
4. Dhar A, Dhar I, Jiang B, Desai KM, Wu L. Chronic methylglyoxal infusion by minipump causes pancreatic beta-cell dysfunction and induces type 2 diabetes in Sprague-Dawley rats. *Diabetes* 60: 899-908, 2011.
5. Feng X, Chen Y, Zhao J, Tang C, Jiang Z, Geng B. Hydrogen sulfide from adipose tissue is a novel insulin resistance regulator. *Biochem Biophys Res Commun* 380: 153-9, 2009.
6. Finck BN, Kelly DP. PGC-1 coactivators: inducible regulators of energy metabolism in health and disease. *J Clin Invest* 116: 615-22, 2006.
7. Fu M, Zhang W, Wu L, Yang G, Li H, Wang R. Hydrogen sulfide (H2S) metabolism in mitochondria and its regulatory role in energy production. *Proc Natl Acad Sci U S A* 109: 2943-8, 2012.
8. Hargrove JL, Trotter JF, Ashline HC, Krishnamurti PV. Experimental diabetes increases the formation of sulfane by transsulfuration and inactivation of tyrosine aminotransferase in cytosols from rat liver. *Metabolism* 38: 666-72, 1989.
9. Harper AE. Glucose-6-phosphatase. In: *Methods of Enzymatic Analysis*. edited by Bergmeyer H. New York, NY: Academic Press; 1963. pp. 788-92.
10. Herzig S, Long F, Jhala US, Hedrick S, Quinn R, Bauer A, Rudolph D, Schutz G, Yoon C, Puigserver P, Spiegelman B, Montminy M. CREB regulates hepatic gluconeogenesis through the coactivator PGC-1. *Nature* 413: 179-83, 2001.
11. Kabil O, Vitvitsky V, Xie P, Banerjee R. The quantitative significance of the transsulfuration enzymes for H2S production in murine tissues. *Antioxid Redox Signal* 15: 363-72, 2011.
12. Kajimura S, Seale P, Kubota K, Lunsford E, Frangioni JV, Gygi SP, Spiegelman BM. Initiation of myoblast to brown fat switch by a PRDM16-C/EBP-beta transcriptional complex. *Nature* 460: 1154-8, 2009.
13. Kartha RV, Zhou J, Hovde LB, Cheung BW, Schroder H. Enhanced detection of hydrogen sulfide generated in cell culture using an agar trap method. *Anal Biochem* 423: 102-8, 2012.
14. Koo SH, Satoh H, Herzig S, Lee CH, Hedrick S, Kulkarni R, Evans RM, Olefsky J, Montminy M. PGC-1 promotes insulin resistance in liver through PPAR-alpha-dependent induction of TRB-3. *Nat Med* 10: 530-4, 2004.
15. Lin J, Wu PH, Tarr PT, Lindenberg KS, St-Pierre J, Zhang CY, Mootha VK, Jager S, Vianna CR, Reznick RM, Cui L, Manieri M, Donovan MX, Wu Z, Cooper MP, Fan MC, Rohas LM, Zavacki AM, Cinti S, Shulman GI, Lowell BB, Krainc D, Spiegelman BM. Defects in adaptive energy metabolism with CNS-linked hyperactivity in PGC-1alpha null mice. *Cell* 119: 121-35, 2004.

16. Longo-Sorbello GSA, Saydam, G., Banerjee, D., Bertino, J.R. . Cytotoxicity and Cell Growth Assays. In: *Cell Biology. A Laboratory Handbook*. edited by Celis JE. Burlington, MA: Elsevier Academic Press; 2006. pp. 315-24.
17. Mani S, Li H, Yang G, Wu L, Wang R. Deficiency of cystathionine gamma-lyase and hepatic cholesterol accumulation during mouse fatty liver development. *Science Bulletin* 60: 336-347, 2015.
18. Mani S, Untereiner A, Wu L, Wang R. Hydrogen sulfide and the pathogenesis of atherosclerosis. *Antioxid Redox Signal* 20: 805-17, 2014.
19. Manmontri B, Sariahmetoglu M, Donkor J, Bou Khalil M, Sundaram M, Yao Z, Reue K, Lehner R, Brindley DN. Glucocorticoids and cyclic AMP selectively increase hepatic lipin-1 expression, and insulin acts antagonistically. *J Lipid Res* 49: 1056-67, 2008.
20. Matsuno F, Chowdhury S, Gotoh T, Iwase K, Matsuzaki H, Takatsuki K, Mori M, Takiguchi M. Induction of the C/EBP beta gene by dexamethasone and glucagon in primary-cultured rat hepatocytes. *J Biochem* 119: 524-32, 1996.
21. Merino B, Alonso-Magdalena P, Lluesma M, Neco P, Gonzalez A, Marroqui L, Garcia-Arevalo M, Nadal A, Quesada I. Pancreatic alpha-cells from female mice undergo morphofunctional changes during compensatory adaptations of the endocrine pancreas to diet-induced obesity. *Sci Rep* 5: 11622, 2015.
22. Mustafa AK, Gadalla MM, Sen N, Kim S, Mu W, Gazi SK, Barrow RK, Yang G, Wang R, Snyder SH. H2S signals through protein S-sulfhydration. *Sci Signal* 2: ra72, 2009.
23. Niehof M, Manns MP, Trautwein C. CREB controls LAP/C/EBP beta transcription. *Mol Cell Biol* 17: 3600-13, 1997.
24. Park EA, Gurney AL, Nizielski SE, Hakimi P, Cao Z, Moorman A, Hanson RW. Relative roles of CCAAT/enhancer-binding protein beta and cAMP regulatory element-binding protein in controlling transcription of the gene for phosphoenolpyruvate carboxykinase (GTP). *J Biol Chem* 268: 613-9, 1993.
25. Rodgers JT, Lerin C, Haas W, Gygi SP, Spiegelman BM, Puigserver P. Nutrient control of glucose homeostasis through a complex of PGC-1alpha and SIRT1. *Nature* 434: 113-8, 2005.
26. Tang G, Zhang L, Yang G, Wu L, Wang R. Hydrogen sulfide-induced inhibition of L-type Ca2+ channels and insulin secretion in mouse pancreatic beta cells. *Diabetologia* 56: 533-41, 2013.
27. Untereiner AA, Dhar A, Liu J, Wu L. Increased renal methylglyoxal formation with downregulation of PGC-1alpha-FBPase pathway in cystathionine gamma-lyase knockout mice. *PLoS One* 6: e29592, 2011.
28. Walker PR. Glycogen metabolism in adult rat liver parenchymal cell primary cultures. *J Cell Physiol* 91: 169-79, 1977.
29. Walker PR, Grindle MJ. Effects of hormones and serum on glycogen metabolism in adult rat liver parenchymal cell primary cultures. *J Cell Physiol* 91: 181-91, 1977.
30. Wang H, Peiris TH, Mowery A, Le Lay J, Gao Y, Greenbaum LE. CCAAT/enhancer binding protein-beta is a transcriptional regulator of peroxisome-proliferator-activated receptor-gamma coactivator-1alpha in the regenerating liver. *Mol Endocrinol* 22: 1596-605, 2008.
31. Wang R. Two's company, three's a crowd – Can H2S be the third endogenous gaseous transmitter. *FASEB J* 16: 1792-1798, 2002.

32. Wang X, Jia X, Chang T, Desai K, Wu L. Attenuation of hypertension development by scavenging methylglyoxal in fructose-treated rats. *J Hypertens* 26: 765-72, 2008.
33. Woo YC, Xu A, Wang Y, Lam KS. Fibroblast growth factor 21 as an emerging metabolic regulator: clinical perspectives. *Clin Endocrinol (Oxf)* 78: 489-96, 2013.
34. Wu L, Yang W, Jia X, Yang G, Duridanova D, Cao K, Wang R. Pancreatic islet overproduction of H2S and suppressed insulin release in Zucker diabetic rats. *Lab Invest* 89: 59-67, 2009.
35. Yang G, Tang G, Zhang L, Wu L, Wang R. The pathogenic role of cystathionine gamma-lyase/hydrogen sulfide in streptozotocin-induced diabetes in mice. *Am J Pathol* 179: 869-79, 2011.
36. Yang G, Wu L, Jiang B, Yang W, Qi J, Cao K, Meng Q, Mustafa AK, Mu W, Zhang S, Snyder SH, Wang R. H2S as a physiologic vasorelaxant: hypertension in mice with deletion of cystathionine gamma-lyase. *Science* 322: 587-90, 2008.
37. Yang W, Yang G, Jia X, Wu L, Wang R. Activation of KATP channels by H2S in rat insulin-secreting cells and the underlying mechanisms. *J Physiol* 569: 519-31, 2005.
38. Yoon JC, Puigserver P, Chen G, Donovan J, Wu Z, Rhee J, Adelmant G, Stafford J, Kahn CR, Granner DK, Newgard CB, Spiegelman BM. Control of hepatic gluconeogenesis through the transcriptional coactivator PGC-1. *Nature* 413: 131-8, 2001.
39. Yusuf M, Kwong Huat BT, Hsu A, Whiteman M, Bhatia M, Moore PK. Streptozotocin-induced diabetes in the rat is associated with enhanced tissue hydrogen sulfide biosynthesis. *Biochem Biophys Res Commun* 333: 1146-52, 2005.
40. Zhang L, Yang G, Untereiner A, Ju Y, Wu L, Wang R. Hydrogen sulfide impairs glucose utilization and increases gluconeogenesis in hepatocytes. *Endocrinology* 154: 114-26, 2013.
41. Zhao W, Zhang J, Lu Y, Wang R. The vasorelaxant effect of H(2)S as a novel endogenous gaseous K(ATP) channel opener. *EMBO J* 20: 6008-16, 2001.

CHAPTER 4

STIMULATORY EFFECT OF THE CSE/H_2S SYSTEM ON HEPATIC MITOCHONDRIAL BIOGENESIS AND THE UNDERLYING MECHANISMS

Ashley A. Untereiner,[1,2,3] Ming Fu,[1,4] YoungJun Ju,[1,5] Rui Wang,[1,4] Katalin Módis,[1,4] and Lingyun Wu[1,2,3,*]

[1] The Cardiovascular and Metabolic Research Unit, Lakehead University, ON, Canada

[2]Department of Health Sciences, Lakehead University, ON, Canada

[3]Thunder Bay Regional Research Institute, ON, Canada

[4]Department of Biology, Laurentian University, ON, Canada

[5]Department of Kinesiology, Lakehead University, ON, Canada

This chapter is in preparation to be submitted as a manuscript to

British Journal of Pharmacology (I.F: 4.842).

Contents of this chapter have been formatted to fit the writing and reference guidelines outlined by the *British Journal of Pharmacology*. The references for this chapter are separately listed at the end of this chapter.

ABSTRACT

BACKGROUND AND PURPOSE

We previously showed that hydrogen sulfide (H_2S) upregulates peroxisome proliferator-activated receptor-γ coactivator (PGC)-1α in primary hepatocytes. PGC-1α is a crucial regulator of mitochondrial biogenesis, a process required to maintain cellular energy homeostasis. We investigated the regulation of hepatic mitochondrial biogenesis by cystathionine γ-lyase (CSE)-generated H_2S under physiological conditions.

EXPERIMENTAL APPROACH

Primary hepatocytes isolated from CSE knockout (KO) and wild-type (WT) mice were used in all experiments. mtDNA (mitochondrial DNA) and mRNA levels were measured *via* real-time PCR. Protein *S*-sulfhydration was determined *via* a modified biotin switch assay. MitoTracker Green was used to quantify mitochondrial content and distribution.

KEY RESULTS

CSE-KO hepatocytes produced less mtDNA compared to WT hepatocytes. Mitochondrial content was decreased in CSE-KO hepatocytes compared to normal hepatocytes, which was restored with NaHS (an H_2S donor) treatment. CSE-KO hepatocytes exhibited lower levels of mitochondrial transcription factors and the mitochondrial transcription coactivator, peroxisome proliferator-activated receptor-γ coactivator-related protein (PPRC) compared to WT hepatocytes. NaHS administration upregulated PPRC, yet downregulated PGC-1β protein level in mouse hepatocytes. Exogenous H_2S induced the S-sulfhydration of PPRC, which was lower in untreated CSE-KO hepatocytes, but not that of PGC-β. Finally, knockdown of either PGC-1α or PPRC significantly decreased NaHS-stimulated mitochondrial biogenesis in hepatocytes, where knockdown of both genes were required to abolish NaHS-induced mitochondrial biogenesis.

CONCLUSIONS AND IMPLICATIONS

Endogenous H_2S-induced liver mitochondrial biogenesis is dependent upon PGC-1α and PPRC signaling in primary hepatocytes. This study may offer clues to the regulation of energy homeostasis under physiological conditions as well as mitochondrial dysregulation.

Keywords: H_2S ● PPRC ● PGC-1α ● mitochondrial biogenesis ● mouse hepatocytes

INTRODUCTION

Mitochondria are highly specialized double membrane organelles that serve a fundamental role in energy production. These intracellular powerhouses generate energy by converting monosaccharide (i.e. glucose) into ATP *via* oxidative phosphorylation. One of the main mechanisms used to accommodate the energy demands of the cell is the initiation and regulation of mitochondrial biogenesis (the growth and division of pre-existing mitochondria). Mitochondrial biogenesis is a complex process governed by a distinguished set of nuclear-encoded transcription factors assisted by transcriptional coactivators. The former group includes nuclear respiratory factor (NRF)-1 and NRF-2 (also known as GABA); whereas the latter set involves the members of the peroxisome proliferator-activated receptor-γ coactivator (PGC) family, including PGC-1α, PGC-β, and peroxisome proliferator-activated receptor-γ coactivator-related protein (PPRC) (Xu *et al.* 2013). This interconnected network of nuclear-encoded transcription factors and transcriptional coactivators allows the cell to maintain and manage the cell's energy-harvesting capacity to meet its energetic demands. Mitochondrial biogenesis is influenced by environmental factors such as caloric restriction, exercise, cold temperatures, as well as cell division and differentiation (Jornayvaz & Shulman, 2010). Evidently, given the crucial role the mitochondria have in energy homeostasis, reduced mitochondrial content (Morino et al. 2005) and mitochondrial genes (Mootha *et al.* 2003; Patti *et al.* 2003) have been linked to age-related diseases such as insulin resistance and type 2 diabetes.

Recently, we demonstrated that the gasotransmitter hydrogen sulfide (H_2S) (Wang, 2002) regulates the expression and activity of PGC-1α in primary liver cells (Untereiner *et al.* 2015). H_2S is endogenously produced in liver cells primarily by cystathionine γ-lyase (CSE) and to a lesser extent by cystathionine β-synthetase (CBS) and 3-mercaptopyruvate sulfurtransferase (Kabil *et al.* 2011). H_2S is involved in an array of physiological systems (Mani *et al.* 2013; Mani

et al. 2015; Untereiner *et al* 2015; Wang, 2012; Yang *et al.* 2008), where among these include the regulation of mitochondrial function. By sensing the oxygen levels in the cytosol, cytosolic CSE translocates into mitochondria to promote H_2S production, subsequently maintaining mitochondrial ATP production under hypoxic conditions in smooth muscle cells (Fu *et al.* 2012). Additionally, liver ischemia promoted the accumulation of CBS proteins in mitochondria resulting in increased H_2S production, which prevented Ca^{2+}-mediated mitochondrial cytochrome *c* release and hypoxia-induced-reactive oxygen species generation (Teng *et al.* 2013). Furthermore, H_2S can act as an inorganic electron donor to complex II, a component of the electron transport chain (ETC) (Modis *et al.* 2013). The donation of electrons from oxidized H_2S was shown to promote mitochondrial ATP generation and support cellular bioenergetics in primary mouse hepatocytes (Modis *et al.* 2013).

The literature reports that the other gasotransmitters, nitric oxide (NO) and carbon monoxide (CO) are involved in adaptive oxidative metabolism by optimizing mitochondrial biogenesis in brown adipocytes (Nisoli *et al.* 2003) and in cardiac tissues (Suliman *et al.* 2007). In fact, both of these gasotransmitters induced PGC-1α activity to upregulate mitochondrial biogenesis. Additionally, NO was shown to upregulate PPRC-mediated induction of mitochondrial biogenesis and respiration in two human cell models of oncocytic thyroid tumours (XTC.UC1 and B-CPAP cell lines) (Raharijaona *et al.* 2009). Therefore, we hypothesized that endogenous H_2S is an important modulator for hepatic mitochondrial biogenesis through the regulation of critical mitochondrial transcriptional coactivator(s) (i.e. PGC-1α, PPRC). In the present study, we investigated whether or not endogenous H_2S stimulates mitochondrial biogenesis and if this mechanism is dependent upon the PGC family, including PGC-1α, PGC-1β, and PPRC in primary hepatocytes.

MATERIALS and METHODS

Animal handling

CSE-KO mice were generated and home-bred as previously described (Yang *et al.* 2008). Eight to twelve-week-old male CSE-KO mice and age-matched male WT mice were used. All animal experiments were conducted in compliance with the Guide for the Care and Use of Laboratory Animals published by the US National Institutes of Health (NIH Publication no. 85-23, revised 1996) and approved by the Animal Care Committee of Lakehead University, Canada. Mice were fed standard rodent chow *ab libitum* with free access to water before isolation of primary liver cells.

Hepatocyte preparation

Primary hepatocytes were isolated from CSE-KO and WT mice as described elsewhere (Zhang *et al.* 2013) with modification. In brief, mouse livers were perfused through the inferior vena cava with a buffer consisting of the following: 140 mM NaCl, 2.6 mM KCl, 0.28 mM Na_2HPO_4, 5 mM glucose, and 10 mM HEPES (pH 7.4). The perfusion was started for 7 min with the buffer supplemented with 0.5 mM EGTA and then for 10 min with the buffer containing 5 mM $CaCl_2$ and 100 U/ml collagenase type IV (Worthington, Lakewood, NJ). The isolated hepatocytes were filtered on nylon mesh (100 μm pore size), and selected by centrifugation in a 26% percoll isodensity gradient and then seeded in medium containing DMEM (5.5 mM glucose), 10% fetal bovine serum (FBS), and 1X penicillin-streptomycin-neomycin. After 2 h at 37ºC in a humidified atmosphere of 5% CO_2, the medium was removed and replaced with DMEM (5.5 mM glucose) supplemented with 10% FBS and 1X penicillin-streptomycin-neomycin. Cell viability was measured *via* trypan blue staining and only cell preparations above 95% of viability were used in experiments.

Endogenous H_2S level

The endogenous H_2S level was measured by the *in situ* methylene blue assay as described elsewhere (Kartha *et al.* 2012) (please see Chapter 2 for method details).

Mitochondrial DNA quantification

Mitochondrial DNA (mtDNA) was quantified *via* real-time PCR analysis of total genomic DNA as described elsewhere (Biesecker *et al.* 2003; Duncan *et al.* 2007; LeBleu *et al.* 2014). Briefly, primary hepatocytes isolated from WT or CSE-KO mice were plated onto collagen I-coated 100 mm petri dishes at a density of 3.3×10^6 cells/plate and maintained in DMEM (5.5 mM glucose) supplemented with 1X penicillin-streptomycin-neomycin and 10% FBS. After 24 h in cell culture, total genomic DNA was extracted from cultured WT and CSE-KO primary hepatocytes *via* QIAamp kit (Qiagen). Total DNA was recorded with a fluorimeter, whereby 50 ng of genomic DNA was amplified in a 25 μL PCR reaction containing SYBR Green PCR Master Mix (Bio-Rad, Mississauga, ON) and 40 nM of each primer. Real-time PCR was performed in an iCycler iQ5apparatus (Bio-Rad) associated with the iCycler optical system software (version 3.1). mtDNA per nuclear genome was calculated by determining the relative levels of a mitochondrial gene (cytochrome b) to a nuclear gene (β-actin). Primer sequences for cytochrome b (cyto b) and β-actin are listed in Table 4-1.

Detection of mitochondrial content

The ratio of the mitochondrial distribution was determined by measuring the fluorescent intensity of MitoTracker Green FM (Molecular Probes, Life Technologies Ltd, Burlington, ON) to Hoechst 33342 (Molecular Probes) in live primary hepatocytes. Briefly, with or without

incubation with 30 μM NaHS for 24 h, liver cells were incubated with 2 μg/mL Hoechst 33342 dye for 30 min at 37ºC, washed twice, then with 50 nM MitoTracker Green FM for 30 min at 37°C. Cells were washed three times with phosphate buffered saline following observation under an inverted Olympus IX70 fluorescent microscope (Tokyo, Japan) or *via* Multiskan Spectrum (MitoTracker Green, 485/520 nm; Hoechst, 350/460 nm).

Real-time PCR

After treatment with or without NaHS (30 μM) for 6 h, the medium was aspirated, and primary liver cells were washed with ice-cold PBS. Afterwards, total RNA was isolated using TRIzol (Sigma), and treated with RNase-free DNase (New England BioLabs). RNA purity and integrity were verified by A260/A280 measurements (Agilent 2100 Biosystem, Mississauga, Ontario, Canada) and by 1% agarose-formaldehyde denaturing gel, respectively. Reverse transcription was performed using the SuperScript First-Strand Synthesis system (Invitrogen). The relative abundance of mRNA in each sample was measured by real-time PCR in a fluorescent temperature cycler (iQ5 Real-Time PCR Detection System) with SYBR Green PCR Master Mix (Bio-Rad), as described previously (Untereiner *et al.* 2011). Mouse primers for PGC-1β, PPRC, Tfam, NRF-1, NRF-2, Na^+/K^+, ATPase-a5 (ATP1a5), and β-actin were used, and the sequences are listed in Table 2-1 on page 55. The specificity of PCR was determined by melt-curve analysis for each reaction. The relative difference in mRNA between samples was calculated using the arithmetic formula $2^{-\Delta\Delta CT}$.

Western blot analysis

Primary hepatocytes were treated with or without NaHS (30 μM) for 24 h. Thereafter, cells were washed twice with ice-cold 1X PBS and harvested in PBS supplemented with protease cocktail solution (1:100). Samples were sonicated three times (10 s/each) on ice using a cell sonicator (Sonic Dismembrator Model 100; Fisher Scientific) and centrifuged at 12,000 rpm for 20 mins at 4ºC. Protein concentration was determined *via* BCA method. Equal amount of proteins was boiled in 1 X SDS sample buffer (62.5 mM Tris-HCl, pH 6.8, 2% SDS, 10% glycerol, 50 mM DTT, and 0.01% bromophenol blue). Total liver cell lysates (10-50 μg per lane) were separated by standard 7.5% SDS/PAGE and then transferred onto PVDF membranes (Millipore) and probed with selected primary antibodies. The primary antibody dilutions were 1:1,000 for anti-PGC-1α (Novus Biologicals, Oakville, ON, Canada), anti-PGC-1β, and anti-CSE (Abnova, Walnut, USA), 1:200 for anti-PPRC and 1:10,000 for anti-β-actin antibodies (Santa Cruz Biotechnology, Santa Cruz, CA). HRF-conjugated secondary antibodies were used at 1:10,000. Immunoreactions were visualized by enhanced chemiluminescence and exposed to X-ray film (Kodak Scientific Imaging Film). Densitometric quantification was determined *via* ImageJ Software (National Institutes of Health).

The modified biotin switch assay

The assay was conducted as described elsewhere (Mustafa *et al.* 2009; Untereiner *et al.* 2015) (please see Chapter 2 for method details).

Gene silencing with siRNA

Primary liver cells were transfected with 100 nM siRNA-A (control), siPGC-1α, siPPRC, or both siPGC-1α and siPPRC for 60 h. The siRNA complexes were diluted in Opti-MEM media (Invitrogen, Burlington, ON, Canada) and Lipofectamine® RNAi/MAX Reagent (Invitrogen) was used as the transfection reagent.

Chemicals and statistical analysis

All chemicals, enzymes, and primers used in this study were obtained from Sigma-Aldrich (Oakville, ON, Canada) unless otherwise stated. siRNA products were obtained from Santa Cruz Biotechnology (Santa Cruz, CA) and antibodies were purchased from Abcam (Burlington, ON, Canada) unless otherwise specified. All data sets are presented as mean ± S.E.M. For primary liver cell experiments, *n* value designates the number of mice used in the experiments. Results were analyzed using Student's *t*-test, or one-way ANOVA followed by a *post hoc* analysis (Tukey's test) when applicable. Statistical significance was set at $P < 0.05$.

RESULTS

H_2S induces mitochondrial biogenesis in primary hepatocytes

CSE is the dominant H_2S-generating enzyme in the liver (Kabil *et al.* 2011). Primary hepatocytes isolated from CSE-KO mice showed a marked reduction in endogenous H_2S level, 32% of that in cultured WT primary hepatocytes (Figure 4-1A). Interestingly, relative mtDNA content was significantly reduced in cultured CSE-KO hepatocytes by 33% compared to normal cells (Figure 4-1B). In agreement, we found that basal mitochondrial content was significantly lower in cultured CSE-KO liver cells than those of WT liver cells, whereas 30 μM NaHS treatment significantly increased mitochondrial mass in both primary liver cells (Figure 4-2A-B). Additionally, both endogenous and exogenous H_2S upregulated at transcription levels of nuclear-encoded transcription factors (NRF-1 and NRF-2), a mitochondrial transcription factor (Tfam), as well as a subunit of complex V (ATP1a5) (Figure 4-2C).

H_2S upregulates the expression and activity of PPRC and downregulates PGC-1β in primary hepatocytes

It is well established that the PGC family orchestrates mitochondrial biogenesis (Andreux *et al.* 2013; Jornayvaz & Shulman, 2010). Recently we demonstrated that H_2S increased the protein level of PGC-1α in primary hepatocytes (Untereiner *et al.* 2015). Therefore, we sought to determine the potential role H_2S may have in regulating the expression levels of PGC-1β and PPRC in hepatocytes. We found basal PPRC mRNA level to be 57% lower, whereas basal PGC-1β mRNA level was 158% higher in untreated CSE-KO hepatocytes that those in untreated WT hepatocytes (Figure 4-3A). In agreement, basal PPRC protein expression level was 44% lower, and basal PGC-1β expression level was 169% higher in untreated CSE-KO liver cells than their

respective basal levels in untreated WT liver cells (Figure 4-3B-D). Stimulation with 30 μM NaHS for 6 h increased PPRC and decreased PGC-1β mRNA levels in both WT and CSE-KO hepatocytes (Figure 4-3A). Moreover, 24 h treatment with 30 μM NaHS significantly enhanced the protein level of PPRC and lowered the protein level of PGC-1β in both WT and CSE-KO hepatocytes (Figure 4-3B-D). For instance, PPRC protein levels were elevated by 47% and 83% and PGC-1β protein levels were reduced by 34% and 82% in NaHS-treated WT and CSE-KO primary hepatocytes, respectively (Figure 4-3B-D).

Recently, we demonstrated that both endogenous and exogenous H_2S increased the sulfhydrated form of PGC-1α in isolated primary hepatocytes (Untereiner *et al.* 2015). The same results were obtained in this study (Figure 4-4A). We further found the basal *S*-sulfhydrated (SSH) form of PPRC to be significantly lower in untreated CSE-KO hepatocytes than that in untreated WT hepatocytes (Figure 4-4B and D). Treatment with 30 μM NaHS for 24 h significantly increased SSH-PPRC protein content in both WT and CSE-KO primary liver cells (Figure 4-4B and D). The *S*-sulfhydrated form of PGC-1β, on the other hand, was not detected by the biotin switch assay (Figure 4-4C).

H_2S-induced mitochondrial biogenesis is dependent on both PGC-1α and PPRC signaling in WT and CSE-KO hepatocytes

To determine whether H_2S-stimulated hepatic mitochondrial biogenesis observed in Figures 4-1 and 4-2 was mediated by PGC-1α and/or PPRC, we transfected WT and CSE-KO primary liver cells with siPGC-1α, siPPRC, or both siPGC-1α and siPPRC for 60 h. These maneuvers significantly knocked down the expression of the respective genes (Figure 4-5A-C). Transfection with either siPGC-1α or siPPRC significantly reduced 30 μM NaHS-stimulated

mitochondrial biogenesis in both WT and CSE-KO hepatocytes when compared to their respective 30 μM NaHS-treated siRNA control groups (Figure 4-5D and E). Interestingly, the induction of NaHS-stimulated mitochondrial biogenesis was completely abolished in co-transfected siPGC-1α and siPPRC WT and CSE-KO primary hepatocytes (Figure 4-5D and E).

DISCUSSION

The present study focused on the crucial role of H_2S in hepatic mitochondrial biogenesis under physiological conditions. CSE-KO mice, with diminished hepatic H_2S production, displayed significantly reduced mtDNA content along with lower cellular mitochondrial content (Figure 4-1 and 4-2). Cultured primary liver cells isolated from CSE-KO mice produced significantly lower mRNA levels of mitochondrial transcription factors (i.e. NRF-1, NRF-2, Tfam), as well as a subunit of complex V (ATP1a5) than WT liver cells (Figure 4-2). Thus, we demonstrated that endogenous H_2S stimulates the transcription of mitochondrial genes in mouse liver, leading to increased mitochondrial biogenesis. Our results also reveal the vital roles of PPRC and PGC-1α in H_2S-induced hepatic mitochondrial mass. One intriguing discovery from our study is the differential responses of H_2S on the members of the PGC family. In comparison with WT hepatocytes, we observed higher levels of PGC-1β in untreated CSE-KO hepatocytes (Figure 4-3 and 4-4), whereby exogenously applied H_2S inhibited the expression of PGC-1β. On the other hand, H_2S upregulated the expression levels of PPRC (Figure 4-3 and 4-4). Furthermore, H_2S selectively mediated the *S*-sulfhydration of PPRC, not PGC-1β, in primary hepatocytes (Figure 4-5). This study not only shows that endogenous H_2S is an important player in hepatic mitochondrial biogenesis but also demonstrates the specific stimulatory role of endogenous H_2S in the regulation of PGC-1β and PPRC.

To investigate the liver-specific effect of H_2S on glucose production, we have used primarily isolated and cultured hepatocytes from CSE-KO and WT mice. Under these conditions, we found that endogenous H_2S upregulated mtDNA content along with the transcription factors that govern mtDNA production, such as NRF-1, NRF-2, and Tfam in primary liver cells (Figure 4-1 and 4-2). Reduced mitochondrial content (Morino *et al.* 2005) and specific mitochondrial-encoded genes (Mootha *et al.* 2003; Patti *et al.* 2003) have been

linked to age-related diseases such as insulin resistance and type 2 diabetes. An early feature in the pathogenesis of type 2 diabetes is the reduction in mitochondrial oxidative and phosphorylation activity, leading to the accumulation of lipids in the hepatocyte, eventually resulting in mitochondrial dysfunction (Andreux *et al.* 2013; Kotronen *et al.* 2008). In fact, the anti-diabetic drugs pioglitazone (Bogacka *et al.* 2005; Fujisawa *et al.* 2009) and rosiglitazone (Fujisawa *et al.* 2009) induced mitochondrial biogenesis in subcutaneous adipose tissue taken from type 2 diabetic patients (Bogacka *et al.* 2005) and in high glucose-treated human umbilical vein endothelial cells (Fujisawa *et al.* 2009) *via* enhancing PGC-1α, NRF-1, and Tfam levels. Insulin resistance and type 2 diabetes are commonly associated with fatty liver disease (Firneisz, 2014). CSE-KO mice fed a high-fat diet (HFD) for 12 weeks developed hepatic injury (i.e. higher aspartate aminotransferase, alanine aminotransferase, and alkaline phosphatase levels) and fatty liver compared to the HFD-fed WT mice (Mani *et al.* 2015). The HFD-fed CSE-KO mice exhibited a metabolic defect that severely affected the clearance of excess dietary fat from the liver, suggesting that mitochondrial fatty acid oxidation was compromised. Overall, the downregulation of mtDNA and its critical mitochondrial transcription factors suggest impairment in the mitochondrial biogenesis and function in CSE-KO liver cells; whereby nutrient overload or environment stress could exacerbate mitochondrial dysregulation.

The PGC family consists of three members, PGC-1α, PGC-1β, and the more distant cousin, PPRC. These three coactivators regulate a broad spectrum of mitochondrial genes and promote mitochondrial biogenesis (Finck & Kelly, 2006; Hock & Kralli, 2009). The PGC proteins contain leucine-rich motifs and a conserved tetrapeptide motif (DHDY) which enable interaction with NRF-1 and NRF-2, respectively, and are thereby recruited to target regulatory sites to initiate transcription of mitochondrial genes (Hock & Kralli, 2009). Recently, our

laboratory demonstrated a link between endogenous H_2S and PGC-1α expression level in both mouse renal tissues (Untereiner *et al.* 2011) and isolated primary hepatocytes (Untereiner *et al.* 2015). In the present study, we focused on the regulatory role of endogenous H_2S on PGC-1β and PPRC expression and activity levels in primary hepatocytes. We found that both endogenous and exogenous H_2S upregulated the mRNA and protein levels of PPRC and downregulated the mRNA and protein level of PGC-1β in WT and CSE-KO liver cells (Figure 2 and 3). Both PGC-1β and PPRC modulate mitochondrial biogenesis but do so under different physiological stimuli leading to different metabolic characteristics. For instance, PGC-1β is induced *via* short-term high-fat feeding (Lin *et al.* 2005), whereas PPRC is upregulated by serum stimulation (Andersson & Scarpulla, 2001). Mitochondrial respiration stimulated by PGC-1β is tightly coupled than PPRC-mediated stimulation (St-Pierre *et al.* 2003), indicating that fewer protons (H^+) leak across the inner mitochondrial membrane and into the intermembrane space (*via* uncoupling proteins), and thereby produces heat instead of ATP. How H_2S regulates PGC-1β and PPRC are unclear. Unlike PGC-1α, the upstream factors that govern the gene upregulation of PGC-1β and PPRC are currently unknown. However, what is intriguing is the selective regulation of PGC-1β and PPRC by H_2S stimulation and the impact this may do for lipogenesis and cell proliferation studies.

Moreover, we also demonstrated that H_2S selectively augmented the *S*-sulfhydration of PPRC, not PGC-1β, in both primary WT and CSE-KO hepatocytes (Figure 4). Protein sulfhydration is a physiological post-transcriptional modification of cysteine residues in the target protein that leads to enhanced protein function (Mustafa *et al.* 2009). Currently, it is unclear whether or not PPRC activity is regulated *via* post-transcriptional modification. Therefore, we propose a novel mechanism by which PPRC activity is regulated at the post-

translational level *via S*-sulfhydration in primary hepatocytes, thus inducing mitochondrial biogenesis.

Both PGC-1α and PPRC are crucial for NaHS-induced mitochondrial biogenesis. Transfection of either siPGC-1α or siPPRC partially lowered NaHS-induced increase in mitochondrial mass, whereas co-transfection of both siPGC-1α and siPPRC completely abolished NaHS effects on mitochondrial biogenesis in both WT and CSE-KO primary hepatocytes (Figure 5). Needless to say, maximal induction of NaHS-stimulated mitochondrial biogenesis requires functional PGC-1α and PPRC signaling pathways in primary hepatocytes. Therefore, we propose endogenous H_2S-induced mitochondrial biogenesis occurs *via* stimulation of PPRC and PGC-1α activity (*via S*-sulfhydration), which induces the upregulation of NRF-1, NRF-2, and consequently Tfam, eventually leading to higher mitochondrial mass in primary hepatocytes (Figure 6).

The present study identifies key targets of the CSE/H_2S system in liver mitochondrial biogenesis, deepening insight on the regulation of hepatic energy homeostasis under physiological conditions and shedding light on the potential impact of endogenous H_2S on mitochondrial dysregulation in insulin-resistant diseases.

Table 4-1: Real-time PCR primer sequences used to quantify mtDNA in mouse hepatocytes

Short name	Forward primer 5´-3´	Reverse primer 5´-3´
cyto b	CCACTTCATCTTACCA-TTTATTATCGC	TTTTATCTGCATCTGAG-TTTAATCCTGT
β-actin	CTGCCTGACGGCCAGG	CTATGGCCTCAGGAGTTTTGTC

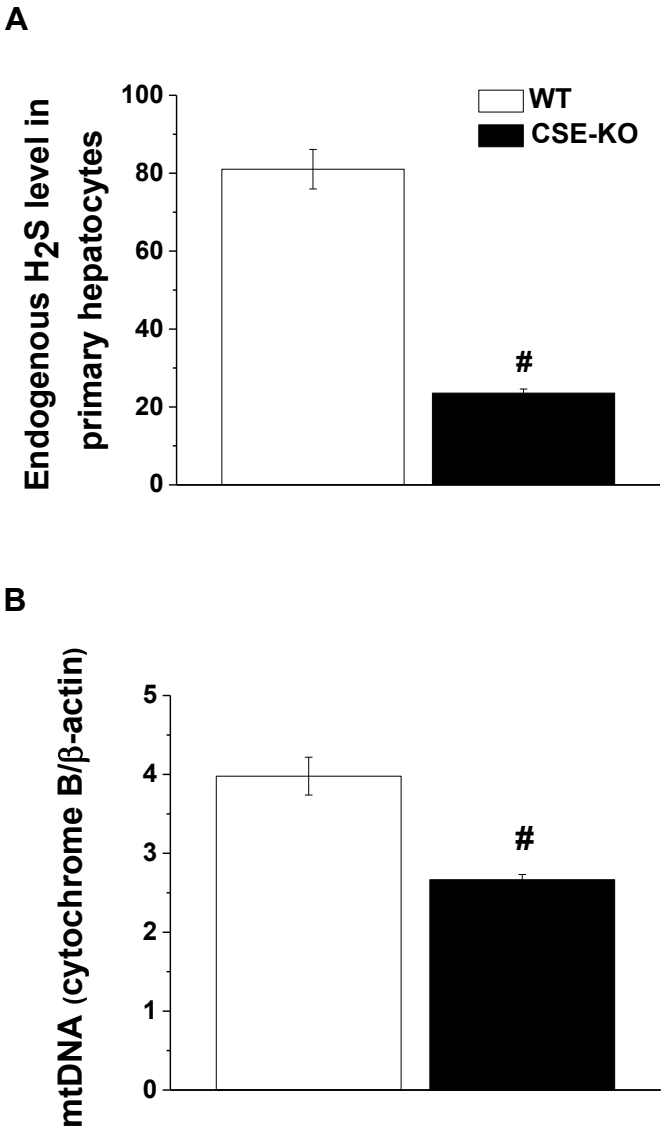

Figure 4-1: Reduced endogenous H_2S production and mtDNA transcripts in CSE-KO primary hepatocytes. Primary liver cells isolated from 8-12 week-old WT and CSE-KO mice were incubated for 24 h. **A)** Endogenous H_2S level was measured *via in situ* methylene blue assay. $n = 5$ for each group. **B)** Relative mtDNA level was calculated as the ratio of cytochrome b DNA to β-actin DNA quantity *via* q-PCR as described in Materials and Methods. $n = 5$-6 for each group. Statistical analysis was performed using the Student's *t*-test. $^{\#}P < 0.05$ *versus* WT group.

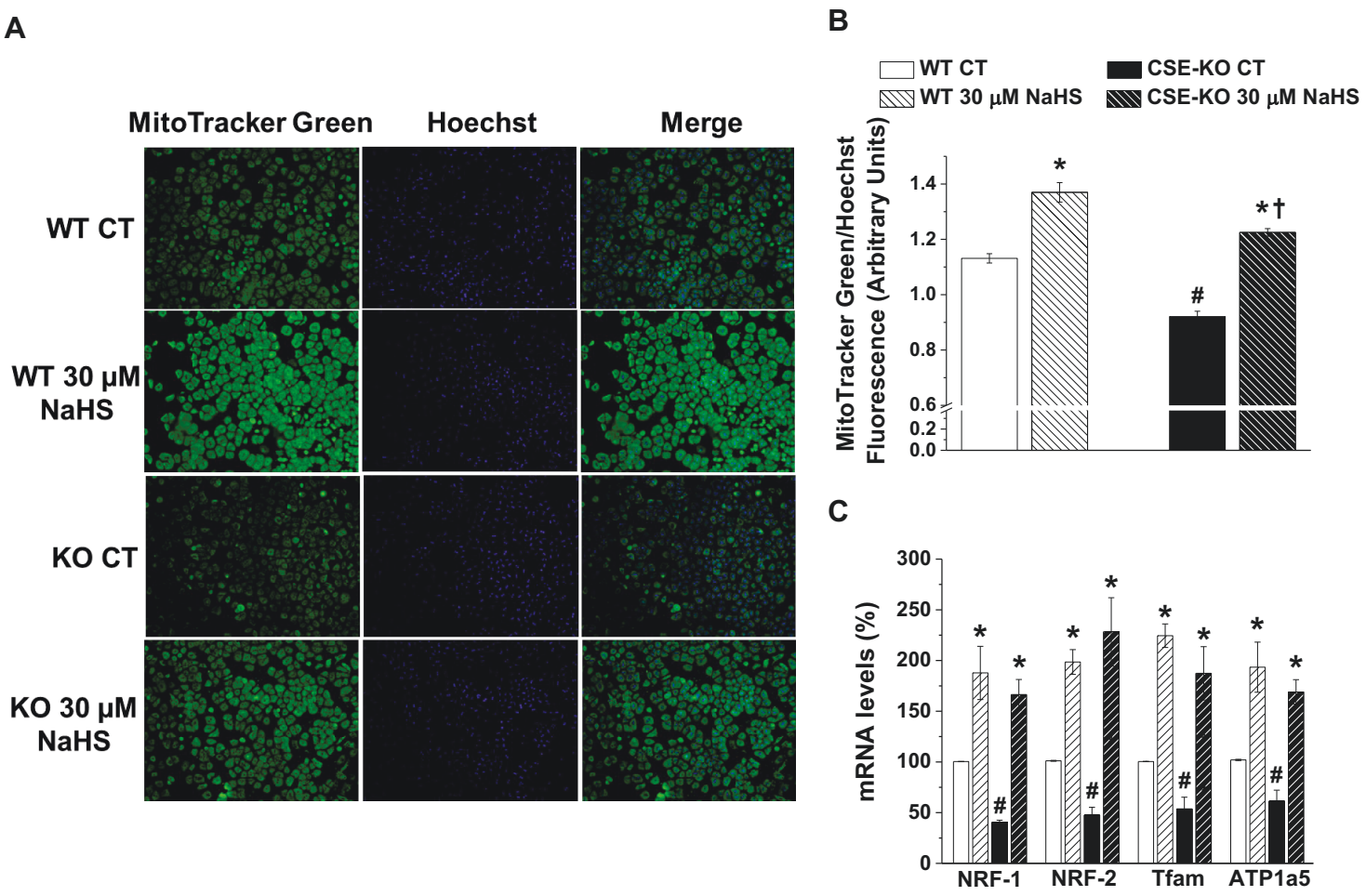

Figure 4-2: Endogenous and exogenous H_2S modulates mitochondrial biogenesis in primary hepatocytes isolated from WT and CSE-KO mice. Primary liver cells isolated from 8-12 week-old WT and CSE-KO mice were treated with or without 30 μM NaHS for 6 h. **A)** Liver hepatocytes were stained with MitoTracker Green FM (50 nM) and Hoechst (2 μg/mL) whereby the fluorescence intensity was measured by an inverted Olympus IX70 microscope. **B)** The ratio of the fluorescence of MitoTracker Green FM (485/520 nm) to Hoechst (350/460 nm) was used to quantify cellular mitochondrial content and distribution *via a* spectrophotometer. *n* = 6 for each group. **C)** Total cellular RNA was isolated and converted to cDNA. Gene

expression levels were analyzed by q-PCR and normalized to β-actin. n = 5-6 for each group. Statistical analysis was performed using the one-way ANOVA followed by a *post hoc* analysis (Tukey's test). $^{*}P < 0.05$ *versus* respective CT (control) group; $^{\#}P < 0.05$ *versus* WT CT group; $^{\dagger}P < 0.05$ *versus* 30 μM NaHS-treated WT group.

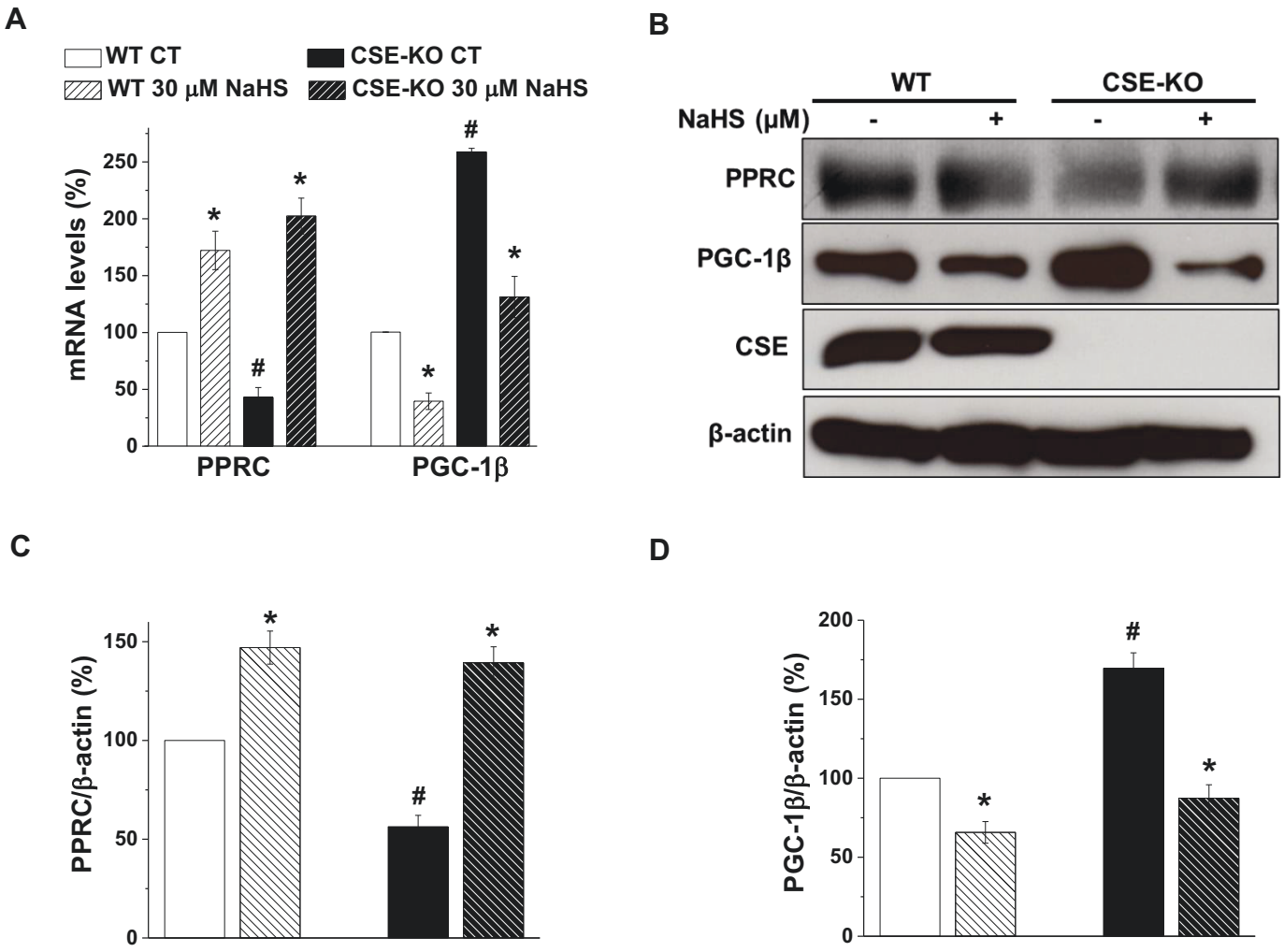

Figure 4-3: H_2S upregulates PPRC and downregulates PGC-1β expression in primary hepatocytes. Liver cells isolated from WT and CSE-KO mice were treated with or without 30 μM NaHS for 6 h **(A)** or 24 h **(B)**. **A)** Total RNA was isolated *via* RNA Isolation Kit. Selected genes were measured *via* q-PCR. PPRC: $n = 4$ for each group; PGC-1β: $n = 6$-8 for each group. **B)** Representative Western blot results of the changed expression levels of selective proteins in isolated WT and CSE-KO hepatocytes. **(C-D)** Summary of the changed expression levels of selective proteins in liver cells. PPRC: $n = 6$ for each group; PGC-1β: $n = 8$ for each group.

Statistical analysis was performed using the one-way ANOVA followed by a *post hoc* analysis (Tukey's test). $^{*}P < 0.05$ *versus* respective CT (control) group; $^{\#}P < 0.05$ *versus* WT CT group.

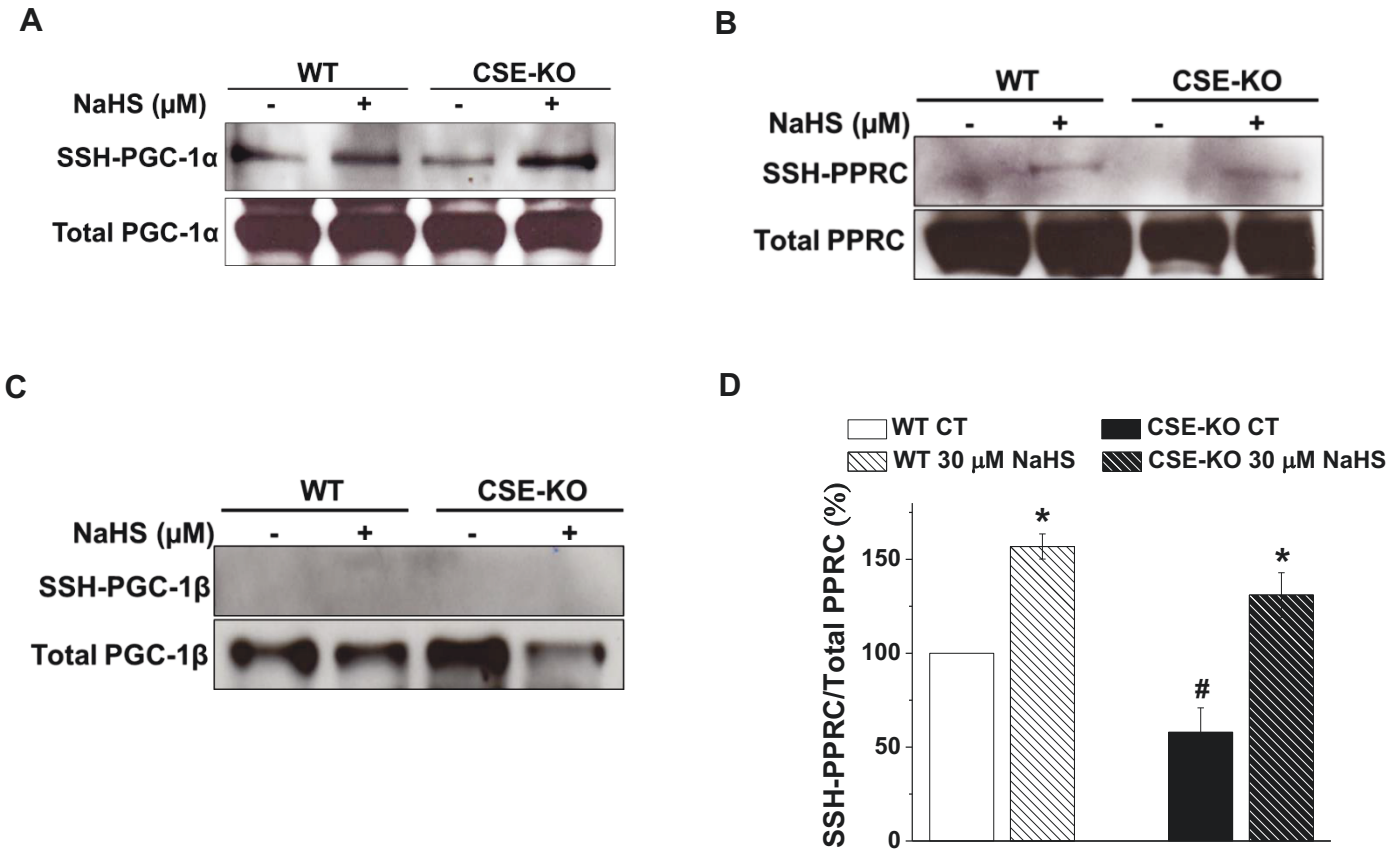

Figure 4-4: Endogenous and exogenous H_2S induces *S*-sulfhydration of PPRC and PGC-1α in isolated primary liver cells. (A-C) Representative Western blot results of the *S*-sulfhydration (SSH) of selective proteins in WT and CSE-KO liver cells. **(D)** The density of SSH-PPRC was normalized to total PPRC protein and expressed as a fold change to that of untreated primary WT hepatocytes. PPRC: n = 5-7 for each group. Statistical analysis was performed using the one-way ANOVA followed by a *post hoc* analysis (Tukey's test). $^{*}P < 0.05$ *versus* respective CT (control) group; $^{\#}P < 0.05$ *versus* WT CT group.

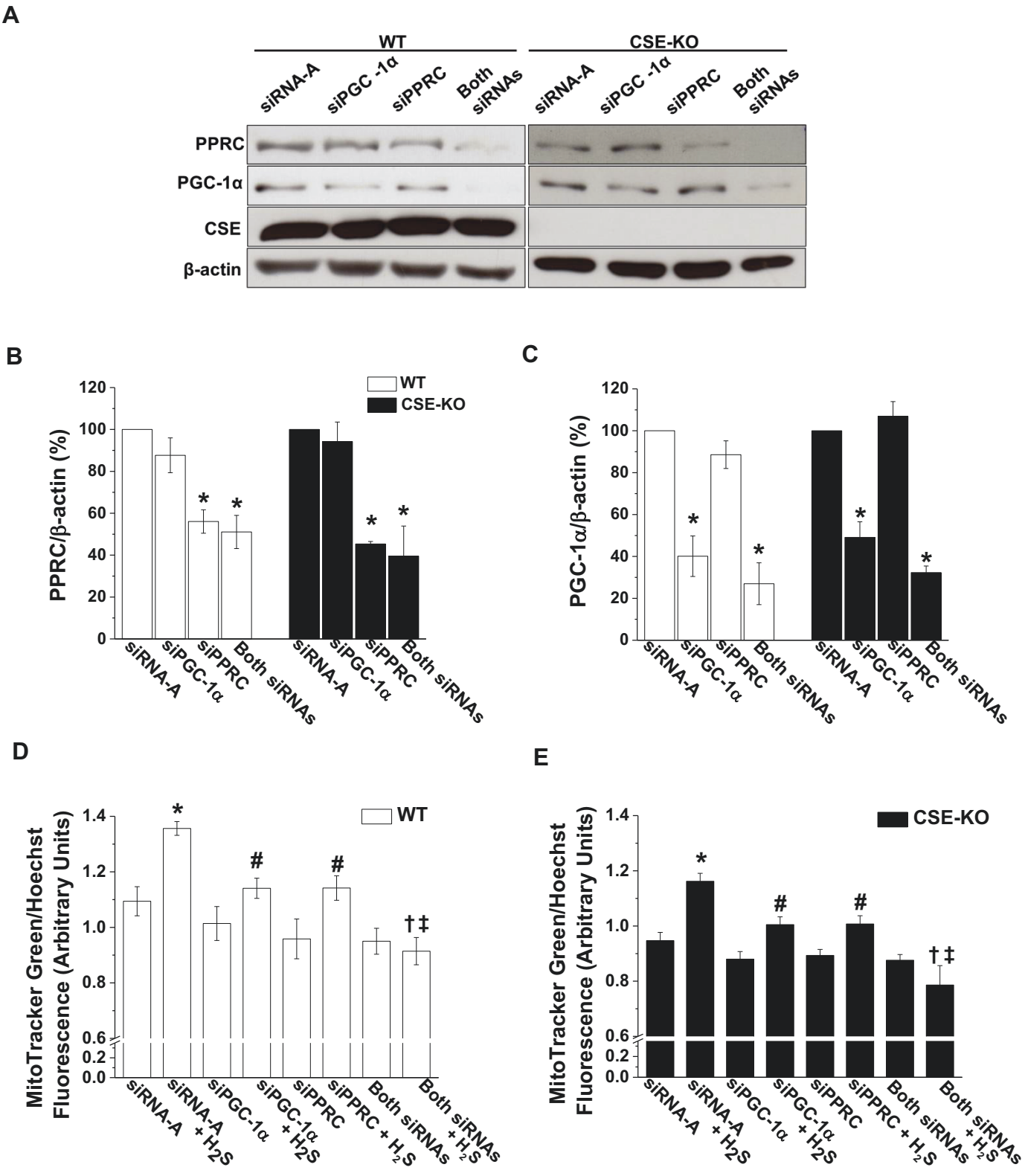
A
WT
CSE-KO
siRNA-A
siPGC -1α
siPPRC
Both siRNAs
PPRC
PGC-1α
CSE
β-actin
B
WT
CSE-KO
PPRC/β-actin (%)
C
PGC-1α/β-actin (%)
D
MitoTracker Green/Hoechst Fluorescence (Arbitrary Units)
siRNA-A + H2S
siPGC-1α + H2S
siPPRC + H2S
Both siRNAs + H2S
E

Figure 4-5: H_2S-stimulated mitochondrial biogenesis is dependent on the signaling pathways of both PGC-1α and PPRC in primary hepatocytes. Primary liver cells isolated from WT and CSE-KO mice were transfected with siRNA-A (control), siPGC-1α, siPPRC, or both siPGC-1α and siPPRC for 60 h. Lipofectamine RNAiMAX was used as the transfection reagent. **(A)** Representative Western blot results of the selected proteins in WT and CSE-KO liver cells. **(B and C)** Summary of the changed protein levels in WT and CSE-KO liver cells with different treatments. The densities of the selected proteins were normalized to that of β-actin and expressed as a percentage of the corresponding siRNA-A transfected WT or CSE-KO liver cells. PPRC: n = 3-4 for each group; PGC-1α: n = 4 for each group. NaHS at 30 μM was used to treat the cells for 24 h, and mitochondrial biogenesis was measured in WT **(D)** (n = 7-9 for each group) and CSE-KO **(E)** (n = 9-11 for each group) hepatocytes *via* normalizing MitoTracker Green fluorescence (485/520 nm) to Hoechst fluorescence (350/460 nm). Statistical analyses performed were: Student's t-test **(B and C)** and one-way ANOVA followed by a *post hoc* analysis (Tukey's test) **(D and E)**. $^{*}P < 0.05$ *versus* respective siRNA-A group; $^{\#}P < 0.05$ *versus* respective 30 μM NaHS-treated siRNA-A group; $^{\dagger}P < 0.05$ *versus* respective 30 μM NaHS-treated siPGC-1α group; $^{\ddagger}P < 0.05$ *versus* respective 30 μM NaHS-treated siPPRC group.

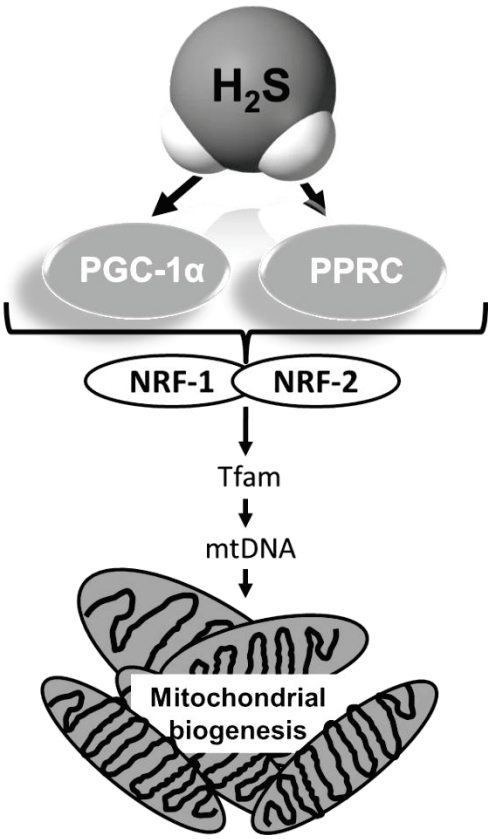

Figure 4-6: Proposed mechanism of H_2S-stimulated mitochondrial biogenesis in hepatocytes. H_2S-mediated induction of mitochondrial biogenesis is dependent upon PGC-1α and PPRC signaling in primary hepatocytes. Once activated *via* H_2S-stimulated *S*-sulfhydration, both PGC-1α and PPRC upregulate the gene transcription of *nrf-1* and *nrf-2*. Once translated into their respective protein forms, both NRF-1 and NRF-2 bind to either PGC-1α or PPRC, whereby these tirade protein complexes work synchronistically to induce mitochondrial biogenesis in liver cells. H_2S: hydrogen sulfide; mtDNA: mitochondrial DNA; NRF: nuclear respiratory factor; PGC-1α: peroxisome proliferator-activated receptor-γ coactivator-1α; PPRC: peroxisome proliferator-activated receptor-γ coactivator-related protein; Tfam: transcription factor A, mitochondrial.

REFERENCES

Andersson U, & Scarpulla RC (2001). Pgc-1-related coactivator, a novel, serum-inducible coactivator of nuclear respiratory factor 1-dependent transcription in mammalian cells. Mol Cell Biol 21**:** 3738-3749.

Andreux PA, Houtkooper RH, & Auwerx J (2013). Pharmacological approaches to restore mitochondrial function. Nat Rev Drug Discov 12**:** 465-483.

Biesecker G, Karimi S, Desjardins J, Meyer D, Abbott B, Bendele R*, et al.* (2003). Evaluation of mitochondrial DNA content and enzyme levels in tenofovir DF-treated rats, rhesus monkeys and woodchucks. Antiviral research 58**:** 217-225.

Bogacka I, Xie H, Bray GA, & Smith SR (2005). Pioglitazone induces mitochondrial biogenesis in human subcutaneous adipose tissue in vivo. Diabetes 54**:** 1392-1399.

Duncan JG, Fong JL, Medeiros DM, Finck BN, & Kelly DP (2007). Insulin-resistant heart exhibits a mitochondrial biogenic response driven by the peroxisome proliferator-activated receptor-alpha/PGC-1alpha gene regulatory pathway. Circulation 115**:** 909-917.

Finck BN, & Kelly DP (2006). PGC-1 coactivators: inducible regulators of energy metabolism in health and disease. J Clin Invest 116**:** 615-622.

Firneisz G (2014). Non-alcoholic fatty liver disease and type 2 diabetes mellitus: The liver disease of our age? World Journal of Gastroenterology : WJG 20**:** 9072-9089.

Fu M, Zhang W, Wu L, Yang G, Li H, & Wang R (2012). Hydrogen sulfide (H2S) metabolism in mitochondria and its regulatory role in energy production. Proc Natl Acad Sci U S A 109**:** 2943-2948.

Fujisawa K, Nishikawa T, Kukidome D, Imoto K, Yamashiro T, Motoshima H*, et al.* (2009). TZDs reduce mitochondrial ROS production and enhance mitochondrial biogenesis. Biochem Biophys Res Commun 379**:** 43-48.

Hock MB, & Kralli A (2009). Transcriptional control of mitochondrial biogenesis and function. Annu Rev Physiol 71**:** 177-203.

Jornayvaz FR, & Shulman GI (2010). Regulation of mitochondrial biogenesis. Essays in biochemistry 47**:** 10.1042/bse0470069.

Kabil O, Vitvitsky V, Xie P, & Banerjee R (2011). The quantitative significance of the transsulfuration enzymes for H2S production in murine tissues. Antioxid Redox Signal 15**:** 363-372.

Kartha RV, Zhou J, Hovde LB, Cheung BW, & Schroder H (2012). Enhanced detection of hydrogen sulfide generated in cell culture using an agar trap method. Anal Biochem 423**:** 102-108.

Kotronen A, Seppala-Lindroos A, Bergholm R, & Yki-Jarvinen H (2008). Tissue specificity of insulin resistance in humans: fat in the liver rather than muscle is associated with features of the metabolic syndrome. Diabetologia 51**:** 130-138.

LeBleu VS, O'Connell JT, Gonzalez Herrera KN, Wikman H, Pantel K, Haigis MC*, et al.* (2014). PGC-1alpha mediates mitochondrial biogenesis and oxidative phosphorylation in cancer cells to promote metastasis. Nat Cell Biol 16**:** 992-1003, 1001-1015.

Lin J, Yang R, Tarr PT, Wu PH, Handschin C, Li S*, et al.* (2005). Hyperlipidemic effects of dietary saturated fats mediated through PGC-1beta coactivation of SREBP. Cell 120**:** 261-273.

Mani S, Li H, Untereiner A, Wu L, Yang G, Austin RC*, et al.* (2013). Decreased endogenous production of hydrogen sulfide accelerates atherosclerosis. Circulation 127**:** 2523-2534.

Mani S, Li H, Yang G, Wu L, & Wang R (2015). Deficiency of cystathionine gamma-lyase and hepatic cholesterol accumulation during mouse fatty liver development. Sci Bull 60**:** 336-347.

Modis K, Coletta C, Erdelyi K, Papapetropoulos A, & Szabo C (2013). Intramitochondrial hydrogen sulfide production by 3-mercaptopyruvate sulfurtransferase maintains mitochondrial electron flow and supports cellular bioenergetics. Faseb j 27**:** 601-611.

Mootha VK, Lindgren CM, Eriksson KF, Subramanian A, Sihag S, Lehar J*, et al.* (2003). PGC-1alpha-responsive genes involved in oxidative phosphorylation are coordinately downregulated in human diabetes. Nature genetics 34**:** 267-273.

Morino K, Petersen KF, Dufour S, Befroy D, Frattini J, Shatzkes N*, et al.* (2005). Reduced mitochondrial density and increased IRS-1 serine phosphorylation in muscle of insulin-resistant offspring of type 2 diabetic parents. J Clin Invest 115**:** 3587-3593.

Mustafa AK, Gadalla MM, Sen N, Kim S, Mu W, Gazi SK*, et al.* (2009). H2S signals through protein S-sulfhydration. Sci Signal 2**:** ra72.

Nisoli E, Clementi E, Paolucci C, Cozzi V, Tonello C, Sciorati C*, et al.* (2003). Mitochondrial biogenesis in mammals: the role of endogenous nitric oxide. Science 299**:** 896-899.

Patti ME, Butte AJ, Crunkhorn S, Cusi K, Berria R, Kashyap S*, et al.* (2003). Coordinated reduction of genes of oxidative metabolism in humans with insulin resistance and diabetes: Potential role of PGC1 and NRF1. Proc Natl Acad Sci U S A 100**:** 8466-8471.

Raharijaona M, Le Pennec S, Poirier J, Mirebeau-Prunier D, Rouxel C, Jacques C*, et al.* (2009). PGC-1-related coactivator modulates mitochondrial-nuclear crosstalk through endogenous nitric oxide in a cellular model of oncocytic thyroid tumours. PLoS One 4**:** e7964.

St-Pierre J, Lin J, Krauss S, Tarr PT, Yang R, Newgard CB*, et al.* (2003). Bioenergetic analysis of peroxisome proliferator-activated receptor gamma coactivators 1alpha and 1beta (PGC-1alpha and PGC-1beta) in muscle cells. J Biol Chem 278**:** 26597-26603.

Suliman HB, Carraway MS, Tatro LG, & Piantadosi CA (2007). A new activating role for CO in cardiac mitochondrial biogenesis. Journal of cell science 120**:** 299-308.

Teng H, Wu B, Zhao K, Yang G, Wu L, & Wang R (2013). Oxygen-sensitive mitochondrial accumulation of cystathionine beta-synthase mediated by Lon protease. Proc Natl Acad Sci U S A 110**:** 12679-12684.

Untereiner AA, Dhar A, Liu J, & Wu L (2011). Increased renal methylglyoxal formation with downregulation of PGC-1alpha-FBPase pathway in cystathionine gamma-lyase knockout mice. PLoS One 6**:** e29592.

Untereiner AA, Wang R, Ju Y, & Wu L (2015). Decreased Gluconeogenesis in the Absence of Cystathionine Gamma-Lyase and the Underlying Mechanisms. Antioxid Redox Signal.

Wang R (2002). Two's company, three's a crowd: can H2S be the third endogenous gaseous transmitter? FASEB J 16**:** 1792-1798.

Wang R (2012). Physiological implications of hydrogen sulfide: a whiff exploration that blossomed. Physiol Rev 92**:** 791-896.

Xu X, Duan S, Yi F, Ocampo A, Liu GH, & Izpisua Belmonte JC (2013). Mitochondrial regulation in pluripotent stem cells. Cell Metab 18**:** 325-332.

Yang G, Wu L, Jiang B, Yang W, Qi J, Cao K*, et al.* (2008). H2S as a physiologic vasorelaxant: hypertension in mice with deletion of cystathionine gamma-lyase. Science 322**:** 587-590.

Zhang L, Yang G, Untereiner A, Ju Y, Wu L, & Wang R (2013). Hydrogen sulfide impairs glucose utilization and increases gluconeogenesis in hepatocytes. Endocrinology 154**:** 114-126.

CHAPTER 5

DISCUSSION AND CONCLUSIONS

GENERAL DISCUSSION

Disturbed H_2S metabolism plays crucial roles in the pathogenesis of insulin resistance and diabetes. However, the role of endogenous H_2S availability in gluconeogenesis and its impact on mitochondrial biogenesis under physiological conditions has been unknown. Therefore, deducing these regulatory mechanisms of H_2S on energy metabolism was the motivation of my Ph.D. thesis.

In this study, we focused on elucidating the mechanisms by which endogenous H_2S regulates hepatic glucose production and mitochondrial biogenesis under physiological conditions. We provide evidence that endogenous H_2S is a critical regulator of these two energy processes under normal conditions. H_2S stimulates glucose production through the PGC-1α-signaling pathway *via* activating either the glucocorticoid receptor pathway or the cAMP/PKA signaling pathway in primary liver cells. By upregulating PGC-1α as well as its activity (*via S*-sulfhydration), H_2S indirectly stimulated the induction of glucose-producing machinery in the liver cell. Both FOXO1 and HNF-4α are critical to the PGC-1α-mediated induction of the major gluconeogenic enzymes, including PEPCK, FBPase, and G6Pase. In fact, we found that H_2S administration increased the gene expression levels of FOXO1 and HNF-4α in $HepG_2$ cells (Supplementary Figure S-1). The enhanced expression of PGC-1α and its gluconeogenic coactivators, FOXO1 and HNF-4α, lead to higher levels of PEPCK, FBPase, and G6Pase in primary liver cells and $HepG_2$ cells (Supplementary Figure S-1). Not only does H_2S play an indirect role in the induction of the gluconeogenic genes, but we also found it to interact directly with their protein transcripts *via* post-translational modification. The activities of G6Pase and FBPase were remarkably enhanced *via* H_2S-mediated *S*-sulfhydration. In another study, we found H_2S increased the enzymatic activity of PC, again through *S*-sulfhydration (109). Clearly, H_2S is a potent inducer of hepatic glucose generation.

We also demonstrated that endogenous H_2S is vital to maintaining mitochondrial homeostasis in isolated hepatocytes. Mitochondria are the powerhouse for ATP and NADPH production, which is cruical to fuel gluconeogenesis. By stimulating the signaling pathways of PPRC and PGC-1α (*via* protein upregulation and *S*-sulfhydration), H_2S induced mitochondrial biogenesis in primary hepatocytes. Once activated by H_2S, both PGC-1α and PPRC upregulated the gene transcription of *nrf-1* and *nrf-2*. Once translated into their respective protein forms, both NRF-1 and NRF-2 where shown to bind to either PGC-1α or PPRC, whereby these tirade protein complexes work synchronistically to induce mitochondrial biogenesis in liver cells (150; 151). Indeed, we observed lower *Tfam* and mtDNA levels in primary hepatocytes lacking the *cse* gene to normal hepatocytes. Additionally, we also found that H_2S enhanced the mitochondrial membrane potential in both WT and CSE-KO primary liver cells (Supplementary Figure S-2), further supporting its role in the induction of ATP generation (43; 113). In the end, the stimulation of hepatic mitochondrial biogenesis and mitochondrial function *via* H_2S stimulation further strengthens with its impact on the induction of hepatic glucose production.

Interestingly, unlike its induction of hepatic glucose production, H_2S simulated hepatic mitochondrial biogenesis either through PGC-1α or PPRC activity, whereby maximal induction of mitochondrial biogenesis was achieved if both pathways were functional. When PGC-1α was knockdown in primary liver cells, NaHS-induction of glucose production as completely eradicated. On the other hand, knockdown of PGC-1α only partially suppressed NaHS-stimulated mitochondrial biogenesis. PGC-1α is a master regulator of hepatic gluconeogenesis. It does this by 1) upregulating the gene expression levels of the main rate-limiting gluconeogenic enzymes, *pc, pepck*, *fbpase*, and *g6pase;* and 2) by stimulating mitochondrial biogenesis and mitochondrial energy production. In this case, with the downregulation of PGC-1α, the

expression levels of the critical glucose-producing machinery (i.e. gluconeogenic enzymes) would have been significantly lower. Although, cellular ATP would have been slightly higher, due to PPRC activation, it was not enough to drive glucose production in primary liver cells upon H_2S stimulation.

Under physiological conditions, a functionally intact CSE/H_2S system is important for human's adaptive energy metabolism. A reduced gluconeogenesis system limits one's physical endurance by impairing both aerobic and anaerobic glycolysis, depending if sufficient oxygen is available. In aerobic respiration, skeletal muscle cells use glucose to generate a substantial amount of ATP through first cytosolic glycolysis, the Krebs cycle, and then mitochondrial oxidative phosphorylation (203). With a diminished glucose supply due to suppressed gluconeogenesis, ATP production would be hampered, causing the individual to quickly fatigue. In fact, not only can H_2S induce the production of new mitochondria it was also demonstrated to regulate bioenergetics by increasing ATP generation (43) *via* serving as an inorganic electron donor (113). When oxygen supply is insufficient, skeletal muscle cells will rely on anaerobic glycolysis, namely the Cori cycle. Under strenuous activity, muscle glycogen is broken down *via* several pathways into lactate, released into the circulation, and taken up by the liver to be converted into glucose *via* gluconeogenesis (203). From there, hepatic glucose is released back into the bloodstream to the muscle (203). With a reduced gluconeogenic process, plasma lactate would accumulate, leading to lactic acidosis and the individual would again quickly fatigue. Additionally, a prolonged period of fasting could put a severe strain on the already weakened gluconeogenic process with a deficient CSE/H_2S system, leading to hypoglycemia.

On the other hand, an over-activated CSE/H_2S system in the liver could predispose an individual to develop metabolic syndrome because H_2S blocks insulin release (33; 204) and

insulin-stimulated glucose uptake into both fat (205) and liver (105) cells. In this regard, it has been reported that both CSE (119; 120) and PGC-1α (139; 140; 162) are robustly active in the liver under diabetic conditions, as is C/EBP-β (189; 194).

Overall, the present study identifies key targets of the CSE/H_2S system in liver gluconeogenesis; thus, deepening our insight on hepatic glucose regulation under physiological conditions and highlighting the potential impact endogenous H_2S may have on the dysregulated gluconeogenic system in metabolic syndrome.

CONCLUSION

The study provides evidence that CSE-generated endogenous H_2S stimulates glucose production as well as mitochondrial biogenesis in the liver, which is critical in regulating glucose metabolism. H_2S stimulates liver glucose production and liver mitochondrial biogenesis through four underlying mechanisms: 1) H_2S upregulates the expression of PGC-1α and PEPCK *via* glucocorticoid receptor pathway. 2) H_2S upregulates the expression of PGC-1α through the activation of the cAMP/PKA pathway, as well as PGC-1α activity *via S*-sulfhydration. 3) H_2S upregulates the expression and the activities (by *S*-sulfhydration) of G6Pase and FBPase. 4) H_2S augments the protein expression level and activity (*via S*-sulfhydration) of PPRC. By stimulating the combined activities of PPRC and PGC-1α, H_2S induces mitochondrial biogenesis in primary hepatocytes (Figure 5-1).

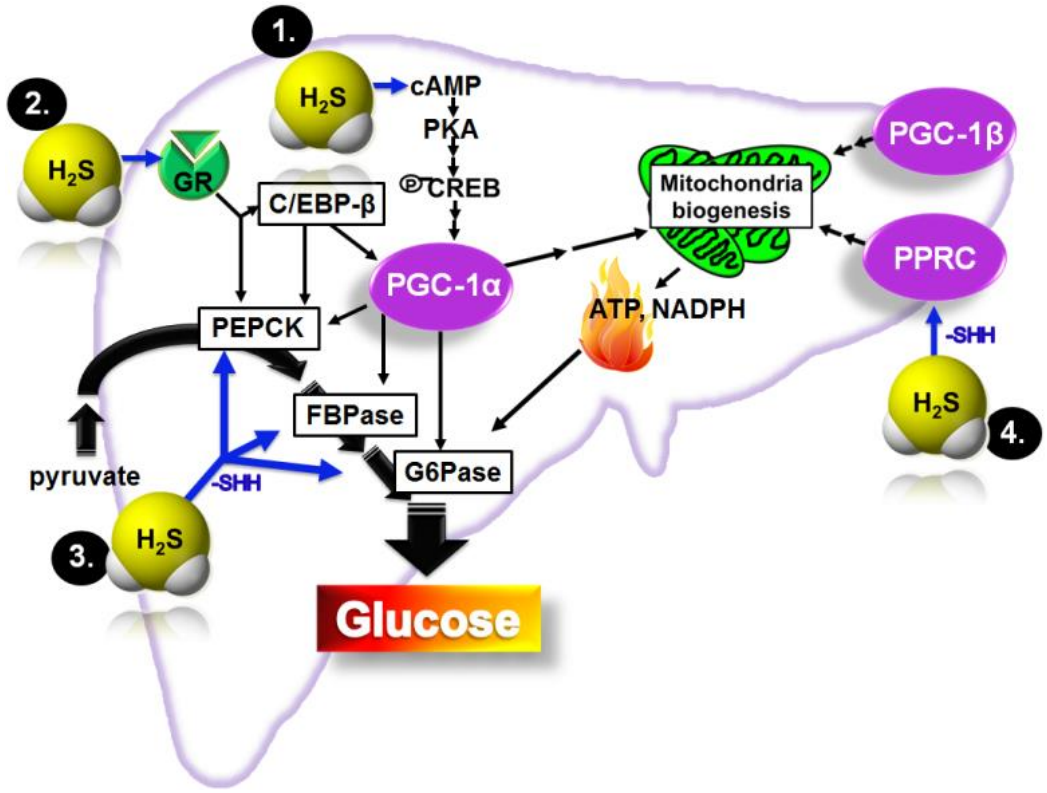

Figure 5-1: Proposed mechanisms by which H_2S stimulates glucose production and mitochondrial biogenesis in primary liver cells.

SIGNIFICANCE of the STUDY

In 2015, one in four Canadians (~9 million people) were estimated to be living with diabetes or prediabetes (13). If nothing is done to curve this trend, by 2020, it will be one in three (13). Without a doubt, diabetes prevalence is growing at epidemic levels across Canada, and urgent action is needed to reduce the cost pressure on the Canadian health care system and economy.

Chronic hyperglycemia is the leading cause of diabetes-related complications, including heart disease, stroke, and hypertension. The major metabolic defect that contributes to hyperglycemia is uncontrolled gluconeogenesis from the insulin-resistant liver. Interestingly, the abnormal metabolisms of CSE (119; 120), PGC-1α (139; 140; 162), and C/EBP-β (189; 194) are

significantly upregulated in livers of T1DM (119; 120; 140; 189; 194) and in T2DM (139; 140; 162) animal models. For the first time, we demonstrate a link between the CSE/H_2S system and PGC-1α and C/EBP-β in the context of gluconeogenesis regulation in the liver. We also highlight the importance of H_2S in the induction of mitochondrial biogenesis in the liver *via* PGC-1α and PPRC signaling. Because gluconeogenesis is abnormally overactive in the insulin-resistant liver, stresses the importance of identifying factors that govern the induction of gluconeogenesis and mitochondrial homeostasis. In fact, the most successful anti-hyperglycemia and anti-diabetic drug currently on the market is the hepatic gluconeogenic suppressor, metformin (206). By clarifying the role the CSE/H_2S system plays in hepatic glucose metabolism under physiological conditions suggests the potential impact it may also have in the induction of an overstimulated gluconeogenic system in metabolic syndrome. The novelty of these discoveries contributes to the growing knowledge of the elaborate underlying mechanisms of the gluconeogenic system, and its abnormalities associated with insulin-resistant diseases. Overall, this study may lead to the development of new and protective interventions or therapeutic treatment for metabolic syndrome and its associated complications.

LIMITATIONS of the STUDY

A. Research Limitations

Primary mouse hepatocytes were selected as the ideal experimental model compared to primary rat or human hepatocytes and the immortalized human hepatoma cell line, $HepG_2$ cells. Naturally, the use of primary human hepatocytes would have been an extremely valuable tool to study the effects of H_2S on glucose metabolism. The homogeneous background of animals, under well-controlled experimental settings, do not always concordant with the diversity of human patients living in heterogeneous conditions (207). However, due to limited availability of

donor material, the large metabolic variability between human donors (208-210), and the cost to obtain commercially available human hepatocytes for all experiments was infeasible. Studies on $HepG_2$ cells, on the other hand, would have easily provided us important insight on human hepatic metabolism; however, the fact that these are cloned carcinoma cells raises questions about whether or not data can be interpreted as physiological than compared to native normal liver cells. In fact, $HepG_2$ cells have lost many liver-specific functions (208; 211). Furthermore, in comparison with primary mouse hepatocytes, rat hepatocytes exhibit a rapid decline in liver-specific functions (i.e. decrease in phase I and phase II genes involved in drug metabolism) (209; 212; 213), suggesting that metabolic competence may also be weakened. This drawback would have been detrimental to the reproducibility of all of our siRNA transfections experiments, as they were to be in cell cultured for 4-5 days. Additionally, our laboratory generated mouse deficient in the *cse* gene (41), thus providing us with a unique opportunity to study the *in vivo* and *in vitro* effects of endogenous H_2S on glucose metabolism. Therefore, taking all of this into consideration, mouse primary hepatocytes were seen as the optimal experimental model for this thesis.

Unfortunately, one of the major drawbacks to working with primary mouse hepatocytes was their quiescent nature once isolated, resulting in the continual need to freshly isolate cells for each experiment. This required careful ordination of experiments, longer work hours to perform the isolation, and a continual replenishment of enzymes and chemicals necessary for the isolation (i.e. collagenase type IV, percoll). Attempts were made to cryopreserve the freshly isolated hepatocytes; however, this yielded hepatocytes with extremely low cell viability (~30% *via* trypan blue assay). Due to the sensitive nature of the primary hepatocytes, a controlled rate cooler (i.e. Kryo from CRYO Biotechnology; $9,000 - $21,000) was needed to time-dependently

lower the internal temperature of the primary hepatocyte mixture (i.e. at 4°C samples are to be cooled at −1°C/min to −6°C and held for 10 minutes then cooled at −1°C/min to −80°C).

In Chapters 3 and 4, the interaction between H_2S and PGC-1α/PPRC were investigated using transient siRNA knockout techniques. siRNA-based gene silencing is not as precise or thorough as a traditional gene deletion. Therefore, using PGC-1α-KO mouse model would provide a further confirmation of our findings. Also, the introduction of an adenovirus overexpressing the *cse* gene into WT mice would have provided additional support for the regulatory role the CSE/H_2S system has in hepatic glucose production and mitochondrial biogenesis. Many researchers have shown the effectiveness of adenovirus delivery *via* tail vein injection, which specifically targets the liver with minimum immune response (140; 214; 215). Our Ad-CSE and β-galactosidase have deletions in the E1, E2, and E4 genes, which prevents the transcription of viral proteins encoded by these DNA sequences, as well as viral self-replication. This safely minimizes the host immune response to adenoviral delivery and prolongs the gene expression *in vivo* (216). Evidence from the adenovirus overexpressing CSE in livers would have contributed to further understanding the roles of endogenous H_2S in hepatic glucose production as well as mitochondrial biogenesis and function. Unfortunately, due to time constraints, we were unable to manufacture and delivery Ad-CSE *via* tail-vein injection into the WT mice.

In Chapter 4, we analyzed mitochondrial biogenesis by measuring the fluorescence of MitoTracker Green FM from a spectrometer. Spectrophotometry measures the bulk volume of the sample where the percentage of absorption and transmission of specific wavelengths are determined. This method is reliable although it may be not as sensitive as flow cytometry, which measures the fluorescence of very single live cell in a sample; whereby fluorescence from dead

cells, cellular debris, and excess probe are excluded from the reading (217). Attempts were made to use the Fluorescence-Activated Cell Sorting (FACS) at the Northern Ontario School of Medicine (NOSM) laboratory at Lakehead University. Unfortunately, complications arose due to sample preservation because of a weakened and unpredictable fluorescence reading as the MitoTracker Green probe only stains live cells. Additionally, if cell treatments were conducted at the NOSM laboratory, isolated primary hepatocytes would have needed to be transported from the CMRU laboratory to the NOSM laboratory (about 15 min driving) for every experiment. Considering the primary hepatocytes easily becomes quiescent once in cell culture, therefore, the flow cytometry analysis was opted out of our experiments due to practicality and time issues.

B. Methodological Limitations

The biotin switch assay, developed by Snyder and colleagues (20), was used for the detection of *S*-sulfhydrated proteins. This assay is considered to be a reliable method to measure protein modification; however, the biotin switch assay indirectly measures protein *S*-sulfhydration. The sensitivity of the biotin switch method depends on the effective blocking of the free thiol by MMTS. After blocking, the modified thiol was labeled with a thiol-reactive biotin (which forms a mixed disulfide with the modified thiol). Finally, the biotinylated proteins were pulled down *via* streptavidin-agarose and analyzed by Western blot. LC-MS/MS, on the other hand, directly measure *S*-sulfhydrated proteins, without the application of MMTS or biotin to protein samples. LC-MS/MS can distinguish *S*-sulfhydration based on protein mass shift; whereas biotin switch assay depends on the thiol-biotin-streptavidin-agarose binding that is then analyzed *via* Western blot. Quantifying *S*-sulfhydrated proteins *via* LC-MS/MS would have provided further supporting evidence in Chapters 3 and 4.

In Chapter 3, we measured hepatic glucose production *via* a colorimetric method; however, the use of a radioactive method would have been more sensitive and precise. As a result of our laboratory limitation, the radioisotope method was not adopted for our study. Additionally, in Chapter 3, we measured the enzymatic activity of G6Pase from total cell lysates. G6Pase is the only gluconeogenic enzyme that is located in the ER. Once glucose is synthesized by G6Pase, it is packaged up in a vesicle and sent to the cell membrane for exocytosis. Therefore, ER isolation from primary liver cells would have produced more precise measurements of G6Pase activity; however, an ultracentrifuge was required to separate the ER from the rest of the cell components and debris. Due to the limitation of our laboratory, ER-isolation *via* ultracentrifugation was not incorporated into our study.

Lastly, the denaturing agarose-formaldehyde gel method was used to determine RNA integrity by visualizing the 2:1 ratio of the 28S and 18S bands (Chapter 4 and Supplementary Figure S-1). While the cost of analyzing RNA integrity by gel electrophoresis is relatively low, analysis requires a significant amount of handling and hands-on time. Also, since ethidium bromide stains bind to nucleic acids, they are potential carcinogens; therefore, careful handling was necessary. Also, gel electrophoresis is not as sensitive as the 2100 Bioanalyzer (Agilent Technologies) or the Experion™ Automated Electrophoresis System (Bio-Rad). These methods consume a substantial small amount of RNA, with faster analysis, and more accurate calculation of RNA quality. However, these methods are expensive and require costly reagents and chips. Considering that the determination of RNA was only a small part in this thesis, incorporating the 2100 Bioanalyzer or the Bio-Rad Experion system would have been considered, if extensive RNA analysis were required.

ETHICAL PERSPECTIVE

Animal research has played a pivotal role in many scientific and medical advances, and it continues to aid our understanding of various diseases. Around the world, people enjoy a better quality of life due to these advances, and the subsequent development of new medicines and treatments, which was made possible by animal research (218). For instance, the discovery of insulin was made possible through animal studies. In 1921, Frederick Banting and Charles Best showed that isolated pancreatic extracts dramatically reduced the hyperglycemia and glycosuria and prolonged the lives of dogs made diabetic by removal of the pancreas. Next, Banting and Best developed a procedure to extract insulin from a bovine pancreas, whereby in the winter of 1922, they treated their first human patient, a young boy, whose life was saved by a treatment achieved through animal research (219). In conjunction with the successful discovery of insulin, animal testing has furthered our understanding of AIDS, asthma, tuberculosis, breast cancer, cystic fibrosis, Huntington's disease, etc. An up-to-date and comprehensive list of all the diseases animal research has aided in our understanding in is chronicled at http://www.animalresearch.info/en/medical-advances/diseases-research/.

However, animal experimentation has been a subject of heated debate for many years. Despite the numerous medical advances, the tight controls governing animal experimentation, and the widespread implementation of the 3Rs [reduction, replacement, and refinement of the use of animals in research (220)], animal-rights groups are lobbying for a complete ban on animal research. Pushing for non-animal replacement methods involves not only the development of the method but also its validation by national and international regulatory authorities, whereby any negligence could endanger human health. Overall, the numerous medical achievements made possibly by animal research has led to critical drug discoveries

throughout the years. Abandonment of animal research could impose severe consequences on medical advances and public health.

FUTURE DIRECTION

As a follow-up to this Ph.D. study, the suggested future directions are divided into two parts:

PART ONE:

1. Perform a functional study on the WT mice *via* overexpressing CSE *in vivo* using our proven Ad-CSE transfection technology (1 x 10^{12} viral particles) (96; 105). Control WT mice would be injected with an adenovirus encoding β-galactosidase (1 x 10^{12} viral particles). Approximately 2-5 days after adenovirus injection, the following observational experiments are suggested:
    a. Measure the rate of gluconeogenesis *via* PTT
    b. Determine insulin resistance in hepatocytes isolated from Ad-CSE treated WT mice by treating the cells with insulin (100 nM for 15 min) and analyze:
        i. glucose production
        ii. phosphorylation of insulin receptor substrate (IRS)
        iii. Akt activation
        iv. phosphorylation of FOXO1
        v. PGC-1α and TRB-3 protein levels
2. Redo the experiments listed in 1) but with PPG-treated Ad-CSE- and Ad- β-galactosidase-treated WT mice. PPG injections (40 mg/kg/day) are to begin one week prior to adenovirus delivery and to continue until the termination of the mice.

PART TWO:

1. Induce T2DM in mice *via* a combination of a single i.p. injection of STZ (50 mg/kg) and high-energy intake diet (58% calories as fat) (Research Diets, New Brunswick, NJ) in both WT and CSE-KO mice. The single STZ injection should be given after two weeks of dietary manipulation. The STZ-HFD treatment was shown to effectively induce T2DM in both rats and mice by altering the related gene expressions in major metabolic tissues, leading to peripheral insulin resistance, which was accompanied by frank hyperglycemia (221-224). Thereafter, the development of diabetes in these mice should be determined and compared. The following experiments are suggested:
    a. Determine insulin sensitivity *via* insulin tolerance test
    b. Test the efficiency of insulin secretion *via* glucose tolerance test
    c. Measure the rate of gluconeogenesis *via* PTT
    d. Measure hepatic PGC-1α and TRB-3 protein levels
    e. Analyze hepatic mitochondrial function by measuring mitochondrial membrane potential (*via* specific mitochondrial probes) and ATP production (*via* commercially available ATP assay kit).
2. Repeat the experiments listed in the above step but with a 3 week treatment of daily PPG injections. It would be crucial to determine if PPG could reverse or alleviate H_2S-related diabetes development in the type 2 diabetic WT and CSE-KO mice. Daily i.p. injections of PPG (40 mg/kg/day) are to begin one week prior to dietary manipulation and to proceed the two weeks of the HFD feeding.

SUPPLEMENTARY MATERIAL

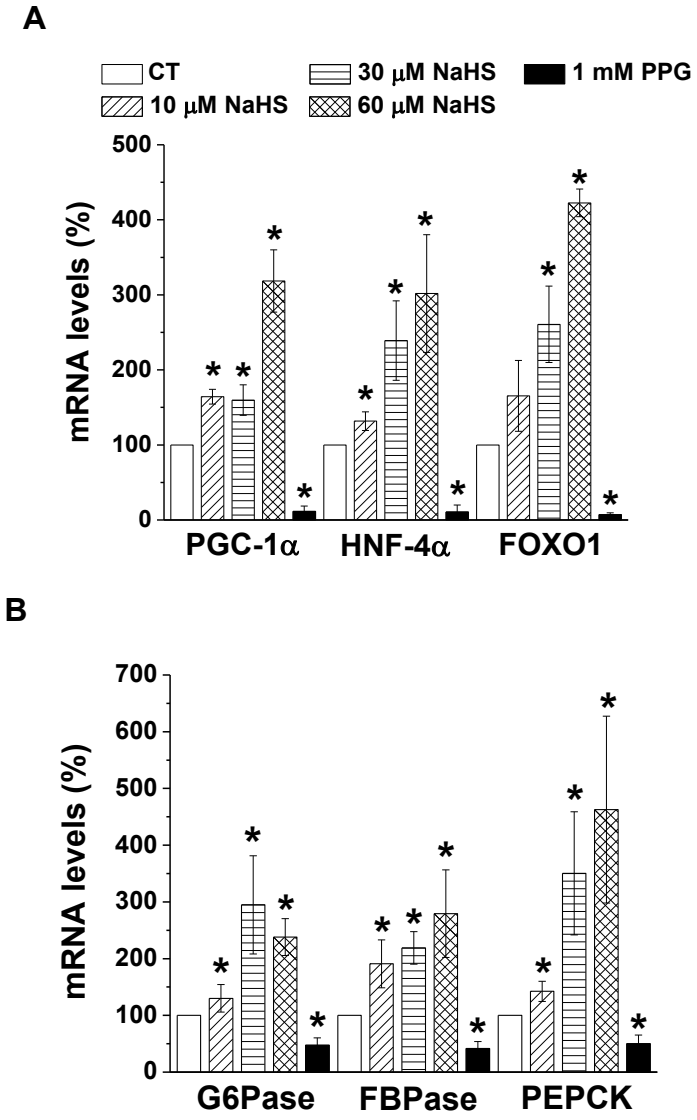

Supplementary Figure S-1: NaHS upregulates the expression levels of gluconeogenic genes in $HepG_2$ cells. $HepG_2$ cells were treated with or without 10, 30, or 60 μM NaHS or 1 mM PPG for 6 h. **A and B)** Selected gene expression levels were analyzed by q-PCR and normalized to total β-actin. n = 3-4 for each group. Statistical analysis was performed using the Student's t-test. $P < 0.05$ *versus* control group (CT).

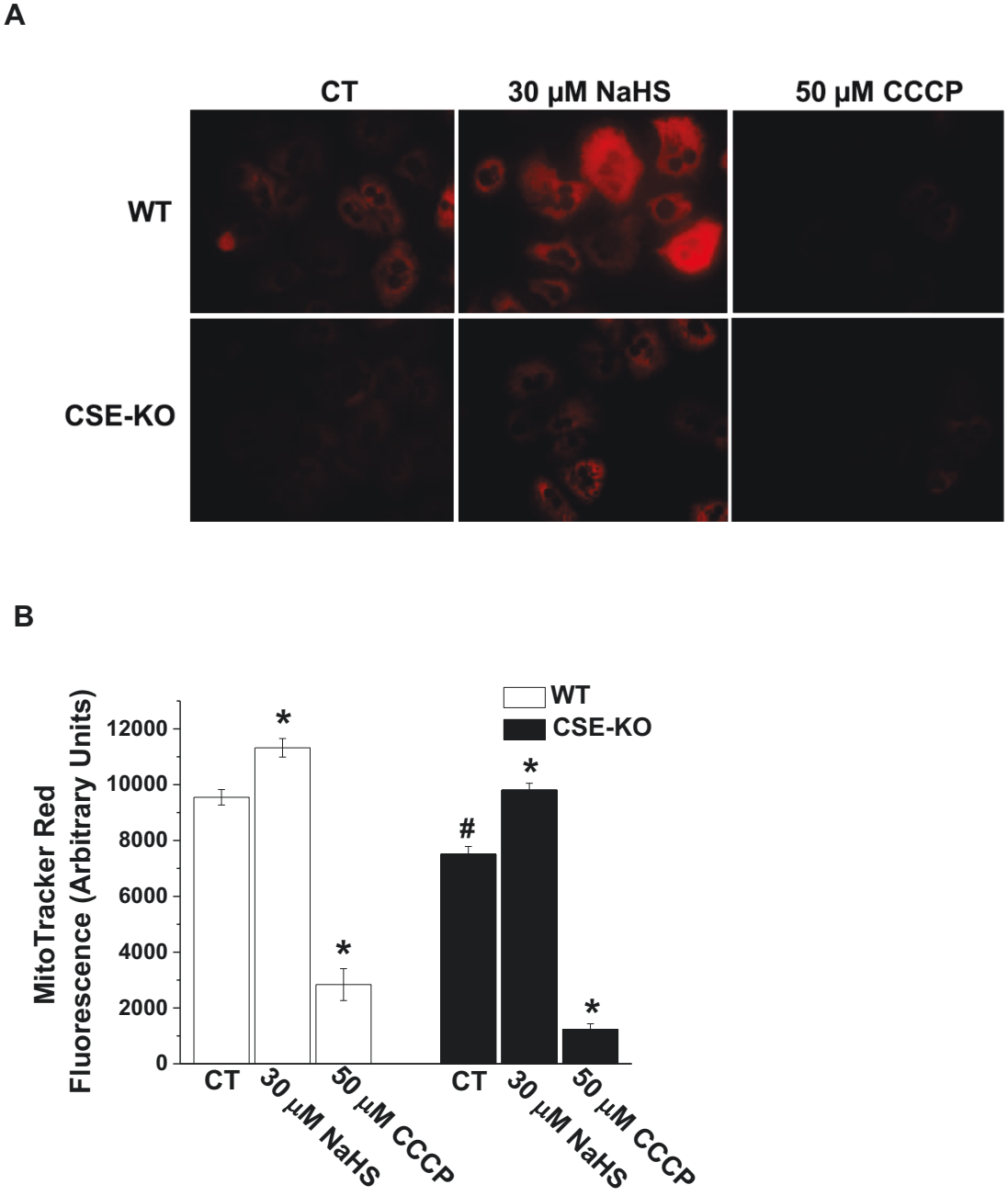

Supplementary Figure S-2: Endogenous and exogenous H_2S upregulates mitochondrial membrane potential in primary hepatocytes. Primary liver cells isolated from WT and CSE-KO mice were treated with 30 μM NaHS for 6 h or 50 μM CCCP, a mitochondrial uncoupling reagent, for 25 min. MitoTracker Red CM-H2XRos was used to measure mitochondrial membrane potential (100 μm). **A)** Cells were images *via* fluorescent microscope. $n = 3$ for each

group. **B)** Summary of MitoTracker Red fluorescence measured *via* spectrophotometer at excitation/emission: 579/599 nm. n = 3-4 for each group. Statistical analysis was performed using the one-way ANOVA followed by a *post hoc* analysis (Tukey's test). $^{*}P < 0.05$ *versus* control group (CT); $^{\#}P < 0.05$ *versus* WT CT group.

REFERENCES

1. Association CD. Clinical Practice Guidelines. http://guidelines.diabetes.ca/screeninganddiagnosis/screening
2. Rojas JM, Schwartz MW. 2014. Control of hepatic glucose metabolism by islet and brain. *Diabetes Obes Metab* 16 Suppl 1:33-40
3. Kleinridders A, Konner AC, Bruning JC. 2009. CNS-targets in control of energy and glucose homeostasis. *Curr Opin Pharmacol* 9:794-804
4. Fu Z, Gilbert ER, Liu D. 2013. Regulation of insulin synthesis and secretion and pancreatic Beta-cell dysfunction in diabetes. *Curr Diabetes Rev* 9:25-53
5. Li X, Monks B, Ge Q, Birnbaum MJ. 2007. Akt/PKB regulates hepatic metabolism by directly inhibiting PGC-1alpha transcription coactivator. *Nature* 447:1012-6
6. Moore MC, Coate KC, Winnick JJ, An Z, Cherrington AD. 2012. Regulation of hepatic glucose uptake and storage in vivo. *Adv Nutr* 3:286-94
7. Gerich MZSaJE. 2010. Principles of Diabetes Mellitus. In *Normal Glucose Homeostatis*, ed. L Poretsky:19-35. New York, NY: Springer Science and Business Media. Number of 19-35 pp.
8. Landau BR, Wahren J, Chandramouli V, Schumann WC, Ekberg K, Kalhan SC. 1996. Contributions of gluconeogenesis to glucose production in the fasted state. *J Clin Invest* 98:378-85
9. Shrayyef MZ, Gerich JE. 2010. Normal Glucose Homeostasis.19-35
10. Gerich JE, Meyer C, Woerle HJ, Stumvoll M. 2001. Renal gluconeogenesis: its importance in human glucose homeostasis. *Diabetes Care* 24:382-91
11. Pilkis SJ, el-Maghrabi MR, Claus TH. 1988. Hormonal regulation of hepatic gluconeogenesis and glycolysis. *Annu Rev Biochem* 57:755-83
12. Alberti KG, Zimmet P, Shaw J. 2005. The metabolic syndrome--a new worldwide definition. *Lancet* 366:1059-62
13. Assoication CD. 2015. Canadian Diabetes Association 2015 Pre-Budget Submission to the House of Common Standing Committee on Finance. http://www.parl.gc.ca/Content/HOC/Committee/412/FINA/WebDoc/WD6615327/412_FINA_PBC2014_Briefs%5CCanadianDiabetesAssociation-e.pdf: The Diabetes Charter of Canada
14. Olokoba AB, Obateru OA, Olokoba LB. 2012. Type 2 diabetes mellitus: a review of current trends. *Oman Med J* 27:269-73
15. Haslam DW, James WP. 2005. Obesity. *Lancet* 366:1197-209
16. WHO. Controlling the global obesity epidemic. http://www.who.int/nutrition/topics/obesity/en/: World Health Organization
17. Wang R. 2002. Two's company, three's a crowd: can H2S be the third endogenous gaseous transmitter? *FASEB J* 16:1792-8
18. Wang R. 2012. Physiological implications of hydrogen sulfide: a whiff exploration that blossomed. *Physiol Rev* 92:791-896
19. Untereiner AA, Wu L, Wang R. 2012. The role of carbon monoxide as a gasotransmitter in cardiovascular and metabolic regulation. In *Gasotransmitters: physiology and pathophysiology*, ed. GFS Anton Hermann, Thomas M. Weiger:37-69. Berlin: Springer Science & Business Media. Number of 37-69 pp.
20. Mustafa AK, Gadalla MM, Sen N, Kim S, Mu W, et al. 2009. H2S signals through protein S-sulfhydration. *Sci Signal* 2:ra72

21. Chen YH, Yao WZ, Gao JZ, Geng B, Wang PP, Tang CS. 2009. Serum hydrogen sulfide as a novel marker predicting bacterial involvement in patients with community-acquired lower respiratory tract infections. *Respirology* 14:746-52
22. Untereiner AA, Dhar A, Liu J, Wu L. 2011. Increased renal methylglyoxal formation with down-regulation of PGC-1alpha-FBPase pathway in cystathionine gamma-lyase knockout mice. *PLoS One* 6:e29592
23. Zhao W, Zhang J, Lu Y, Wang R. 2001. The vasorelaxant effect of H(2)S as a novel endogenous gaseous K(ATP) channel opener. *EMBO J* 20:6008-16
24. Furne J, Saeed A, Levitt MD. 2008. Whole tissue hydrogen sulfide concentrations are orders of magnitude lower than presently accepted values. *Am J Physiol Regul Integr Comp Physiol* 295:R1479-85
25. Doeller JE, Isbell TS, Benavides G, Koenitzer J, Patel H, et al. 2005. Polarographic measurement of hydrogen sulfide production and consumption by mammalian tissues. *Anal Biochem* 341:40-51
26. Whitfield NL, Kreimier EL, Verdial FC, Skovgaard N, Olson KR. 2008. Reappraisal of H2S/sulfide concentration in vertebrate blood and its potential significance in ischemic preconditioning and vascular signaling. *Am J Physiol Regul Integr Comp Physiol* 294:R1930-7
27. Reiffenstein RJ, Hulbert WC, Roth SH. 1992. Toxicology of hydrogen sulfide. *Annu Rev Pharmacol Toxicol* 32:109-34
28. Nagai Y, Tsugane M, Oka J, Kimura H. 2004. Hydrogen sulfide induces calcium waves in astrocytes. *FASEB J* 18:557-9
29. Garcia-Bereguiain MA, Samhan-Arias AK, Martin-Romero FJ, Gutierrez-Merino C. 2008. Hydrogen sulfide raises cytosolic calcium in neurons through activation of L-type Ca2+ channels. *Antioxid Redox Signal* 10:31-42
30. Szabo C. 2007. Hydrogen sulphide and its therapeutic potential. *Nat Rev Drug Discov* 6:917-35
31. Ishii I, Akahoshi N, Yu XN, Kobayashi Y, Namekata K, et al. 2004. Murine cystathionine gamma-lyase: complete cDNA and genomic sequences, promoter activity, tissue distribution and developmental expression. *Biochem J* 381:113-23
32. Tripatara P, Patel NS, Brancaleone V, Renshaw D, Rocha J, et al. 2009. Characterisation of cystathionine gamma-lyase/hydrogen sulphide pathway in ischaemia/reperfusion injury of the mouse kidney: an in vivo study. *Eur J Pharmacol* 606:205-9
33. Wu L, Yang W, Jia X, Yang G, Duridanova D, et al. 2009. Pancreatic islet overproduction of H2S and suppressed insulin release in Zucker diabetic rats. *Lab Invest* 89:59-67
34. Chang T, Untereiner A, Liu J, Wu L. 2010. Interaction of methylglyoxal and hydrogen sulfide in rat vascular smooth muscle cells. *Antioxid Redox Signal* 12:1093-100
35. Yang G, Sun X, Wang R. 2004. Hydrogen sulfide-induced apoptosis of human aorta smooth muscle cells via the activation of mitogen-activated protein kinases and caspase-3. *FASEB J* 18:1782-4
36. Chen YH, Yao WZ, Ding YL, Geng B, Lu M, Tang CS. 2008. Effect of theophylline on endogenous hydrogen sulfide production in patients with COPD. *Pulm Pharmacol Ther* 21:40-6
37. Wang P, Zhang G, Wondimu T, Ross B, Wang R. 2011. Hydrogen sulfide and asthma. *Exp Physiol* 96:847-52

38. Erickson PF, Maxwell IH, Su LJ, Baumann M, Glode LM. 1990. Sequence of cDNA for rat cystathionine gamma-lyase and comparison of deduced amino acid sequence with related Escherichia coli enzymes. *Biochem J* 269:335-40
39. Abe K, Kimura H. 1996. The possible role of hydrogen sulfide as an endogenous neuromodulator. *J Neurosci* 16:1066-71
40. Stipanuk MH, Beck PW. 1982. Characterization of the enzymic capacity for cysteine desulphhydration in liver and kidney of the rat. *Biochem J* 206:267-77
41. Yang G, Wu L, Jiang B, Yang W, Qi J, et al. 2008. H2S as a physiologic vasorelaxant: hypertension in mice with deletion of cystathionine gamma-lyase. *Science* 322:587-90
42. Ogasawara Y, Isoda S, Tanabe S. 1994. Tissue and subcellular distribution of bound and acid-labile sulfur, and the enzymic capacity for sulfide production in the rat. *Biol Pharm Bull* 17:1535-42
43. Fu M, Zhang W, Wu L, Yang G, Li H, Wang R. 2012. Hydrogen sulfide (H2S) metabolism in mitochondria and its regulatory role in energy production. *Proc Natl Acad Sci U S A* 109:2943-8
44. Renga B. 2011. Hydrogen sulfide generation in mammals: the molecular biology of cystathionine-beta- synthase (CBS) and cystathionine-gamma-lyase (CSE). *Inflamm Allergy Drug Targets* 10:85-91
45. Tan BH, Wong PT, Bian JS. 2010. Hydrogen sulfide: a novel signaling molecule in the central nervous system. *Neurochem Int* 56:3-10
46. Teng H, Wu B, Zhao K, Yang G, Wu L, Wang R. 2013. Oxygen-sensitive mitochondrial accumulation of cystathionine beta-synthase mediated by Lon protease. *Proc Natl Acad Sci U S A* 110:12679-84
47. Jhee KH, Kruger WD. 2005. The role of cystathionine beta-synthase in homocysteine metabolism. *Antioxid Redox Signal* 7:813-22
48. Singh S, Padovani D, Leslie RA, Chiku T, Banerjee R. 2009. Relative contributions of cystathionine beta-synthase and gamma-cystathionase to H2S biogenesis via alternative trans-sulfuration reactions. *J Biol Chem* 284:22457-66
49. Robert K, Vialard F, Thiery E, Toyama K, Sinet PM, et al. 2003. Expression of the cystathionine beta synthase (CBS) gene during mouse development and immunolocalization in adult brain. *J Histochem Cytochem* 51:363-71
50. Lee M, Schwab C, Yu S, McGeer E, McGeer PL. 2009. Astrocytes produce the antiinflammatory and neuroprotective agent hydrogen sulfide. *Neurobiol Aging* 30:1523-34
51. Vitvitsky V, Thomas M, Ghorpade A, Gendelman HE, Banerjee R. 2006. A functional transsulfuration pathway in the brain links to glutathione homeostasis. *J Biol Chem* 281:35785-93
52. Shibuya N, Tanaka M, Yoshida M, Ogasawara Y, Togawa T, et al. 2009. 3-Mercaptopyruvate sulfurtransferase produces hydrogen sulfide and bound sulfane sulfur in the brain. *Antioxid Redox Signal* 11:703-14
53. Shibuya N, Mikami Y, Kimura Y, Nagahara N, Kimura H. 2009. Vascular endothelium expresses 3-mercaptopyruvate sulfurtransferase and produces hydrogen sulfide. *J Biochem* 146:623-6
54. Mani S, Untereiner A, Wu L, Wang R. 2014. Hydrogen sulfide and the pathogenesis of atherosclerosis. *Antioxid Redox Signal* 20:805-17

55. Searcy DG, Lee SH. 1998. Sulfur reduction by human erythrocytes. *J Exp Zool* 282:310-22
56. Curtis CG, Bartholomew TC, Rose FA, Dodgson KS. 1972. Detoxication of sodium 35 S-sulphide in the rat. *Biochemical pharmacology* 21:2313-21
57. Magee EA, Curno R, Edmond LM, Cummings JH. 2004. Contribution of dietary protein and inorganic sulfur to urinary sulfate: toward a biomarker of inorganic sulfur intake. *Am J Clin Nutr* 80:137-42
58. Furne J, Springfield J, Koenig T, DeMaster E, Levitt MD. 2001. Oxidation of hydrogen sulfide and methanethiol to thiosulfate by rat tissues: a specialized function of the colonic mucosa. *Biochemical pharmacology* 62:255-9
59. Weisiger RA, Pinkus LM, Jakoby WB. 1980. Thiol S-methyltransferase: suggested role in detoxication of intestinal hydrogen sulfide. *Biochemical pharmacology* 29:2885-7
60. Levitt MD, Furne J, Springfield J, Suarez F, DeMaster E. 1999. Detoxification of hydrogen sulfide and methanethiol in the cecal mucosa. *J Clin Invest* 104:1107-14
61. Smith RP, Abbanat RA. 1966. Protective effect of oxidized glutathione in acute sulfide poisoning. *Toxicol Appl Pharmacol* 9:209-17
62. Beauchamp RO, Jr., Bus JS, Popp JA, Boreiko CJ, Andjelkovich DA. 1984. A critical review of the literature on hydrogen sulfide toxicity. *Crit Rev Toxicol* 13:25-97
63. Morselli-Labate AM, Fantini L, Pezzilli R. 2007. Hydrogen sulfide, nitric oxide and a molecular mass 66 u substance in the exhaled breath of chronic pancreatitis patients. *Pancreatology* 7:497-504
64. Suarez F, Springfield J, Furne J, Levitt M. 1999. Differentiation of mouth versus gut as site of origin of odoriferous breath gases after garlic ingestion. *Am J Physiol* 276:G425-30
65. Insko MA, Deckwerth TL, Hill P, Toombs CF, Szabo C. 2009. Detection of exhaled hydrogen sulphide gas in rats exposed to intravenous sodium sulphide. *Br J Pharmacol* 157:944-51
66. Mok YY, Atan MS, Yoke Ping C, Zhong Jing W, Bhatia M, et al. 2004. Role of hydrogen sulphide in haemorrhagic shock in the rat: protective effect of inhibitors of hydrogen sulphide biosynthesis. *Br J Pharmacol* 143:881-9
67. Fiorucci S, Antonelli E, Distrutti E, Rizzo G, Mencarelli A, et al. 2005. Inhibition of hydrogen sulfide generation contributes to gastric injury caused by anti-inflammatory nonsteroidal drugs. *Gastroenterology* 129:1210-24
68. Cheng Y, Ndisang JF, Tang G, Cao K, Wang R. 2004. Hydrogen sulfide-induced relaxation of resistance mesenteric artery beds of rats. *Am J Physiol Heart Circ Physiol* 287:H2316-23
69. Ali MY, Ping CY, Mok YY, Ling L, Whiteman M, et al. 2006. Regulation of vascular nitric oxide in vitro and in vivo; a new role for endogenous hydrogen sulphide? *Br J Pharmacol* 149:625-34
70. Lee SW, Cheng Y, Moore PK, Bian JS. 2007. Hydrogen sulphide regulates intracellular pH in vascular smooth muscle cells. *Biochem Biophys Res Commun* 358:1142-7
71. Kiss L, Deitch EA, Szabo C. 2008. Hydrogen sulfide decreases adenosine triphosphate levels in aortic rings and leads to vasorelaxation via metabolic inhibition. *Life Sci* 83:589-94

72. Webb GD, Lim LH, Oh VM, Yeo SB, Cheong YP, et al. 2008. Contractile and vasorelaxant effects of hydrogen sulfide and its biosynthesis in the human internal mammary artery. *J Pharmacol Exp Ther* 324:876-82
73. Bucci M, Papapetropoulos A, Vellecco V, Zhou Z, Pyriochou A, et al. 2010. Hydrogen sulfide is an endogenous inhibitor of phosphodiesterase activity. *Arterioscler Thromb Vasc Biol* 30:1998-2004
74. Bauer CC, Boyle JP, Porter KE, Peers C. 2010. Modulation of Ca(2+) signalling in human vascular endothelial cells by hydrogen sulfide. *Atherosclerosis* 209:374-80
75. Zhao W, Wang R. 2002. H(2)S-induced vasorelaxation and underlying cellular and molecular mechanisms. *Am J Physiol Heart Circ Physiol* 283:H474-80
76. Wang R. 2009. Hydrogen sulfide: a new EDRF. *Kidney Int* 76:700-4
77. Yan SK, Chang T, Wang H, Wu L, Wang R, Meng QH. 2006. Effects of hydrogen sulfide on homocysteine-induced oxidative stress in vascular smooth muscle cells. *Biochem Biophys Res Commun* 351:485-91
78. Kimura Y, Dargusch R, Schubert D, Kimura H. 2006. Hydrogen sulfide protects HT22 neuronal cells from oxidative stress. *Antioxid Redox Signal* 8:661-70
79. Kimura Y, Kimura H. 2004. Hydrogen sulfide protects neurons from oxidative stress. *FASEB J* 18:1165-7
80. Whiteman M, Armstrong JS, Chu SH, Jia-Ling S, Wong BS, et al. 2004. The novel neuromodulator hydrogen sulfide: an endogenous peroxynitrite 'scavenger'? *J Neurochem* 90:765-8
81. Tyagi N, Moshal KS, Sen U, Vacek TP, Kumar M, et al. 2009. H2S protects against methionine-induced oxidative stress in brain endothelial cells. *Antioxid Redox Signal* 11:25-33
82. Zhang H, Zhi L, Moochhala S, Moore PK, Bhatia M. 2007. Hydrogen sulfide acts as an inflammatory mediator in cecal ligation and puncture-induced sepsis in mice by upregulating the production of cytokines and chemokines via NF-kappaB. *Am J Physiol Lung Cell Mol Physiol* 292:L960-71
83. Li L, Rossoni G, Sparatore A, Lee LC, Del Soldato P, Moore PK. 2007. Anti-inflammatory and gastrointestinal effects of a novel diclofenac derivative. *Free Radic Biol Med* 42:706-19
84. Fiorucci S, Orlandi S, Mencarelli A, Caliendo G, Santagada V, et al. 2007. Enhanced activity of a hydrogen sulphide-releasing derivative of mesalamine (ATB-429) in a mouse model of colitis. *Br J Pharmacol* 150:996-1002
85. Zanardo RC, Brancaleone V, Distrutti E, Fiorucci S, Cirino G, Wallace JL. 2006. Hydrogen sulfide is an endogenous modulator of leukocyte-mediated inflammation. *Faseb j* 20:2118-20
86. Wallace JL, Wang R. 2015. Hydrogen sulfide-based therapeutics: exploiting a unique but ubiquitous gasotransmitter. *Nat Rev Drug Discov* 14:329-45
87. Hill BC, Woon TC, Nicholls P, Peterson J, Greenwood C, Thomson AJ. 1984. Interactions of sulphide and other ligands with cytochrome c oxidase. An electron-paramagnetic-resonance study. *Biochem J* 224:591-600
88. Lowicka E, Beltowski J. 2007. Hydrogen sulfide (H2S) - the third gas of interest for pharmacologists. *Pharmacol Rep* 59:4-24

89. Nicholson RA, Roth SH, Zhang A, Zheng J, Brookes J, et al. 1998. Inhibition of respiratory and bioenergetic mechanisms by hydrogen sulfide in mammalian brain. *J Toxicol Environ Health A* 54:491-507
90. Zhi L, Ang AD, Zhang H, Moore PK, Bhatia M. 2007. Hydrogen sulfide induces the synthesis of proinflammatory cytokines in human monocyte cell line U937 via the ERK-NF-kappaB pathway. *J Leukoc Biol* 81:1322-32
91. Whiteman M, Li L, Rose P, Tan CH, Parkinson DB, Moore PK. 2010. The effect of hydrogen sulfide donors on lipopolysaccharide-induced formation of inflammatory mediators in macrophages. *Antioxid Redox Signal* 12:1147-54
92. Yang W, Yang G, Jia X, Wu L, Wang R. 2005. Activation of KATP channels by H2S in rat insulin-secreting cells and the underlying mechanisms. *J Physiol* 569:519-31
93. Ali MY, Whiteman M, Low CM, Moore PK. 2007. Hydrogen sulphide reduces insulin secretion from HIT-T15 cells by a KATP channel-dependent pathway. *J Endocrinol* 195:105-12
94. Kaneko Y, Kimura Y, Kimura H, Niki I. 2006. L-Cysteine Inhibits Insulin Release From the Pancreatic -Cell: Possible Involvement of Metabolic Production of Hydrogen Sulfide, a Novel Gasotransmitter. *Diabetes* 55:1391-7
95. Kaneko Y, Kimura T, Taniguchi S, Souma M, Kojima Y, et al. 2009. Glucose-induced production of hydrogen sulfide may protect the pancreatic beta-cells from apoptotic cell death by high glucose. *FEBS Lett* 583:377-82
96. Yang G, Yang W, Wu L, Wang R. 2007. H2S, endoplasmic reticulum stress, and apoptosis of insulin-secreting beta cells. *J Biol Chem* 282:16567-76
97. Kaneko Y, Kimura Y, Kimura H, Niki I. 2006. L-cysteine inhibits insulin release from the pancreatic beta-cell: possible involvement of metabolic production of hydrogen sulfide, a novel gasotransmitter. *Diabetes* 55:1391-7
98. Cao Y, Adhikari S, Ang AD, Moore PK, Bhatia M. 2006. Mechanism of induction of pancreatic acinar cell apoptosis by hydrogen sulfide. *Am J Physiol Cell Physiol* 291:C503-10
99. Desai KM, Chang T, Untereiner A, Wu L. 2011. Hydrogen sulfide and the metabolic syndrome. *Expert Rev Clin Pharmacol* 4:63-73
100. Inc. AT. 2014. ANTIBE THERAPEUTICS COMPLETES SINGLE ASCENDING DOSE PORTION OF ATB-346 PHASE I PROGRAM. ed. AT Inc. http://www.antibethera.com/s/PressReleases.asp?ReportID=677531&_Type=Press-Releases&_Title=ANTIBE-THERAPEUTICS-COMPLETES-SINGLE-ASCENDING-DOSE-PORTION-OF-ATB-346-PHAS
101. Chattopadhyay M, Kodela R, Olson KR, Kashfi K. 2012. NOSH-aspirin (NBS-1120), a novel nitric oxide- and hydrogen sulfide-releasing hybrid is a potent inhibitor of colon cancer cell growth in vitro and in a xenograft mouse model. *Biochem Biophys Res Commun* 419:523-8
102. Kashfi K. 2014. Anti-cancer activity of new designer hydrogen sulfide-donating hybrids. *Antioxid Redox Signal* 20:831-46
103. Li L, Whiteman M, Guan YY, Neo KL, Cheng Y, et al. 2008. Characterization of a novel, water-soluble hydrogen sulfide-releasing molecule (GYY4137): new insights into the biology of hydrogen sulfide. *Circulation* 117:2351-60

104. Li L, Salto-Tellez M, Tan CH, Whiteman M, Moore PK. 2009. GYY4137, a novel hydrogen sulfide-releasing molecule, protects against endotoxic shock in the rat. *Free Radic Biol Med* 47:103-13
105. Zhang L, Yang G, Untereiner A, Ju Y, Wu L, Wang R. 2013. Hydrogen sulfide impairs glucose utilization and increases gluconeogenesis in hepatocytes. *Endocrinology* 154:114-26
106. Yang G, Tang G, Zhang L, Wu L, Wang R. 2011. The pathogenic role of cystathionine gamma-lyase/hydrogen sulfide in streptozotocin-induced diabetes in mice. *Am J Pathol* 179:869-79
107. Winnick JJ, An Z, Ramnanan CJ, Smith M, Irimia JM, et al. 2011. Hepatic glycogen supercompensation activates AMP-activated protein kinase, impairs insulin signaling, and reduces glycogen deposition in the liver. *Diabetes* 60:398-407
108. Viana AY, Sakoda H, Anai M, Fujishiro M, Ono H, et al. 2006. Role of hepatic AMPK activation in glucose metabolism and dexamethasone-induced regulation of AMPK expression. *Diabetes research and clinical practice* 73:135-42
109. Ju Y, Untereiner A, Wu L, Yang G. 2015. HS-induced S-sulfhydration of pyruvate carboxylase contributes to gluconeogenesis in liver cells. *Biochim Biophys Acta* 1850:2293-303
110. Módis K KZ, Wang R. 2015. Regulation of liver mitochondrial function by hydrogen sulfide. In *Mitochondria in Liver Disease*, ed. I Taylor and Francis Books:(in press): CRC press. Number of (in press) pp.
111. Cooper CE, Brown GC. 2008. The inhibition of mitochondrial cytochrome oxidase by the gases carbon monoxide, nitric oxide, hydrogen cyanide and hydrogen sulfide: chemical mechanism and physiological significance. *J Bioenerg Biomembr* 40:533-9
112. Szabo C, Coletta C, Chao C, Modis K, Szczesny B, et al. 2013. Tumor-derived hydrogen sulfide, produced by cystathionine-beta-synthase, stimulates bioenergetics, cell proliferation, and angiogenesis in colon cancer. *Proc Natl Acad Sci U S A* 110:12474-9
113. Modis K, Coletta C, Erdelyi K, Papapetropoulos A, Szabo C. 2013. Intramitochondrial hydrogen sulfide production by 3-mercaptopyruvate sulfurtransferase maintains mitochondrial electron flow and supports cellular bioenergetics. *Faseb j* 27:601-11
114. Modis K, Asimakopoulou A, Coletta C, Papapetropoulos A, Szabo C. 2013. Oxidative stress suppresses the cellular bioenergetic effect of the 3-mercaptopyruvate sulfurtransferase/hydrogen sulfide pathway. *Biochem Biophys Res Commun* 433:401-7
115. Goubern M, Andriamihaja M, Nubel T, Blachier F, Bouillaud F. 2007. Sulfide, the first inorganic substrate for human cells. *Faseb j* 21:1699-706
116. Lagoutte E, Mimoun S, Andriamihaja M, Chaumontet C, Blachier F, Bouillaud F. 2010. Oxidation of hydrogen sulfide remains a priority in mammalian cells and causes reverse electron transfer in colonocytes. *Biochim Biophys Acta* 1797:1500-11
117. Bouillaud F, Blachier F. 2011. Mitochondria and sulfide: a very old story of poisoning, feeding, and signaling? *Antioxid Redox Signal* 15:379-91
118. Szabo C, Ransy C, Modis K, Andriamihaja M, Murghes B, et al. 2014. Regulation of mitochondrial bioenergetic function by hydrogen sulfide. Part I. Biochemical and physiological mechanisms. *Br J Pharmacol* 171:2099-122
119. Yusuf M, Kwong Huat BT, Hsu A, Whiteman M, Bhatia M, Moore PK. 2005. Streptozotocin-induced diabetes in the rat is associated with enhanced tissue hydrogen sulfide biosynthesis. *Biochem Biophys Res Commun* 333:1146-52

120. Hargrove JL, Trotter JF, Ashline HC, Krishnamurti PV. 1989. Experimental diabetes increases the formation of sulfane by transsulfuration and inactivation of tyrosine aminotransferase in cytosols from rat liver. *Metabolism* 38:666-72
121. Nieman KM, Rowling MJ, Garrow TA, Schalinske KL. 2004. Modulation of methyl group metabolism by streptozotocin-induced diabetes and all-trans-retinoic acid. *J Biol Chem* 279:45708-12
122. Jacobs RL, House JD, Brosnan ME, Brosnan JT. 1998. Effects of streptozotocin-induced diabetes and of insulin treatment on homocysteine metabolism in the rat. *Diabetes* 47:1967-70
123. Manna P, Gungor N, McVie R, Jain SK. 2014. Decreased cystathionine-gamma-lyase (CSE) activity in livers of type 1 diabetic rats and peripheral blood mononuclear cells (PBMC) of type 1 diabetic patients. *J Biol Chem* 289:11767-78
124. Hwang SY, Sarna LK, Siow YL, O K. 2013. High-fat diet stimulates hepatic cystathionine beta-synthase and cystathionine gamma-lyase expression. *Can J Physiol Pharmacol* 91:913-9
125. Mani S, Li H, Untereiner A, Wu L, Yang G, et al. 2013. Decreased endogenous production of hydrogen sulfide accelerates atherosclerosis. *Circulation* 127:2523-34
126. Peh MT, Anwar AB, Ng DS, Atan MS, Kumar SD, Moore PK. 2014. Effect of feeding a high fat diet on hydrogen sulfide (H2S) metabolism in the mouse. *Nitric Oxide* 41:138-45
127. Geng B, Cai B, Liao F, Zheng Y, Zeng Q, et al. 2013. Increase or decrease hydrogen sulfide exert opposite lipolysis, but reduce global insulin resistance in high fatty diet induced obese mice. *PLoS One* 8:e73892
128. Suzuki K, Olah G, Modis K, Coletta C, Kulp G, et al. 2011. Hydrogen sulfide replacement therapy protects the vascular endothelium in hyperglycemia by preserving mitochondrial function. *Proc Natl Acad Sci U S A* 108:13829-34
129. Guan Q, Zhang Y, Yu C, Liu Y, Gao L, Zhao J. 2012. Hydrogen sulfide protects against high-glucose-induced apoptosis in endothelial cells. *J Cardiovasc Pharmacol* 59:188-93
130. Finck BN, Kelly DP. 2006. PGC-1 coactivators: inducible regulators of energy metabolism in health and disease. *J Clin Invest* 116:615-22
131. Handschin C, Spiegelman BM. 2006. Peroxisome proliferator-activated receptor gamma coactivator 1 coactivators, energy homeostasis, and metabolism. *Endocr Rev* 27:728-35
132. Lin J, Handschin C, Spiegelman BM. 2005. Metabolic control through the PGC-1 family of transcription coactivators. *Cell Metab* 1:361-70
133. Andersson U, Scarpulla RC. 2001. Pgc-1-related coactivator, a novel, serum-inducible coactivator of nuclear respiratory factor 1-dependent transcription in mammalian cells. *Mol Cell Biol* 21:3738-49
134. Vega RB, Huss JM, Kelly DP. 2000. The coactivator PGC-1 cooperates with peroxisome proliferator-activated receptor alpha in transcriptional control of nuclear genes encoding mitochondrial fatty acid oxidation enzymes. *Mol Cell Biol* 20:1868-76
135. Knutti D, Kressler D, Kralli A. 2001. Regulation of the transcriptional coactivator PGC-1 via MAPK-sensitive interaction with a repressor. *Proc Natl Acad Sci U S A* 98:9713-8
136. Lin J, Puigserver P, Donovan J, Tarr P, Spiegelman BM. 2002. Peroxisome proliferator-activated receptor gamma coactivator 1beta (PGC-1beta), a novel PGC-1-related transcription coactivator associated with host cell factor. *J Biol Chem* 277:1645-8

137. Handschin C, Kobayashi YM, Chin S, Seale P, Campbell KP, Spiegelman BM. 2007. PGC-1alpha regulates the neuromuscular junction program and ameliorates Duchenne muscular dystrophy. *Genes Dev* 21:770-83
138. Vercauteren K, Gleyzer N, Scarpulla RC. 2008. PGC-1-related coactivator complexes with HCF-1 and NRF-2beta in mediating NRF-2(GABP)-dependent respiratory gene expression. *J Biol Chem* 283:12102-11
139. Herzig S, Long F, Jhala US, Hedrick S, Quinn R, et al. 2001. CREB regulates hepatic gluconeogenesis through the coactivator PGC-1. *Nature* 413:179-83
140. Yoon JC, Puigserver P, Chen G, Donovan J, Wu Z, et al. 2001. Control of hepatic gluconeogenesis through the transcriptional coactivator PGC-1. *Nature* 413:131-8
141. Bernal-Mizrachi C, Weng S, Feng C, Finck BN, Knutsen RH, et al. 2003. Dexamethasone induction of hypertension and diabetes is PPAR-alpha dependent in LDL receptor-null mice. *Nat Med* 9:1069-75
142. Rodgers JT, Lerin C, Haas W, Gygi SP, Spiegelman BM, Puigserver P. 2005. Nutrient control of glucose homeostasis through a complex of PGC-1alpha and SIRT1. *Nature* 434:113-8
143. Rodgers JT, Puigserver P. 2007. Fasting-dependent glucose and lipid metabolic response through hepatic sirtuin 1. *Proc Natl Acad Sci U S A* 104:12861-6
144. Patten IS, Arany Z. 2012. PGC-1 coactivators in the cardiovascular system. *Trends Endocrinol Metab* 23:90-7
145. Nisoli E, Clementi E, Paolucci C, Cozzi V, Tonello C, et al. 2003. Mitochondrial biogenesis in mammals: the role of endogenous nitric oxide. *Science* 299:896-9
146. Suliman HB, Carraway MS, Tatro LG, Piantadosi CA. 2007. A new activating role for CO in cardiac mitochondrial biogenesis. *J Cell Sci* 120:299-308
147. Puigserver P. 2005. Tissue-specific regulation of metabolic pathways through the transcriptional coactivator PGC1-alpha. *Int J Obes (Lond)* 29 Suppl 1:S5-9
148. Puigserver P, Rhee J, Donovan J, Walkey CJ, Yoon JC, et al. 2003. Insulin-regulated hepatic gluconeogenesis through FOXO1-PGC-1alpha interaction. *Nature* 423:550-5
149. Wu Z, Puigserver P, Andersson U, Zhang C, Adelmant G, et al. 1999. Mechanisms controlling mitochondrial biogenesis and respiration through the thermogenic coactivator PGC-1. *Cell* 98:115-24
150. Garesse R, Vallejo CG. 2001. Animal mitochondrial biogenesis and function: a regulatory cross-talk between two genomes. *Gene* 263:1-16
151. Larsson NG, Wang J, Wilhelmsson H, Oldfors A, Rustin P, et al. 1998. Mitochondrial transcription factor A is necessary for mtDNA maintenance and embryogenesis in mice. *Nat Genet* 18:231-6
152. Lehman JJ, Barger PM, Kovacs A, Saffitz JE, Medeiros DM, Kelly DP. 2000. Peroxisome proliferator-activated receptor gamma coactivator-1 promotes cardiac mitochondrial biogenesis. *J Clin Invest* 106:847-56
153. Leone TC, Lehman JJ, Finck BN, Schaeffer PJ, Wende AR, et al. 2005. PGC-1alpha deficiency causes multi-system energy metabolic derangements: muscle dysfunction, abnormal weight control and hepatic steatosis. *PLoS Biol* 3:e101
154. Lin J, Wu PH, Tarr PT, Lindenberg KS, St-Pierre J, et al. 2004. Defects in adaptive energy metabolism with CNS-linked hyperactivity in PGC-1alpha null mice. *Cell* 119:121-35

155. Hara K, Tobe K, Okada T, Kadowaki H, Akanuma Y, et al. 2002. A genetic variation in the PGC-1 gene could confer insulin resistance and susceptibility to Type II diabetes. *Diabetologia* 45:740-3
156. Vimaleswaran KS, Radha V, Ghosh S, Majumder PP, Deepa R, et al. 2005. Peroxisome proliferator-activated receptor-gamma co-activator-1alpha (PGC-1alpha) gene polymorphisms and their relationship to Type 2 diabetes in Asian Indians. *Diabet Med* 22:1516-21
157. Andrulionyte L, Zacharova J, Chiasson JL, Laakso M. 2004. Common polymorphisms of the PPAR-gamma2 (Pro12Ala) and PGC-1alpha (Gly482Ser) genes are associated with the conversion from impaired glucose tolerance to type 2 diabetes in the STOP-NIDDM trial. *Diabetologia* 47:2176-84
158. Ek J, Andersen G, Urhammer SA, Gaede PH, Drivsholm T, et al. 2001. Mutation analysis of peroxisome proliferator-activated receptor-gamma coactivator-1 (PGC-1) and relationships of identified amino acid polymorphisms to Type II diabetes mellitus. *Diabetologia* 44:2220-6
159. Lacquemant C, Chikri M, Boutin P, Samson C, Froguel P. 2002. No association between the G482S polymorphism of the proliferator-activated receptor-gamma coactivator-1 (PGC-1) gene and Type II diabetes in French Caucasians. *Diabetologia* 45:602-3; author reply 4
160. Stumvoll M, Fritsche A, t'Hart LM, Machann J, Thamer C, et al. 2004. The Gly482Ser variant in the peroxisome proliferator-activated receptor gamma coactivator-1 is not associated with diabetes-related traits in non-diabetic German and Dutch populations. *Exp Clin Endocrinol Diabetes* 112:253-7
161. Muller YL, Bogardus C, Pedersen O, Baier L. 2003. A Gly482Ser missense mutation in the peroxisome proliferator-activated receptor gamma coactivator-1 is associated with altered lipid oxidation and early insulin secretion in Pima Indians. *Diabetes* 52:895-8
162. Koo SH, Satoh H, Herzig S, Lee CH, Hedrick S, et al. 2004. PGC-1 promotes insulin resistance in liver through PPAR-alpha-dependent induction of TRB-3. *Nat Med* 10:530-4
163. Oberkofler H, Linnemayr V, Weitgasser R, Klein K, Xie M, et al. 2004. Complex haplotypes of the PGC-1alpha gene are associated with carbohydrate metabolism and type 2 diabetes. *Diabetes* 53:1385-93
164. Rhee J, Inoue Y, Yoon JC, Puigserver P, Fan M, et al. 2003. Regulation of hepatic fasting response by PPARgamma coactivator-1alpha (PGC-1): requirement for hepatocyte nuclear factor 4alpha in gluconeogenesis. *Proc Natl Acad Sci U S A* 100:4012-7
165. Meirhaeghe A, Crowley V, Lenaghan C, Lelliott C, Green K, et al. 2003. Characterization of the human, mouse and rat PGC1 beta (peroxisome-proliferator-activated receptor-gamma co-activator 1 beta) gene in vitro and in vivo. *Biochem J* 373:155-65
166. Lin J, Yang R, Tarr PT, Wu PH, Handschin C, et al. 2005. Hyperlipidemic effects of dietary saturated fats mediated through PGC-1beta coactivation of SREBP. *Cell* 120:261-73
167. Lin J, Tarr PT, Yang R, Rhee J, Puigserver P, et al. 2003. PGC-1beta in the regulation of hepatic glucose and energy metabolism. *J Biol Chem* 278:30843-8

168. Arany Z, Lebrasseur N, Morris C, Smith E, Yang W, et al. 2007. The transcriptional coactivator PGC-1beta drives the formation of oxidative type IIX fibers in skeletal muscle. *Cell Metab* 5:35-46
169. Sonoda J, Laganiere J, Mehl IR, Barish GD, Chong LW, et al. 2007. Nuclear receptor ERR alpha and coactivator PGC-1 beta are effectors of IFN-gamma-induced host defense. *Genes Dev* 21:1909-20
170. Lelliott CJ, Medina-Gomez G, Petrovic N, Kis A, Feldmann HM, et al. 2006. Ablation of PGC-1beta results in defective mitochondrial activity, thermogenesis, hepatic function, and cardiac performance. *PLoS Biol* 4:e369
171. St-Pierre J, Lin J, Krauss S, Tarr PT, Yang R, et al. 2003. Bioenergetic analysis of peroxisome proliferator-activated receptor gamma coactivators 1alpha and 1beta (PGC-1alpha and PGC-1beta) in muscle cells. *J Biol Chem* 278:26597-603
172. Hock MB, Kralli A. 2009. Transcriptional control of mitochondrial biogenesis and function. *Annu Rev Physiol* 71:177-203
173. Gleyzer N, Vercauteren K, Scarpulla RC. 2005. Control of mitochondrial transcription specificity factors (TFB1M and TFB2M) by nuclear respiratory factors (NRF-1 and NRF-2) and PGC-1 family coactivators. *Mol Cell Biol* 25:1354-66
174. Vercauteren K, Pasko RA, Gleyzer N, Marino VM, Scarpulla RC. 2006. PGC-1-related coactivator: immediate early expression and characterization of a CREB/NRF-1 binding domain associated with cytochrome c promoter occupancy and respiratory growth. *Mol Cell Biol* 26:7409-19
175. Vercauteren K, Gleyzer N, Scarpulla RC. 2009. Short hairpin RNA-mediated silencing of PRC (PGC-1-related coactivator) results in a severe respiratory chain deficiency associated with the proliferation of aberrant mitochondria. *J Biol Chem* 284:2307-19
176. Raharijaona M, Le Pennec S, Poirier J, Mirebeau-Prunier D, Rouxel C, et al. 2009. PGC-1-related coactivator modulates mitochondrial-nuclear crosstalk through endogenous nitric oxide in a cellular model of oncocytic thyroid tumours. *PLoS One* 4:e7964
177. He X, Sun C, Wang F, Shan A, Guo T, et al. 2012. Peri-implantation lethality in mice lacking the PGC-1-related coactivator protein. *Dev Dyn* 241:975-83
178. Scarpulla RC. 2008. Nuclear control of respiratory chain expression by nuclear respiratory factors and PGC-1-related coactivator. *Ann N Y Acad Sci* 1147:321-34
179. Goto H, Motomura S, Wilson AC, Freiman RN, Nakabeppu Y, et al. 1997. A single-point mutation in HCF causes temperature-sensitive cell-cycle arrest and disrupts VP16 function. *Genes Dev* 11:726-37
180. Vogel JL, Kristie TM. 2000. The novel coactivator C1 (HCF) coordinates multiprotein enhancer formation and mediates transcription activation by GABP. *Embo j* 19:683-90
181. Cao Z, Umek RM, McKnight SL. 1991. Regulated expression of three C/EBP isoforms during adipose conversion of 3T3-L1 cells. *Genes Dev* 5:1538-52
182. Williams SC, Cantwell CA, Johnson PF. 1991. A family of C/EBP-related proteins capable of forming covalently linked leucine zipper dimers in vitro. *Genes Dev* 5:1553-67
183. Descombes P, Chojkier M, Lichtsteiner S, Falvey E, Schibler U. 1990. LAP, a novel member of the C/EBP gene family, encodes a liver-enriched transcriptional activator protein. *Genes Dev* 4:1541-51

184. Descombes P, Schibler U. 1991. A liver-enriched transcriptional activator protein, LAP, and a transcriptional inhibitory protein, LIP, are translated from the same mRNA. *Cell* 67:569-79
185. Akira S, Isshiki H, Sugita T, Tanabe O, Kinoshita S, et al. 1990. A nuclear factor for IL-6 expression (NF-IL6) is a member of a C/EBP family. *Embo j* 9:1897-906
186. Poli V, Mancini FP, Cortese R. 1990. IL-6DBP, a nuclear protein involved in interleukin-6 signal transduction, defines a new family of leucine zipper proteins related to C/EBP. *Cell* 63:643-53
187. Wang H, Peiris TH, Mowery A, Le Lay J, Gao Y, Greenbaum LE. 2008. CCAAT/enhancer binding protein-beta is a transcriptional regulator of peroxisome-proliferator-activated receptor-gamma coactivator-1alpha in the regenerating liver. *Mol Endocrinol* 22:1596-605
188. Ayala-Sumuano JT, Velez-delValle C, Beltran-Langarica A, Marsch-Moreno M, Hernandez-Mosqueira C, Kuri-Harcuch W. 2013. Glucocorticoid paradoxically recruits adipose progenitors and impairs lipid homeostasis and glucose transport in mature adipocytes. *Sci Rep* 3:2573
189. Arizmendi C, Liu S, Croniger C, Poli V, Friedman JE. 1999. The transcription factor CCAAT/enhancer-binding protein beta regulates gluconeogenesis and phosphoenolpyruvate carboxykinase (GTP) gene transcription during diabetes. *The Journal of biological chemistry* 274:13033-40
190. Croniger CM, Millward C, Yang J, Kawai Y, Arinze IJ, et al. 2001. Mice with a deletion in the gene for CCAAT/enhancer-binding protein beta have an attenuated response to cAMP and impaired carbohydrate metabolism. *J Biol Chem* 276:629-38
191. Park EA, Gurney AL, Nizielski SE, Hakimi P, Cao Z, et al. 1993. Relative roles of CCAAT/enhancer-binding protein beta and cAMP regulatory element-binding protein in controlling transcription of the gene for phosphoenolpyruvate carboxykinase (GTP). *J Biol Chem* 268:613-9
192. Niehof M, Manns MP, Trautwein C. 1997. CREB controls LAP/C/EBP beta transcription. *Mol Cell Biol* 17:3600-13
193. Matsuno F, Chowdhury S, Gotoh T, Iwase K, Matsuzaki H, et al. 1996. Induction of the C/EBP beta gene by dexamethasone and glucagon in primary-cultured rat hepatocytes. *J Biochem* 119:524-32
194. Bosch F, Sabater J, Valera A. 1995. Insulin inhibits liver expression of the CCAAT/enhancer-binding protein beta. *Diabetes* 44:267-71
195. Kajimura S, Seale P, Kubota K, Lunsford E, Frangioni JV, et al. 2009. Initiation of myoblast to brown fat switch by a PRDM16-C/EBP-beta transcriptional complex. *Nature* 460:1154-8
196. Canto C, Auwerx J. 2010. Clking on PGC-1alpha to inhibit gluconeogenesis. *Cell Metab* 11:6-7
197. Burgess SC, Leone TC, Wende AR, Croce MA, Chen Z, et al. 2006. Diminished hepatic gluconeogenesis via defects in tricarboxylic acid cycle flux in peroxisome proliferator-activated receptor gamma coactivator-1alpha (PGC-1alpha)-deficient mice. *J Biol Chem* 281:19000-8
198. Kartha RV, Zhou J, Hovde LB, Cheung BW, Schroder H. 2012. Enhanced detection of hydrogen sulfide generated in cell culture using an agar trap method. *Anal Biochem* 423:102-8

199. Walker PR. 1977. Glycogen metabolism in adult rat liver parenchymal cell primary cultures. *J Cell Physiol* 91:169-79
200. Walker PR, Grindle MJ. 1977. Effects of hormones and serum on glycogen metabolism in adult rat liver parenchymal cell primary cultures. *J Cell Physiol* 91:181-91
201. Longo-Sorbello GSA, Saydam, G., Banerjee, D., Bertino, J.R. . 2006. Cytotoxicity and Cell Growth Assays. In *Cell Biology. A Laboratory Handbook*, ed. JE Celis, 1:315-24. Burlington, MA: Elsevier Academic Press. Number of 315-24 pp.
202. Kouadjo KE, Nishida Y, Cadrin-Girard JF, Yoshioka M, St-Amand J. 2007. Housekeeping and tissue-specific genes in mouse tissues. *BMC genomics* 8:127
203. Hirabara SM, Silveira LR, Abdulkader FR, Alberici LC, Procopio J, et al. 2006. Role of fatty acids in the transition from anaerobic to aerobic metabolism in skeletal muscle during exercise. *Cell Biochem Funct* 24:475-81
204. Tang G, Zhang L, Yang G, Wu L, Wang R. 2013. Hydrogen sulfide-induced inhibition of L-type Ca2+ channels and insulin secretion in mouse pancreatic beta cells. *Diabetologia* 56:533-41
205. Feng X, Chen Y, Zhao J, Tang C, Jiang Z, Geng B. 2009. Hydrogen sulfide from adipose tissue is a novel insulin resistance regulator. *Biochem Biophys Res Commun* 380:153-9
206. Hundal RS, Krssak M, Dufour S, Laurent D, Lebon V, et al. 2000. Mechanism by which metformin reduces glucose production in type 2 diabetes. *Diabetes* 49:2063-9
207. Olson H, Betton G, Robinson D, Thomas K, Monro A, et al. 2000. Concordance of the toxicity of pharmaceuticals in humans and in animals. *Regulatory toxicology and pharmacology : RTP* 32:56-67
208. Schaeffner I, Petters J, Aurich H, Frohberg P, Christ B. 2005. A microtiterplate-based screening assay to assess diverse effects on cytochrome P450 enzyme activities in primary rat hepatocytes by various compounds. *Assay and drug development technologies* 3:27-38
209. Mathijs K, Kienhuis AS, Brauers KJ, Jennen DG, Lahoz A, et al. 2009. Assessing the metabolic competence of sandwich-cultured mouse primary hepatocytes. *Drug metabolism and disposition: the biological fate of chemicals* 37:1305-11
210. Bhogal RH, Curbishley SM, Weston CJ, Adams DH, Afford SC. 2010. Reactive oxygen species mediate human hepatocyte injury during hypoxia/reoxygenation. *Liver transplantation : official publication of the American Association for the Study of Liver Diseases and the International Liver Transplantation Society* 16:1303-13
211. Xu JJ, Diaz D, O'Brien PJ. 2004. Applications of cytotoxicity assays and pre-lethal mechanistic assays for assessment of human hepatotoxicity potential. *Chemico-biological interactions* 150:115-28
212. Hoen PA, Commandeur JN, Vermeulen NP, Van Berkel TJ, Bijsterbosch MK. 2000. Selective induction of cytochrome P450 3A1 by dexamethasone in cultured rat hepatocytes: analysis with a novel reverse transcriptase-polymerase chain reaction assay section sign. *Biochemical pharmacology* 60:1509-18
213. Boess F, Kamber M, Romer S, Gasser R, Muller D, et al. 2003. Gene expression in two hepatic cell lines, cultured primary hepatocytes, and liver slices compared to the in vivo liver gene expression in rats: possible implications for toxicogenomics use of in vitro systems. *Toxicological sciences : an official journal of the Society of Toxicology* 73:386-402

214. Miyake K, Ogawa W, Matsumoto M, Nakamura T, Sakaue H, Kasuga M. 2002. Hyperinsulinemia, glucose intolerance, and dyslipidemia induced by acute inhibition of phosphoinositide 3-kinase signaling in the liver. *J Clin Invest* 110:1483-91
215. Qiao L, MacLean PS, You H, Schaack J, Shao J. 2006. knocking down liver ccaat/enhancer-binding protein alpha by adenovirus-transduced silent interfering ribonucleic acid improves hepatic gluconeogenesis and lipid homeostasis in db/db mice. *Endocrinology* 147:3060-9
216. Schiedner G, Morral N, Parks RJ, Wu Y, Koopmans SC, et al. 1998. Genomic DNA transfer with a high-capacity adenovirus vector results in improved in vivo gene expression and decreased toxicity. *Nat Genet* 18:180-3
217. Christensen P, Stenvang JP, Godfrey WL. 2004. A flow cytometric method for rapid determination of sperm concentration and viability in mammalian and avian semen. *J Androl* 25:255-64
218. Festing S, Wilkinson R. 2007. The ethics of animal research. Talking Point on the use of animals in scientific research. *EMBO Reports* 8:526-30
219. Karamitsos DT. 2011. The story of insulin discovery. *Diabetes research and clinical practice* 93 Suppl 1:S2-8
220. Russell WMS, Burch RL. 1959. The principles of humane experimental technique.
221. Wang HJ, Jin YX, Shen W, Neng J, Wu T, et al. 2007. Low dose streptozotocin (STZ) combined with high energy intake can effectively induce type 2 diabetes through altering the related gene expression. *Asia Pac J Clin Nutr* 16 Suppl 1:412-7
222. Tahara A, Matsuyama-Yokono A, Shibasaki M. 2011. Effects of antidiabetic drugs in high-fat diet and streptozotocin-nicotinamide-induced type 2 diabetic mice. *Eur J Pharmacol* 655:108-16
223. Watts LM, Manchem VP, Leedom TA, Rivard AL, McKay RA, et al. 2005. Reduction of hepatic and adipose tissue glucocorticoid receptor expression with antisense oligonucleotides improves hyperglycemia and hyperlipidemia in diabetic rodents without causing systemic glucocorticoid antagonism. *Diabetes* 54:1846-53
224. Srinivasan K, Viswanad B, Asrat L, Kaul CL, Ramarao P. 2005. Combination of high-fat diet-fed and low-dose streptozotocin-treated rat: a model for type 2 diabetes and pharmacological screening. *Pharmacol Res* 52:313-20

APPENDIX

This section details the work and accomplishments achieved during my time as a PhD student at Lakehead University under the supervision of both Drs. Lily Wu and Rui Wang.

PUBLISHED REFEREED PAPERS:

IF: Impact Factor

1. Untereiner A.A, Wang R, Wu L. 2015. H_2S-induced increase in hepatic glucose production and the underlying mechanisms. *Antioxidants & Redox Signaling* **(IF: 7.407)**. *In press*.

2. Ju Y, Untereiner A, Wu L, Yang G. 2015. H_2S-induced S-sulfhydration of pyruvate carboxylase contributes to gluconeogenesis in liver cells. *Biochimica et Biophysica Acta,* **1850**: 2293-2303 **(IF: 4.66)**.

3. Mani S, Li H, Untereiner A, Yang G, Austin RC, Dickhout JG, Lhoták S, Meng QH, Wu L, Wang R. 2013. Decreased endogenous production of hydrogen sulfide accelerates atherosclerosis. *Circulation*, **127**: 2523-2534 (**IF: 14.429**).

4. Mani S, Untereiner A, Wu L, Wang R. 2013. Hydrogen sulfide and the pathogenesis of atherosclerosis. *Antioxidants & Redox Signaling,* **20**: 805-817 **(IF: 7.407)**.

5. Zhang L, Yang G, Untereiner A, Ju Y, Wu L, Wang R. 2013. H_2S impairs glucose utilization and increases gluconeogenesis in hepatocytes. *Endocrinology,* **154**: 114-126. (**IF: 4.459**).

MANUSCRIPT UNDER REVIEW:

1. Untereiner A.A, Fu M, Ju Y, Wang R, Módis K, Wu L. 2015. Stimulatory effect of the CSE/H_2S system on hepatic mitochondrial biogenesis and the underlying mechanisms. Submitted to *British Journal of Pharmacology* **(IF: 4.842)**.

BOOK CHAPTER

1. Untereiner A.A, Wu L, Wang R. Chapter 2: The role of carbon monoxide as a gasotransmitter in cardiovascular and metabolic regulation. In Gasotransmitters: physiology and pathophysiology. Hermann, Anton; Sitdikova, Guzel F.; Weiger, Thomas M. (Eds). Spinger, p. 37-70, 2012.

ABSTRACTS:

1. Untereiner A.A, Wang R, Wu L. 2015. H_2S-induced increase in hepatic glucose production and the underlying mechanisms. *Nitric Oxide* **47**, S26 (Abstract #PP33). 3rd European Conference on the Biology of Hydrogen Sulfide, May 3-6 2015, Athens, Greece. **(Only graduate student selected to present abstract as an oral presentation)**

2. Módis K, Ju Y, Altaany Z, Untereiner A.A, Yang G, Wu L, Szabo C, Wang R. 2015. Hydrogen sulfide-induced S-sulfhydration of ATP synthase stimulates mitochondrial bioenergetics. *Nitric Oxide* 47, S53 (Abstract #PP98). 3rd European Conference on the Biology of Hydrogen Sulfide, May 3-6 2015, Athens, Greece.

3. Untereiner A, Wang R, Wu L. 2014. Hydrogen sulphide increases glucose production from the liver and the underlying mechanisms. TBRRI 2014 Annual Collaborative Retreat: The Rainbow of Clinical Research. Thunder Bay Regional Health Sciences Centre, Thunder Bay, Ontario. (10/24-25/2014).

4. Mani S, Li H, Untereiner A, Yang G, Wu L, Wang R. 2013. Atherosclerosis development in cystathionine gamma-lyase knockout mice: Systemic detection using ultrasound biomicroscopy. Canadian Institute of Health Research-Institute of Circulatory and Respiratory Health. Toronto, Ontario.

5. Untereiner A, Wang R, Wu L. 2013. Hydrogen sulphide enhances glucose production in primary liver cells. Innovation and Research Week. Lakehead University, Thunder Bay, Ontario. (02/12/2013).
   (Awarded the Best-of-the-Best Poster Award: $250)

TEACHING EXPERIENCE

1. **Graduate Assistant III (2012-2015):** For this assistantship, I lectured for 6 hours to master students enrolled in Dr. Lily Wu's course: "Obesity & Type 2 Diabetes" (PUBL-5710) in the School of Public Health at Lakehead University:
   a. "Human Physiology Overview"
      Lecture length: 2 hours
   b. "Obesity and type 2 diabetes, and related pathophysiological changes in the human body"
      Lecture length: 2.5 hours
   c. "Genetics related to obesity and type 2 diabetes"
      Lecture length: 1.5 hours
2. **Graduate Assistant II (2011-2012):** For this assistantship, I lectured for 3.5 hours to master students enrolled in Dr. Lily Wu's course: "Obesity & Type 2 Diabetes" (PUBL-5710) in the School of Public Health at Lakehead University:
   a. "Human Physiology Overview"
      Lecture length: 1 hour

b. “Obesity and type 2 diabetes, and related pathophysiological changes in the human body”
   Lecture length: 1 hour
c. “Genetics related to obesity and type 2 diabetes”
   Lecture length: 1.5 hours